Kholumolumo ellenbergerorum, gen. et sp. nov., a new basal sauropodomorph from the Lower Elliot Formation (Late Triassic) of Maphutseng, Lesotho

Claire Peyre de Fabrègues, Ronan Allain

Kholumolumo ellenbergerorum, gen. et sp. nov., a new basal sauropodomorph from the Lower Elliot Formation (Late Triassic) of Maphutseng, Lesotho

CLAIRE PEYRE DE FABRÈGUES*, [1] and RONAN ALLAIN[1]

[1] Muséum National d'Histoire Naturelle, Centre de Recherche sur la Paléobiodiversité et les Paléoenvironnements (CR2P, UMR 7207), Sorbonne Universités-MNHN, CNRS, UPMC, 57 rue Cuvier, CP 38, F-75005, Paris, France, claire.peyre-de-fabregues@edu.mnhn.fr, ronan.allain@mnhn.fr

*Corresponding author

ABSTRACT—A dozen basal sauropodomorph genera are currently known from Southern Africa. The vast majority of the specimens were unearthed in South Africa, but a few were found in Lesotho. We provide here the first complete anatomical description of a historical specimen from Lesotho: “the Maphutseng dinosaur.” The first rests of this animal were uncovered in 1955 and cited in a scientific publication just one year after that, in 1956. Since then, the Maphutseng assemblage has been mentioned in several papers and named on two occasions but was never formally published. The bone bed has delivered a huge amount of material from all the regions of the skeleton, of which a small part is described herein. Based on these skeletal elements, and given the unique anatomy of this basal sauropodomorph, the new species *Kholumolumo ellenbergerorum* gen. nov., sp. nov. is erected. Although the rests come from a large number of individuals, the species is the most complete to date in the lower Elliot Formation. Considering all the material known from the upper Triassic of Gondwana, it is also one of the longest specimens (adults could probably reach 10m long). Despite this important size, the anatomy supported by the phylogenetic results remove any doubts concerning a putative quadrupedality of the animal, and thus a possible link with the origin of sauropoda.

INTRODUCTION

Historical Background

Paul Ellenberger was, at first, a Protestant missionary like both his grandfathers and his father before him. Like his father, he was most curious about life and evolution. He worked in Lesotho for 17 years, from 1953 to 1970, period during which he prospected a lot looking for fossils. As a result, he published more than 15 papers on the paleontology of Lesotho.

In 1930, scattered remains were discovered by Samuel Motsoane, principal of the Paris Evangelical Mission School in Bethesda. He communicated their location to P. Ellenberger much later, in 1955. Following these indications, P. Ellenberger prospected near a fossiliferous lens in Maphutseng, not far from the Protestant mission, in August 1955 (Fig. 1A-B). He was assisted by his brother, François Ellenberger, geologist, and their research was in part financed by the CNRS (the French National Center for Scientific Research). In September 1955, they uncovered a pile of well-preserved bones at the place called "Thotobolo ea 'Ma-Beata." They will write later on it: "The bones of this pile (femora, tibias, various long bones, ribs, phalanges, claws, vertebrae, etc.) are distributed without order nor connection, in mass or trail, within a bed of 20 to 30 cm… […]. This deposit displays a previously unseen richness in the South African Stormberg." (Ellenberger and Ellenberger, 1956b: 100). The extent of the Maphutseng deposit being beyond the material and technical means of the brothers Ellenberger, they asked for the help of two South African colleagues, A.W. Crompton, head of the paleontology department at the National Museum of Bloemfontein, and R.F. Ewer from Rhodes University in Grahamstown. Their first collaboration, in November 1955, was the very first paleontological field campaign in Lesotho (Table 1). The same year, P. Ellenberger published a preliminary note, in which Maphutseng and the ongoing fieldwork, are quoted (Ellenberger, 1955). The following year,

in 1956, the same four-man team continued the excavations in Maphutseng (Table 1). Very soon, the Ellenberger brothers realized they were dealing with a very rich deposit (Ellenberger and Ellenberger, 1956a, 1956b). Overall, these first two field campaigns led to 683 collected pieces, of which approximately 450 complete bones, in a 35 m^2 surface (Fig. 1C). In 1957, the whole of the material was brought back to the Iziko Museum (formerly South African Museum), Cape Town, in temporary storage. Nowadays, it has been moved to the University of Cape Town, where part of it is under study (E. Krupandan, pers. comm., 2014). After this first joint experience, the relationships between the Ellenberger brothers and Crompton began to deteriorate, probably because the preparation and, therefore, the study of the 1955-56 material sent in Bloemfontein were not completed in time and the material not returned to Lesotho. In a 1964 letter to L. Ginsburg, Paul Ellenberger complained that the Maphutseng material was "cromptonized" (Supplementary Data Figure 1S).

The deposit being far from drained, another field campaign took place in Maphutseng in 1959. It was funded by the CNRS, and the team included not only the brothers Ellenberger, but also Léonard Ginsburg and Jean Fabre, two researchers from the National Museum of Natural History in Paris (MNHN), as well as Hélène Ellenberger, the wife of F. Ellenberger (Table 1). The exact quantity of fossils collected during this campaign is unknown, but according to the excavation plan drawn by F. Ellenberger (Fig. 1C), it probably comes close to two hundred pieces. A small part of it was housed in Morija Museum & Archives, and some vertebrae were lent to the Iziko Museum in Cape Town. Most of the material was sent to Paris MNHN, in temporary storage. In 1960, F. and P. Ellenberger published an article about a slab found in Maphutseng and exhibiting dozens of tracks. According to them, the 70 m^2 slab displayed at least eight different trackways (Ellenberger and Ellenberger, 1960). Several other tracks were found in Maphutseng. At least three original tracks were brought to Montpellier University, as well as 18 other tracks, presumably casts. Most of it is indicated as

"missing" in the inventory, the whereabouts of this material is thus currently unknown (pers. obs., 2016). The following excavations in Maphutseng occurred in 1963. The team consisted of P. Ellenberger, L. Ginsburg, J. Fabre and Christiane Mendrez (MNHN) (Table 1). The expedition was followed by the first description of the bones of the Maphutseng dinosaur, and their attribution to *Euskelosaurus browni* (Ellenberger and Ginsburg, 1966).

In September 1970, P. Ellenberger oversaw the last expedition in Maphutseng, with the assistance of L. Ginsburg, J. Fabre and Bernard Battail (MNHN) (Table 1; Fig. 2). The bones collected were brought to Paris. Between 1959 and 1970, based on the excavation plan of 1959 and the total number of excavated pieces given by P. Ellenberger (Ellenberger, 1970: 345), we estimate to approximately 400 the number of Maphutseng fossils sent to France. The brothers Ellenberger attributed a field number to each excavated bone between 1959 and 1970. Given that the numbers range from 684 to 1303, the number of fossils is extended to 600. However, only 210 are nowadays housed in the MNHN, in Paris. This significant difference can be explained if we consider that, on the field, several numbers can be attributed to fragments of the same bone. Consequently, some subcomplete bones of the collections display until 4 field numbers. The Ellenberger themselves wrote in 1956: "The second [fieldwork], in February 1956, increased this number to almost 700 (which should represent more than 450 complete and distinct bones), […]" (Ellenberger and Ellenberger, 1956b: 100).

In 1970, Paul Ellenberger returned for good to France, and continued his work on Lesotho fossils in Montpellier (Southern France). The same year, he wrote a review about Lesotho stratigraphy, in which appear all the fossils, ichnofossils and deposits he discovered during his expeditions. In this paper appears the first name attributed to the Maphutseng dinosaur, which was, at that time, no longer considered as a specimen of *Euskelosaurus*. Indeed, P. Ellenberger wrote: "A new type of 'Euskelosauridae', perhaps closer to sauropods: 'The Maphutseng Beast' or '*Thotobolosaurus mabeatae*' (under study), 1150 bones extracted with

various rests of lower jaws and skulls from a *Dicroidium* marl of this age, in Maphutseng." (Ellenberger, 1970: 345). This proposed binomen was inspired by the Sesotho name of the place where the first pile of bones was found, not far from the huts of the village of Maphutseng ("Thotobolo ea 'Ma-Beata", meaning "Beata's mother's trash heap"). This new species was never formally published, even if numerous publications have dealt with this material (Ellenberger, 1955; Ellenberger and Ellenberger, 1956a, 1956b; Ellenberger and Ginsburg, 1966; Ellenberger et al., 1970; Ellenberger, 1970). It is thus currently considered as a nomen nudum. Gauffre (1993) coined the name *Kholumolumosaurus ellenbergerorum* for the Maphutseng dinosaur and described the material in more details in his PhD Thesis (Gauffre, 1996). The latter, too, was never formally published, and this second binomen is thus also considered as a nomen nudum.

Stratigraphical Overview and the Age of the "Maphutseng Dinosaur"

Maphutseng is a mission located in the Mohale's Hoek District, in the southwest of Lesotho (Fig. 3). Many outcrops, corresponding to different stratigraphic levels, have yielded numerous fossils, including mainly footprints, but also plants and dinosaur bones in the vicinity of Maphutseng (Ellenberger, 1970).

As for most sauropodomorphs taxa from the Elliot Formation of southern Africa (McPhee et al., 2017), uncertainties remain on the exact stratigraphic provenance of the Maphutseng dinosaur. In the first three articles mentioning the latter, the Ellenberger brothers stated that the bones come from the base of Red Beds (Ellenberger, 1955; Ellenberger and Ellenberger, 1956a; 1956b), i.e. the base of the lower Elliot Formation (LEF) (SACS, 1980; Johnson et al., 1996; Bordy et al., 2004). According to the Ellenberger brothers, the bone bed presents sedimentary facies typical of the top of the Molteno Formation. It is mainly composed of grey to yellowish-green sandy clays and soft gritty sandstones that contain abundant plant fossils,

with the foliage species *Dicroidium odontopteroides* dominating the assemblage. Laterally, the bone bed grades into red sandstones typical of the LEF (Ellenberger and Ellenberger, 1956b). In their subsequent publications (Ellenberger and Ginsburg, 1966; Ellenberger et al., 1970), the same authors changed their mind and referred the bone bed of Maphutseng to the top of the Molteno Formation. In 1970, Paul Ellenberger established a subdivision for the Molteno, Elliot and Clarens Formations in Lesotho, and precised the stratigraphic position of the Maphutseng bone bed, which is placed in the Zone A/4 ("Molteno supérieur b du Lesotho"). The zone A/4 is now considered to form part of the LEF (e.g. Kitching and Raath, 1984; Gauffre, 1993, 1996; Bordy et al., 2004). Based on lithostratigraphic assessments (van Gend et al., 2015), it has been recently suggested that the Maphutseng bone bed is in the uppermost part of the LEF, and thus is of a latest Triassic age (around 205 Myr). This has been contradicted by other lithostratigraphic observations (Ellenberger and Ellenberger, 1956b; Battail, pers. comm., 2018) and a magnetostratigraphic study (Scissio et al., 2017) which place the site in the lower part of the LEF, suggesting a Norian age (around 210 Myr) for the bone bed.

Abbreviations

Institutional Abbreviations—BP, Evolutionary Studies Institute, Johannesburg, South Africa (formerly Bernard Price Institute); **CM**, Carnegie Museum, Pittsburgh, USA; **CPSGM**, Collections Paléontologiques du Service Géologique du Maroc, Rabat, Morocco; **ISEM**, Institut des Sciences de l'Évolution Montpellier, Montpellier, France; **MB**, Museum für Naturkunde, Berlin, Germany; **MNHN**, Muséum National d'Histoire Naturelle, Paris, France; **NM QR**, National Museum, Bloemfontein, South Africa; **OUMNH**, Oxford University Museum of Natural History, Oxford, England; **PVL**, Universidad Nacional de

Tucumán, San Miguel de Tucumán, Argentina; **SAM-PK**, Iziko South African Museum, Cape Town, South Africa; **YPM**, Peabody Museum of Natural History, New Haven, USA.

SYSTEMATIC PALAEONTOLOGY

DINOSAURIA Owen, 1842

SAURISCHIA Seeley, 1887

SAUROPODOMORPHA Huene, 1932

KHOLUMOLUMO, gen. nov.

Etymology—The Kholumolumo [xodumodumo] is a mythological creature of the sotho folklore. It is often described as a type of dragon, an enormous monster, or sometimes a big lizard or crocodile. When referring to dinosaurs, Basotho frequently use this term.

Type species—*Kholumolumo ellenbergerorum*.

Diagnosis—As for the species.

KHOLUMOLUMO ELLENBERGERORUM, sp. nov.

(Figs. 4–22)

"forme nouvelle de Prosauropode": Ellenberger and Ellenberger, 1956a: 100.

"Prosauropode quadrupède (voisin de *Melanorosaurus* ou *Euskelosaurus*)": Ellenberger and Ellenberger, 1960: 236.

Euskelosaurus Huxley, 1866: Ellenberger et al., 1964: 326.

Melanosauridae indet: Charig et al., 1965: 201.

Euskelosaurus browni Huxley, 1866: Ellenberger and Ginsburg, 1966: 1944.

Thotobolosaurus mabeatae Ellenberger, 1970, nomen nudum: Ellenberger, 1970: 345.

Euskelosaurus Huxley, 1866: Gauffre, 1993: 147.

Kholumolumosaurus ellenbergerorum Gauffre, 1996, nomen nudum: Gauffre, 1996: 3.

Euskelosaurus Huxley, 1866: de Ricqlès et al., 2003: 72.

Plateosauridae indet.: Knoll, 2004: 79.

"Bloem Dino": McPhee et al., 2014: 157.

"Maphutseng dinosaur": Peyre de Fabrègues and Allain, 2016: 2.

Etymology—In honor of the brothers Ellenberger, Paul and François, who discovered the Maphutseng deposit, and have done a tremendous amount for Lesotho, particularly in terms of paleontology and geology.

Holotype—MNHN.F.LES381m. A right complete tibia (Fig. 20). We consider that all the specimens from the bone bed are congeneric and conspecific, but all the skeletons being disarticulated, we designate this bone because of its diagnostic features. The rest of the material is relegated to the status of paratype.

Paratypes and referred material—The bones from multiple individuals figured herein are considered as paratypes: an incomplete left postorbital (MNHN.F.LES153); an incomplete right postorbital (MNHN.F.LES54); a posterior cervical vertebra (MNHN.F.LES169); an incomplete anterior dorsal neural arch (MNHN.F.LES397); an incomplete middle dorsal vertebra (MNHN.F.LES32); a sacral vertebra (MNHN.F.LES155); two incomplete anterior caudal vertebrae (MNHN.F.LES168, 376); a left scapula (MNHN.F.LES386) ; a left humerus (MNHN.F.LES379); a right ulna (MNHN.F.LES159); a right radius (MNHN.F.LES147); a right metacarpal I (MNHN.F.LES26); a left metacarpal II (MNHN.F.LES92); a right metacarpal III (MNHN.F.LES93); an incomplete right metacarpal IV (MNHN.F.LES76); a left phalanx I-1 (MNHN.F.LES29); a right ilium

(MNHN.F.LES375a); a left pubis (MNHN.F.LES378); an incomplete left ischium (MNHN.F.LES152); a right femur (MNHN.F.LES394); a right fibula (MNHN.F.LES374); a left metatarsal I (MNHN.F.LES89); a left metatarsal II (MNHN.F.LES81); a left metatarsal III (MNHN.F.LES82); a left metatarsal V (MNHN.F.LES77).

The rest of the material housed in the MNHN is referred to *Kholumolumo ellenbergerorum*, as well as the Maphutseng remains stored in the University of Cape Town. A complete list of the material stored in Paris is available in supplementary data (Supplementary Data Table 1S).

Type locality—Maphutseng, Mohale's Hoek District, Lesotho (Fig. 3).

Type horizon—Lower Elliot Formation, Upper Triassic.

Diagnosis—A basal sauropodomorph with the following unique combination of characters on the holotype: very short and stout tibia (circumference/length ratio = 53%. All the other basal sauropodomorphs have ratios < 49%, except Antetonitrus and Blikanasaurus) with a diaphysis becoming finer distally in lateral and medial views and showing straight anterior and posterior margins, unlike in Antetonitrus. By contrast with Blikanasaurus, fourth metatarsal elongated relatively to the tibia and with a proximal extremity larger transversely and less extended anteroposteriorly. Diagnostic characters of the paratype: posterior cervical vertebra particularly short and high with a centrum elongation of 1.2. On the anterior dorsal vertebra, base of the neural spine anterior to the anterior margin of the diapophysis in dorsal view. On the sacral vertebra, centrum very short anteroposteriorly, with an elongation (ratio of the ventral length of the centrum on its anterior height) of 0.7. On the scapula, two marked posterodorsal and anterodorsal ridges on the lateral surface of the blade.

Associated fauna—Two large teeth of a carnivore have also been collected. Referred to a theropod by Ellenberger (1970: 345), they most probably belong to a rauisuchian, given their size.

DESCRIPTION

Skull

Two postorbitals were found in the Maphutseng bone bed: a left one (MNHN.F.LES153) and a right one (MNHN.F.LES54), both incomplete. According to the marked size difference, they belong to two different specimens (Fig. 4).

The postorbital is stout and triradiate. There is no marked step between the anterior and posterior processes in lateral view, as in *Coloradisaurus*, *Melanorosaurus* or *Sarahsaurus*. However, the dorsal margin of the postorbital still appears concave in lateral and medial views. The anterior process of the postorbital is transversely wide. A part of the articular facet for the frontal is visible on its ventrolateral surface (Fig. 4A, C). The medial surface of the anterior process also bears a depression, which probably accommodated the parietal (Fig. 4B). The lateral surface of the process is strongly convex. A small depression on the dorsomedial portion of the anterior process is indicative of the extension of the supratemporal fossa on the postorbital. The anterior margin of the postorbital constitutes the posterodorsal margin of the orbit. In anterior view, it gets wider dorsally.

In lateral view, the ventral process of the postorbital is bent forward as in most basal sauropodomorphs (Fig. 4A-B). In some genera however, the ventral process is straighter. It is the case in *Anchisaurus* or *Jingshanosaurus*. The transverse thickness of the ventral process equals 60% of its anteroposterior width. The posterior process of the postorbital is much thinner than the two other processes, both in lateral and dorsal views. The preserved part of the posterior process does not taper distally. Unlike the ventral process, the posterior process is straight and rod-like, with slightly dorsoventrally convex lateral surface (Fig. 4C-D). In some basal sauropodomorphs, such as *Melanorosaurus*, *Xixiposaurus* and *Yunnanosaurus*, the posterior process is not straight in dorsal view, but laterally convex.

Cervical Vertebrae

Middle Cervical Vertebrae (MNHN.F.LES338 & MNHN.F.LES342)—Two incomplete middle cervical vertebrae were found in Maphutseng. Both vertebrae consist in a damaged and incomplete centrum. The lowest and most elongated one (LES342) is more complete than the other (LES338). LES342 was probably slightly anterior to LES338 in the cervical series.

The centra are amphicoelous, as well as acamerate. LES342 has been transversely compressed: its centrum elongation (ratio of the ventral length of the centrum on its anterior height) is of 2.4 (Table 3) but was probably closer to 2.7 given the compression (2.7 is the average Elongation Index: aEI as described in Chure et al., 2010). In anterior view, the transverse compression is well visible on both centra. In LES338, the anterior articular surface appears 1.2 times higher than wide. In LES342, it is 1.3 times higher than wide (Table 3). In ventral view, a keel is visible on both centra as in many other basal sauropodomorphs. It is absent in some other genera like *Coloradisaurus, Riojasaurus* or *Yunnanosaurus*. In lateral view, the ventral border of both centra is concave. Their lateral surface appears slightly concave dorsally. It bears the parapophysis, which is located in the anterior third of the centrum, closer to the ventral margin than to the neurocentral suture. The parapophysis on LES338 is poorly developed and oval.

On LES342, the diapophysis is not much developed, subtriangular and oriented lateroventrally. It is situated in the anterior half of the centrum.

Given the length of the centrum, the position of the diapophysis and parapophysis, and compared to *Adeopapposaurus* and *Plateosaurus,* both vertebrae are considered to be part of the middle cervical series.

Posterior Cervical Vertebra (C10?) (MNHN.F.LES169)—One complete cervical vertebra was found on the Maphutseng site (Fig. 5). The only missing parts of the bone are the distal extremities of the postzygapophyses. The centrum is both amphicoelous and

acamerate and the neural arch displays low laminae. The centrum elongation (ratio of the ventral length of the centrum on its anterior height) is of 1.2 (Table 3): that is much inferior to the ratio of the middle cervical vertebra MNHN.F.LES342. These proportions are not observed in many posterior cervical vertebrae of basal sauropodomorphs, as most of them have very elongated and low cervicals. Some of the few other genera to present posterior cervical vertebrae with high articulation surfaces compared to their length are *Plateosaurus*, *Riojasaurus* and *Ruehleia*. However, as in the middle cervical vertebrae, the centrum articular surfaces are slightly higher than wide (Table 3). In ventral view, the cervical vertebra displays a marked median constriction and a ventral keel, of which the distal border is eroded. The ventral keel extends on all the length of the centrum (Fig. 5F). This morphology is similar to that observed in most basal sauropodomorphs, as in *Massospondylus*, even though in some genera such as *Plateosaurus* or *Riojasaurus*, the ventral surface of the cervical vertebrae is flat until the C9.

In lateral view, the ventral border of the vertebra is strongly concave. As it is the case in C9 and C10 of most basal sauropodomorphs, a hypapophysis is visible on the anteroventral part of the centrum, in the axis of the ventral keel. The lateral surfaces of the vertebra are slightly excavated and display the parapophysis in the anterior third of the centrum, centered between the ventral margin and the neurocentral suture. The right parapophysis is broken, but the left one is complete (Fig. 5A-B). They are rather developed dorsoventrally and form a well-developed tuber on the surface of the centrum. The dorsal portion of the parapophysis is the most extended laterally. More ventrally, the parapophysis gets lower and merges gradually in the centrum surface. The contact surface with the capitulum is oriented laterally to lateroventrally.

The diapophysis are developed, subrectangular and oriented lateroventrally (Fig. 5C-D). In ventral view, the anterocentrodiapophyseal and posterocentrodiapophyseal laminae are

visible. They are short and concealed by the diapophysis. The prezygodiapophyseal lamina is well-marked on the right size of the vertebra. The postzygodiapophyseal lamina is visible on the left side of the cervical vertebra. The prezygapophyses are still in articulation with the postzygapophyses and the hyposphene of the preceding vertebra. They are short, rounded and anteriorly projected. Their articular surface is oriented dorsomedially and seem to be flat. There is no visible intraprezygapophyseal lamina, whereas posterior cervical vertebrae of *Adeopapposaurus*, *Plateosaurus*, *Ruehleia* or *Massospondylus* bear this lamina. The ventral surface of the prezygapophyses is planar to slightly convex and connected to the centrum through the centroprezygapophyseal lamina. The postzygapophyses of the preceding vertebra project posteriorly with a lateral component in dorsal view. They are elongated, stout and bear an extensive planar to slightly concave articular surface directed ventrolaterally. The position of the postzygapophyses and the presence of a protuberant hyposphene make it unlikely the presence of an intrapostzygapophyseal lamina. Although broken, the postzygapophyses extended beyond the posterior margin of the centrum. In posterior view, the centropostzygapophyseal laminae are well visible. The dorsal surface of the postzygapophyses bears an epipophysis, which seems to extend on most of their length. The epipophyses are low and merged with the postzygapophyses on all their length, without well-delimited medial or lateral borders. The dorsal surface of the postzygapophyses of the preceding vertebra bears a spinopostzygapophyseal lamina coming into contact with the lateral margins of the neural spine. This lamina is also observed on the posterior cervicals of *Adeopapposaurus*, *Mussaurus* and *Ruehleia*. The neural spine is almost as long as wide in dorsal view and appears globulous and subcircular (Fig. 5E). In lateral view, a small posterior projection of its posterodorsal corner is visible. The anterior margin of the neural spine is convex, the dorsal margin is straight to slightly convex and the posterior one is concave. In anterior and posterior views, the neural spine shows a slight distal expansion.

The position of the parapophysis, at mid-height of the centrum, the presence of a hypapophysis, and the distance between the diapophysis and the postzygapophysis in lateral view allow to identify this element as a cervical vertebra. The height of the vertebra, the elongation of the centrum, the strongly concave ventral margin, the central rather than ventral position of the parapophysis, the shape of the diapophysis, the presence of the prezygodiapophyseal and postzygodiapophyseal laminae and the shape of the neural spine allow to identify the vertebra as a posterior cervical, most likely a C10.

Dorsal Vertebrae

Anterior Dorsal (D1?) Neural Arch [MNHN.F.LES397]— The neural arch is well-preserved and not deformed at all. The left postzygapophysis and the neural spine are broken at their base, but all the remaining anatomical structures are complete (Fig. 6; Table 3). No parapophysis, complete or partial, is visible in lateral view (Fig. 6B). It means that it was located on the centrum and that we deal with an anterior dorsal vertebra. No beginning of prezygoparapophyseal laminae (prpl) is visible near the prezygapophysis. The diapophyses are not much developed relatively to what is observed in other taxa such as *Plateosaurus* or *Ruehleia*. They are longer anteroposteriorly than large transversely. The left diapophysis is the most complete. In dorsal view, it is subrectangular. The diapophyses project laterally with a small posterior component in dorsal view. In anterior and posterior views, they are oriented slightly ventrally (Fig. 6C-D). In lateral view, their extremity has a subtriangular shape. The diapophyses are supported by four laminae (acdl or ppdl, pcdl, prdl and podl), delimiting four associated fossae. On the lateral surface of the neural arch, ventrally to the diapophyses, a vertical lamina, which was probably extending on the centrum of the vertebra, is visible in anterior view. Given that the parapophysis cannot be observed, this lamina could be an anterocentrodiapophyseal (acdl) or a paradiapophyseal lamina (ppdl). Anteriorly and

posteriorly to the diapophysis, the prezygodiapophyseal (prdl) and postzygodiapophyseal (podl) laminae are visible. The postzygodiapophyseal lamina (podl) is interrupted at the level of the hyposphen ("stranded lamina", Wilson, 2012). This interruption is observed in some basal sauropodomorph taxa, including *Ruehleia*. In the latter, it occurs on the posterior cervicals. *Kholumolumo* is apparently the only one in which this lamina is visible on an anterior dorsal. On the posterior margin of the diapophysis, the postzygodiapophyseal lamina (podl) defines, with the posterocentrodiapophyseal lamina (pcdl), a postzygapophyseal centrodiapophyseal fossa (pocdf). In dorsal view, the postzygapophyses project more laterally than the prezygapophyses relatively to the longitudinal axis of the vertebra.

The prezygapophyses project anteriorly in dorsal and lateral views (Fig. 6A). In dorsal view, they are rather short and have a rounded extremity. They present flat dorsal articular surfaces which are dorsomedially oriented. The prezygapophyses are not interconnected by an intraprezygapophyseal lamina (tprl), conversely to what is observed on the first dorsal vertebra of *Massospondylus*, *Plateosaurus* or *Ruehleia*. In anterior view, the centroprezygapophyseal lamina (cprl) is well visible on each side of the vertebra. With the prezygodiapophyseal lamina (prdl) and the anterocentrodiapophyseal (acdl) or paradiapophyseal lamina (ppdl), it defines a deep prezygapophyseal centrodiapophyseal fossa (prcdf). No spinoprezygapophyseal lamina (sprl) is visible. The right postzygapophysis is the only one preserved. It is located very high on the neural arch, thus the dorsoventral distance between the postzygapophysis and the diapophysis is important. However, the anteroposterior distance between these two structures is reduced in lateral view relatively to the posterior cervical vertebra described herein. The postzygapophysis project posterolaterally in dorsal view, with a significant lateral component contrary to *Plateosaurus*. In lateral view, its orientation is slightly dorsal. The articular ventral surface of the postzygapophysis is flat and ventrolaterally oriented. In dorsal view, the postzygapophysis is wider transversely than long

anteroposteriorly and thus appears short and stocky. There is no intrapostzygapophyseal lamina (tpol) visible, the small gap between the postzygapophyses being occupied by a developed hyposphene. In posterior view, the centropostzygapophyseal lamina (cpol) is present. In dorsal view, there is no visible epipophysis on the right postzygapophysis. On the anterior part of the dorsal surface of the postzygapophysis, the beginning of a spinopostzygapophyseal lamina (spol) is visible. The neural spine is broken at its base. The location of the base of the spine is unusual: it is anterior to the anterior margin of the diapophysis (Fig. 6A). On the anterior dorsal vertebrae of *Plateosaurus* or *Ruehleia*, the base of the spine is located at the same level as the middle of the diapophysis or between the middle and the posterior margin of the diapophysis. The neural spine seems to be anteroposteriorly very short relatively to the length of the neural arch. In many basal sauropodomorphs, neural spines of anterior dorsal vertebrae display a reduced base and widen distally. However, the widening is usually transverse, and the anteroposterior length of the neural spine is more or less steady from the base to the top, as it is observed in *Plateosaurus* or *Ruehleia*.

The development of the diapophyses, and particularly the absence of epipophysis on the postzygapophysis, show that we do not deal with a cervical vertebra. The absence of parapophysis on the neural arch show that this is an anterior dorsal. Based on the location of the parapophyses on the dorsal series of *Plateosaurus*, this vertebra is located between D1 and D5. Given the development of the diapophyses (especially compared to that of the posterior cervical vertebra MNHN.F.LES169, which is quite similar), the thick anterocentrodiapophyseal (acdl) and posterocentrodiapophyseal (pcdl) laminae, and the absence of intraprezygapophyseal laminae (tprl), the neural arch probably comes from one of the first dorsals, much likely a D1.

Anterior Dorsal (D2-3?) Centrum [MNHN.F.LES172]—One centrum from an anterior dorsal vertebra was found in the collected material. It fits well, in size and morphology, with the anterior dorsal neural arch described above (MNHN.F.LES397), and is thus probably from a very close vertebra. The centrum is slightly transversely compressed and deformed, this is particularly visible in anterior and posterior views. It is both amphicoelous and acamerate and the visible laminae are low. The centrum elongation ratio is of 1, the ventral length of the centrum being roughly equal to its anterior height (Table 3). In anterior and posterior views, the articular surfaces are 1.3 times higher than wide, like for the other vertebrae (Table 3). In ventral view, the centrum displays a marked median constriction and a ventral keel. The ventral keel, of which the distal border is broken, extends throughout the length of the centrum. This morphology is similar to that observed in most basal sauropodomorphs with complete dorsal series. In *Massospondylus*, the keel is present on the entire length of the centrum only in D1 and D2.

In lateral view, the ventral border of the vertebra is slightly concave. We can infer the presence of a hypapophysis following the ventral keel on the anteroventral part of the centrum, even though the area is eroded. The lateral surfaces of the vertebra are slightly excavated. They bear the parapophyses, which are located closer to the middle of the vertebra than to its anterior border. Dorsoventrally, the parapophysis is situated on the dorsal half of the centrum, overlying the neurocentral suture. The parapophysis is oval, almost three times longer dorsoventrally than anteroposteriorly. It has a rough surface and forms an important protrusion on the surface of the centrum. Laterally, the parapophysis protrudes on approximately 1 cm.

The proportions of the centrum and the high position of the parapophysis suggest a dorsal vertebra. The position and shape of the parapophysis combined with the presence of a ventral keel permit to identify this element as an anterior dorsal vertebra. The parapophysis overlying

the neurocentral suture and the thickness of the anterocentrodiapophyseal (acdl) and posterocentrodiapophyseal (pcdl) laminae, which are thinner than in the anterior dorsal neural arch MNHN.F.LES397, allow us to think that this centrum belongs to a D2 or D3.

Posterior Dorsal (D8-12?) [MNHN.F.LES32]—Overall, this vertebra is badly preserved. The postzygapophyses, neural spine, as well as some structures from the right side, are missing. The anterior surface of the centrum is substantially broken and eroded. Conversely, its posterior surface is almost complete. The neural arch is very eroded on its lower part. On the left side, the diapophysis is broken and the parapophysis is not visible any more. The whole of the vertebra has undergone a transverse compression (Fig. 7), as evidenced by the articular surfaces of the centrum 1.5 higher than wide, when the ratio should be more of 1.2 as in all the other vertebrae (Table 3).

The posterior articular surface of the centrum is concave (Fig. 7C). The lateral surfaces show a slight dorsal concavity. The centrum elongation (ratio of the ventral length of the centrum on its anterior height) is of 1.2. Given the observed deformation, the real ratio (aEI) was probably closer to 1.5. These values are slightly superior to the ratio of 1 observed on the anterior dorsal MNHN.F.LES172, but clearly inferior to the 2.4 ratio of the middle cervical vertebra MNHN.F.LES342 (Table 3). In ventral view, the centrum shows a median constriction. Its ventral surface is flat and does not exhibit a keel. Even though the anterior part of the centrum is partially broken, it does not seem to present a hypapophysis. In lateral view, the ventral margin of the centrum is concave.

The separation between the centrum and the neural arch is very clear. The neural arch shows marked but relatively thick laminae, typical of what is usually observed in basal sauropodomorphs. It is remarkably higher than the neural arch of the anterior dorsal MNHN.F.LES397 described above (Table 3). The parapophysis is located on the neural arch.

It is visible on the right side of the neural arch, but much damaged on the left side. It is situated at mid-height on the anterior part of the neural arch (Fig. 7A). It is large and suboval in shape, even though its ventral region is abraded and not much more visible. The long axis of the parapophysis is oblique relatively to the longitudinal axis of the vertebra. On the right side of the vertebra, the parapodiapophyseal lamina (ppdl) can be clearly distinguished. The bone surface being much damaged under the parapophysis and on the anterodorsal part of the centrum, it is impossible to determine if there is an anterocentroparapophyseal lamina (acpl). The right diapophysis is the only one to be preserved. It is high on the neural arch and projects posterodorsally in lateral view. It is not much developed, and the distal extremity is broken, making it impossible to appreciate the total extension of the diapophysis. Without a distal extremity, it appears subrectangular in dorsal view and projects strictly laterally. The diapophysis is surrounded, ventrally and anteriorly, by three laminae (prdl, ppdl and pcdl). Anteriorly, the prezygodiapophyseal lamina (prdl) is well developed. It borders dorsally the prezygapophyseal centrodiapophyseal fossa (prcdf). The parapodiapophyseal lamina (ppdl) extends over 45 mm between the diapophysis and the parapophysis. It replaces the anterocentrodiapophyseal lamina (acdl), which is absent because of the high position of the parapophysis. A posterocentrodiapophyseal lamina (pcdl) connects the diapophysis to the posterior part of the centrum. The ventral part of this lamina is not visible, because it is located on the damaged part of the neural arch and centrum. A shallow centrodiapophyseal fossa (cdf) is present between the posterocentrodiapophyseal lamina (pcdl) and the parapodiapophyseal lamina (ppdl). Posteromedially to the posterocentrodiapophyseal lamina (pcdl), a deep postzygapophyseal centrodiapophyseal fossa (pocdf) is visible in lateral and posterior views. In posterior view, the beginning of a postzygodiapophyseal lamina (podl) seems to be present on the posterior margin of the diapophysis. However, in the absence of postzygapophyses, we cannot attest to the presence of this lamina. The prezygapophyses are

elongated and project strictly anteriorly in dorsal view. In lateral view, their orientation shows a dorsal component. Their dorsal articular surface is flat and oriented dorsally with a slight medial component. The prezygapophyses are not interconnected by an intraprezygapophyseal lamina. The anterior part of the neural arch being damaged and poorly prepared, we cannot state with certainty that centroprezygapophyseal laminae (cprl) extend ventrally under the prezygapophyses, even if it appears to be the case. The dorsal surface of the neural arch is relatively well-preserved, despite the absence of neural spine, and does not bear a spinoprezygapophyseal lamina (sprl). The postzygapophyses were not preserved. However, a stout and well-developed hyposphene is visible above the neural canal in posterior view. In height, the hyposphene equals 25% of the total height of the neural arch without the neural spine. The neural spine is broken at its base. The missing parts and the plaster added on the dorsal surface of the neural arch prevent from locating the zone where the base of the neural spine was situated.

The position of the parapophysis on the neural arch and the height of the transverse process demonstrate that we deal with a dorsal vertebra. The height of the parapophysis on the neural arch, above the neurocentral suture, shows that it is a middle or posterior dorsal vertebra. However, it cannot be one of the last two dorsals given that the parapophysis and the diapophysis are well separated from each other. By comparing with the position of the parapophysis in other basal sauropodomorphs, we can situate this vertebra between D7 and D12.

Sacral Vertebra

Primordial Sacral 2? [MNHN.F.LES155]—The sacral vertebra is almost complete, without deformation, and its bone surface is relatively well-preserved. The anterior surface of the centrum and neural spine are eroded in some places and the prezygapophyses are missing

(Fig. 8). This can be explained by the fact that another sacral vertebra was probably articulated and partially fused anteriorly to this one. As a rule, prosauropod dinosaurs possess two primordial sacral vertebrae associated with a dorsosacral and/or a caudosacral, depending on the considered taxa (Galton, 1999; Galton and Upchurch, 2004). Because of their limited number and their contribution to the sacrum, sacral vertebrae usually have quite distinct morphologies from one another.

This sacral vertebra is stout, large and its centrum height equals approximately 60% of the neural arch height (Table 3). The sacral ribs, projecting on each side of the vertebra, are meant to meet the ilium (Fig. 8A). The centrum is very short anteroposteriorly, its elongation (ratio of the ventral length of the centrum on its anterior height) is of 0.7 (Table 3), that is inferior to that of the posterior cervical vertebra and dorsal vertebrae (ratios between 1 and 1.2) and much inferior the elongation ratio of the middle cervical vertebra (2.4). This stocky morphology is unusual among basal sauropodomorphs given that numerous taxa like *Adeopapposaurus* (1.5), *Leonerasaurus* (1.6) or *Plateosaurus* (exact ratio unknown) have sacral vertebrae with much higher elongation ratios. The anterior articular surface of the centrum is 1.3 times higher than wide, as in most other vertebrae. In ventral view, the centrum has a quite odd morphology, its anterior width equals 60% of its posterior width (Table 3). The state of preservation of the anterior part of the vertebra must have an impact on this difference, but probably an insignificant one, given that the bone surface is visible in some places. This width variation is quite representative of the sacral vertebrae of some sauropods like *Apatosaurus*, but is not observed in *Adeopapposaurus*, *Massospondylus* or *Plateosaurus*. The centrum shows a median constriction and its ventral surface is flat. It is circular in posterior view, the height and the width of the posterior articular surface being almost identical (Table 3), and its posterior surface is concave. In lateral view, the ventral margin of the centrum is concave and its posterior border

projects more ventrally than its anterior one. The lateral surface is slightly concave and partially covered by the rib, which occupies the dorsal third of its height.

The neural arch is anteroposteriorly short and located on the anterior two thirds of the centrum. On the neural arch, the diapophyses are developed and subrectangular. They are merged with the ribs and, taken together, their transverse width is much superior to the anteroposterior length of the diapophyses at their base. In posterior view, a small bulge visible on the dorsal surface of the fused diapophyses and ribs corresponds to the location where they are merging. Anteroposteriorly, each diapophysis occupies the entire length of the neural arch. In dorsal view, the length of the diapophyses decreases distally. The point where it is thinner seems to match the location where it merges with the sacral rib. The anteroposterior extension of the sacral rib is increasing towards its distal extremity. Despite this, there is no marked constriction between the diapophysis and the sacral rib in dorsal view (Fig. 8C). The fused diapophysis and rib show concave anterior and posterior margins and project laterally with a small posterior component. The shape and the direction of the process and rib in dorsal view resemble what is observed on the second primordial sacral of *Lufengosaurus* and *Mussaurus*. In posterior view, the rib exhibits a marked ventral depression, of which the dorsal margin is situated at the level of the neural canal and extending until the ventral border of the sacral rib. The lateral margin of the fused diapophysis and rib is concave. In lateral view, the extremity of the rib has a subrectangular shape and an oblique main axis (Fig. 8B). It extends on more than 100 mm dorsoventrally, that is approximately two thirds of the height of the centrum. The dorsal part of the rib is more extended anteroposteriorly than its ventral extremity. The articular facet for the ilium is simple. In lateral view, the dorsal border of the sacral rib is slightly convex, its anterior and posterior margins are concave, and its ventral border appears to be flat to slightly concave. The biconcavity (anterior and posterior) is mentioned by Pol et al. (2011) as being representative of the first primordial sacral among

sauropodomorphs. However, the shape and dorsoventral extension of the contact area with the ilium are inconsistent with what is observed on the first primordial sacral of *Leonerasaurus* or *Riojasaurus*. Moreover, the shape of the anteroventral margin of the rib and the state of preservation of the anterior surface of the sacral vertebra and rib clearly indicate that they were fused with the previous vertebra. It then cannot be the first primordial sacral. By comparing the shape of the contact area for the ilium with those visible on the sacral vertebrae of *Adeopapposaurus*, *Leonerasaurus*, *Mussaurus* or *Riojasaurus*, it appears that we are closer to the second primordial sacral. Among these three taxa, *Riojasaurus* is the one where the shape and the orientation of the contact area for the ilium best match what is observed on the Maphutseng specimen. The prezygapophyses of the sacral vertebra are, unfortunately, not preserved. The postzygapophyses are short, not extended transversely and project posterolaterally in dorsal view. Their ventral articular surfaces are flat and ventrolaterally oriented. The postzygapophyses arise from the base of the neural spine posterior margin and flush with the latter. They are separated by an interpostzygapophyseal notch. Underneath the postzygapophyses there is a large hyposphene, which is approximately the same height as the neural canal. The neural canal is circular. The neural spine is quite high and located anterior to the sacral vertebra centrum. In lateral view, the neural spine is clearly higher than anteroposteriorly long (its length equals 42% of its height) and shows a constant length (Table 3; Fig. 8). Its proportions remind those of the sacrum neural spines of *Plateosaurus*, most of the other sauropodomorph taxa presenting neural spines usually anteroposteriorly longer with respect to their height. The neural spine is oriented posterodorsally, but not as dramatically as in *Adeopapposaurus* or *Plateosaurus*. Its anterior border is slightly convex, whereas its posterior border is concave. Its dorsal margin is posteriorly inclined. The distal extremity of the neural spine is oval in dorsal view. In posterior view, the lateral borders of the neural

spine are concave given that the proximal and distal extremities are slightly transversely extended compared with the median part of the neural spine.

Given the dorsoventral extension of the contact area for the ilium, the anterior surface of the vertebra which was probably fused with another one, the shape and the orientation of the fused diapophyses and ribs in dorsal view, and, considering that the majority of basal sauropodomorphs have three to four sacral vertebrae, including two primordial sacrals, we suggest this vertebra to be identified as a second primordial sacral.

Caudal Vertebrae

Anterior Caudal (Ca1-Ca5) [MNHN.F.LES168]—The first caudal from Maphutseng is damaged, but does not appear to have undergone important deformation. The posterior surface of the centrum is complete, but its anterior surface is quite incomplete, particularly on the borders. The largest missing parts are located at the base of the neural arch, for that reason the centropostzygapophyseal ridges were replaced by plaster, and on the lateral sides of the vertebra, where the transverse processes are absent. The left prezygapophysis and postzygapophysis are broken, those from the right side are in part reinforced with plaster, but complete. The neural spine is complete (Fig. 9).

The centrum is very high and short, as it is the case on the anterior caudal vertebrae of some basal sauropodomorph taxa like *Aardonyx*, *Lufengosaurus* or *Melanorosaurus* (NM QR1551). Its aEI equals 0.56 (Table 3), that is to say well inferior to what has been measured on all the preceding vertebrae, including the sacral vertebra. In posterior view, the centrum articular surface is overhung by a matrix residue. The latter could give the impression that the centrum shows a dorsal protuberance, but it is not the case and the centrum is, in reality, circular. The posterior articular surface of the centrum is concave (Fig. 9B). Similarly, its lateral surfaces show a slight dorsal concavity. In lateral view, the ventral margin of the centrum is strongly

concave (Fig. 9A). In ventral view, the centrum shows a marked median constriction, not located on a central point as it is the case on the posterior cervical (MNHN.F.LES169), but on the entire length of the centrum, apart from the anterior and posterior borders. The ventral surface of the centrum is smooth and does not bear a longitudinal groove as in *Adeopapposaurus*, *Eoraptor* or *Riojasaurus*. This groove is observed on the anterior caudal vertebrae of several basal sauropodomorphs, but usually appears after a few vertebrae on the caudal series (for instance, in *Plateosaurus*, it is well visible from the Ca6).

The neural arch is badly preserved. Laterally to the neural canal, a small part of the base of the neural arch is still in place on both sides. It is difficult to judge the anteroposterior extension of the neural arch, given that the posterior borders are broken, but it seems to be quite short, as an extension of the centrum. The neural arch is very high, almost as high as the one of the sacral vertebra MNHN.F.LES155 (260 and 265 mm, respectively). The transverse processes are missing. The right prezygapophysis of the vertebra, the only one preserved, is projecting strictly anteriorly. It is relatively long in comparison to the anteroposterior extension of the vertebra, but is not mounted on high pedicels. It has got a rounded shape in dorsal view and a subtriangular one in lateral view (Fig. 9A). The dorsal articular surface of the prezygapophysis is flat and oriented strictly dorsally. In dorsal view, an interprezygapophyseal notch is visible. The right postzygapophysis is the only one preserved. It projects strictly posteriorly in lateral view. It is robust, rounded in dorsal view and coupled over its entire height to the posterior margin of the neural spine. The spinopostzygapophyseal lamina is broken, but apparently exceeded the mid-height of the neural spine. The ventral articular surface of the postzygapophysis is flat to slightly concave and oriented ventrally to ventrolaterally (Fig. 9B). Judging by the remnants of the left postzygapophysis on the left side of the posterior surface of the neural spine, the postzygapophysis articular surfaces were probably very close to each other. The neural spine is complete, high and located at the same

level as the centrum on an anteroposterior axis. The anteroposterior length on the top of the neural spine equals 36% of its total height (Table 3). This length is constant on the entire height of the neural spine, if we do not take into account the postzygapophysis. Transversely, the neural spine is compressed and its width goes slightly increasing towards its distal extremity. In posterior view, the lateral margins of the neural spine are straight above the postzygapophyses. In lateral view, the vertebra neural spine is oriented strictly dorsally and not posterodorsally, as on the most posterior caudal vertebra. The distal extremity of the neural spine is convex, its anterior border is slightly convex and its posterior border, dorsally to the postzygapophysis, appears slightly concave. In dorsal view, the distal extremity of the neural spine is oval.

The proportions of this vertebra, the absence of laminae or fossae on the preserved parts of the neural arch and the height of the neural spine allow us to confirm that we deal with a caudal vertebra. Considering the proportions of the vertebra, including the very short centrum, the size of the vertebra, very close to the one of the sacral vertebra MNHN.F.LES155, the absence of posterodorsal projection on the neural spine and the fact that the pedicels of the prezygapophyses and postzygapophyses are almost non-existent, we identify this vertebra as a very anterior caudal (Ca1-Ca5).

Anterior Caudal (Ca5-Ca15) [MNHN.F.LES376]—This anterior caudal vertebra is well-preserved. On the neural arch, the left transverse process is broken at its extremity. The right transverse process is broken at its base. Both postzygapophyses are broken. However the prezygapophyses are complete, as well as the neural spine, in spite of some slight damages on the anterior and posterior margins (Fig. 10).

This caudal vertebra is clearly smaller than the other one (MNHN.F.LES168). Its height equals approximately 80% of the one described above (Table 3). Other differences were also found, like a more elongated centrum, much more developed pedicels bearing the

prezygapophyses and a posterodorsally projecting neural spine. It is unlikely that these two caudal vertebrae had belonged to the same individual, but we can affirm that this second vertebra was situated more posteriorly in the caudal series than the previous one. The caudal centrum is amphicoelous and its lateral surfaces are flat. The aEI is 0.91 that is superior to the ones of the sacral and the more anterior caudal vertebrae. The articular surfaces are oval, their long axis being dorsoventral. The width of the centrum equals approximately 85% of its height (Table 3). In lateral view, the ventral margin of the centrum is concave, but in a much less marked way than on the previous caudal vertebra (Fig. 10C). In ventral view, the centrum does not show a median constriction, but lateral borders are concave all the same. On the median area of the centrum, a slight longitudinal groove is visible (Fig. 10E).

The neural arch equals approximately 60% of the entire height of the vertebra (Table 3). The neural canal, visible in posterior view, is circular. The left transverse process is the only one to be partially preserved. Its base is quite wide dorsoventrally and extends slightly on the dorsal part of the centrum. The base quickly sharpens dorsoventrally, thus imparting a subtriangular shape to the transverse process in anterior and posterior views (Fig. 10A-B). In dorsal view, the transverse process is thin and seems to be subrectangular, even though it is not complete. It is projecting posterolaterally. On the caudal series of *Plateosaurus* or *Riojasaurus*, we can observe that the transverse processes oriented posterolaterally are usually situated on the most anterior caudal vertebrae. In *Riojasaurus*, for instance, the processes recover a strictly lateral orientation between Ca10 and Ca15. The prezygapophyses are located further from the median axis of the vertebra than the postzygapophyses (Fig. 10D). The prezygapophyses of the vertebra are projecting anteriorly with, in lateral view, a dorsal component. They are small, but seem to be mounted on pedicels, which was not the case on the previous caudal vertebra. They bear flat dorsal articular surfaces, which are dorsomedially oriented. The postzygapophyses are broken. As on the previous caudal vertebra, they arise

from the base of the neural spine, on the posterior margin of the latter (Fig. 10C). The neural spine is complete and projects posterodorsally. The angle of the main axis of the neural spine relatively to the longitudinal axis of the vertebra is sometimes fairly important from the first caudal vertebra. It is, for example, the case in *Lufengosaurus* or *Mussaurus*. In some other basal sauropodomorph taxa, the neural spine is not angled at all on the first caudals and switches to a more and more posterodorsal orientation along the anterior part of the caudal series. It is the case in the Maphutseng specimen, but also in *Melanorosaurus*. The neural spine is very high and located at the level of the posterior half of the centrum. The anteroposterior length of the top of the neural spine equals 35% of its total height, that is almost the same value as on the more anterior caudal vertebra (Table 3). In lateral view, the anteroposterior extension of the neural spine is constant along its entire height (Fig. 10C). In anterior or posterior view, the neural spine is transversely compressed. Its lateral borders are straight and its distal extremity, although eroded, appears to be slightly superior in width than the rest of the neural spine. In anterior or posterior view, the distal part of the neural spine is slightly deflected towards the right side of the vertebra, arguably because of breakages and fossilization process of the vertebra (Fig. 10A-B). In lateral view, the distal extremity of the neural spine is convex, but slightly eroded. The anterior margin of the neural spine is somewhat damaged, but seems straight, and its posterior margin is concave. In dorsal view, the top of the neural spine is clearly longer than wide and oval (Table 3, Fig. 10D).

The proportions of this vertebra, the absence of laminae or fossae on its neural arch, the height of the neural spine and the arrangement of the postzygapophyses help to conclude that we deal with a caudal vertebra. As already said, it is, without doubt, more posterior than the caudal vertebra MNHN.F.LES168. We deduce this mainly by looking at the elongation of the centrum, the position of the neural arch relatively to the latter, and the orientation of the neural spine. Considering the elongation of the centrum on this caudal vertebra, the presence

of a very light ventral longitudinal groove, the orientation of the transverse processes, the elongation of the prezygapophyses, and comparing with a few complete caudal series, it is most likely that we deal with an anterior caudal vertebra, probably located between Ca5 and Ca15.

Middle Caudal (Ca15-Ca25) [MNHN.F.LES177]—This middle caudal vertebra is particularly well-preserved. The centrum is subcomplete, having just a few fragments missing on the borders. It is the only middle caudal vertebra to have most of its neural arch preserved. On the latter, the right prezygapophysis is broken and the left postzygapophysis is missing. The neural spine is broken at its base. This vertebra shows a typical "middle caudal morphology", that is anteroposteriorly elongated and quite low in height.

The centrum is amphicoelous and its lateral surfaces are flat. The aEI is quite important, as it equals 1.5. One of the most anterior caudal vertebrae (MNHN.F.LES168) has the same anteroposterior length (90 mm), but a much superior width, and hence a 0.56 aEI. In anterior and posterior views, the articular surfaces are rounded, very slightly wider than high. The width of the centrum equals 113% of its height (Table 3). In lateral view, the ventral margin of the centrum is concave. In ventral view, the centrum shows a slight median constriction and, on its median area, a faint longitudinal groove is visible.

The neural canal, visible both in anterior and posterior views, is subcircular. The prezygapophyses are located further than the postzygapophyses relative to the median axis of the vertebra. The prezygapophyses are projecting anteriorly with a slight lateral component in dorsal view, and a dorsal component in lateral view. They are mounted on pedicels and quite small. Unfortunately, the articular surfaces are not preserved. The postzygapophyses are located at the base of the neural spine, on its posterior margin. The neural spine base is situated at the level of the last posterior quarter of the centrum. It appears transversely compressed.

The proportions and morphology of this vertebra, the absence of laminae or fossae on its neural arch, and the arrangement of the prezygapophyses and postzygapophyses allow to conclude that we deal with a caudal vertebra. Considering the proportions of the centrum on this caudal vertebra, the absence of transverse processes, the presence of a faint ventral longitudinal groove, and the location and shape of the zygapophyses, it is most likely that we deal with a middle caudal vertebra, probably located between Ca15 and Ca25.

Posterior Caudals (Ca25 and beyond) [MNHN.F.LES35&37]—These vertebrae are among the few well-preserved posterior caudals. For most of them, the centrum is the only preserved part and is often damaged. The centra of these two vertebrae are subcomplete, having just a few fragments missing on their extremities. It is practically the only posterior caudals in which a part of the neural arch is preserved. On MNHN.F.LES35, the lower part of the neural arch as well as the base of the postzygapophyses and neural spine are preserved. On MNHN.F.LES37, the anterior part of the neural arch is preserved, along with the right prezygapophysis. The following description is based on both vertebrae. Measurements are made on MNHN.F.LES35. These vertebrae exhibit a morphology close to that of the middle caudal vertebra, with an anteroposteriorly elongated and dorsoventrally low centrum.

The centrum is amphicoelous and its lateral surfaces are flat. The aEI is more important than in the middle caudal vertebra, as it equals 1.9. In anterior and posterior views, the articular surfaces are circular. On these surfaces, the width of the centrum equals approximately 100% of its height (Table 3). In lateral view, the ventral margin of the centrum is slightly concave. In ventral view, the centrum shows a slight median constriction. On its median area, a wide but shallow longitudinal groove is visible.

At the interface between the centrum and the neural arch, the neural canal is subcircular. The prezygapophyses are located more laterally than the postzygapophyses relative to the median axis of the vertebra. The prezygapophysis is projecting anteriorly with a slight lateral

component in dorsal view. In lateral view, it has a dorsal component. It is mounted on a short pedicel and terminated by an oval articular surface which is medially, and slightly dorsally, oriented. The postzygapophyses are located at the base of the neural spine. They are at the level of the last posterior quarter of the centrum.

The proportions and morphology of these vertebrae, the absence of laminae or fossae on their neural arch, and the unique morphology of the centrum, allow to conclude that we deal with caudal vertebrae. Considering the proportions of the centra, the absence of transverse processes, and the arrangement of the neural arches, it is most likely that we deal with posterior caudal vertebrae, probably located beyond Ca25.

Ribs and Chevrons

Ribs—No complete ribs could be reconstructed from the many rib sections found in the collected material. A single middle dorsal rib (MNHN.F.LES138) has been identified with confidence, based on the circular to triangular proximal cross section of the rib shaft, and on the well-differenciated tuberculum and capitulum. In articulation with its corresponding dorsal vertebra; this rib should have a posterolateral orientation.

Chevrons [MNHN.F.LES53]—Several isolated haemapophyses (chevrons), more or less complete, were recovered in Maphutseng. The description will focus on MNHN.F.LES53, which is the more complete and better-preserved element. The chevron is a robust Y-shaped bone. It is 320 mm long. Both its proximal and distal extremities are damaged and, all along the chevron, six fractures are visible, but the structure is nonetheless subcomplete.

The proximal extremity of the chevron consists of an eroded and partially broken arch. The arch is dorsally concave and corresponds to the articular surface for the caudal vertebrae. Beneath this surface is located the haemal canal. It has a pronounced oval shape, with a

dorsoventral long axis. More ventrally, the chevron sharpens distally and, therefore, appears V-shaped in anterior and posterior views. Transversely, the haemal spine is 2.6 times thicker proximally than at its distal end. Following the haemal canal, the anterior surface of the chevron bears a marked groove extending on the median axis of the bone for about one third of its entire length. On both sides, small ridges frame the longitudinal groove. The posterior surface of the haemal spine is flat beneath the haemal canal, but being more sharpened than the anterior surface, it exhibits a marked ridge on its distal half. In lateral view, the anterior and posterior margins of the chevron are subparallel. The thinnest part of the chevron is located at the level of the haemal canal. The haemal spine is anteroposteriorly more extended distally than proximally. Its distal extremity is about 1.7 wider than its proximal part. The distal extremity of the haemal spine is not entirely preserved, but its distal margin seems to be straight in lateral view.

We identify this chevron as a very proximal one (around the fourth and fifth caudal vertebrae or so), based on its size and global morphology, and on what is observed in *Plateosaurus* (Huene, 1926, Taf. III: Fig. 1).

Pectoral Girdle

Left Scapula [MNHN.F.LES386]—The scapula described hereinafter is considered with its long axis positioned vertically. Following this orientation, the contact surface with the coracoid is ventral, the acromion is on the anterior part of the scapula and the glenoid is posterior. We assume that, in vivo, the scapula was oriented obliquely with respect to the longitudinal axis of the animal, with the contact surface bearing the coracoid directed anteroventrally.

The scapula is almost complete, its distal extremity being the only part of the bone not fully preserved. The preserved dorsal and ventral margins present a relatively marked wear. The

bone surface of the scapula is damaged, and the bone exhibits multiple fractures, particularly on the blade. Nonetheless, the scapula does not show any deformation. It is not articulated with the coracoid (Fig. 11). The Maphutseng specimen scapula is quite short and stout, like the one of *Antetonitrus*. Its proximal extremity is clearly anteroposteriorly extended with respect to the blade. The distal extremity of the scapula seems to be widened too, but the lack of the distal part of the bone prevents the estimation of its anterior projection.

The distal part of the scapular blade is incomplete, but judging by the orientation of its anterior border, by the crack, it was fan-shaped, as in most basal sauropodomorph taxa (Remes, 2008:figs. 7-3). The posterodorsal corner of the scapula is incomplete too, but probably did not project behind the posteroventral corner.

The scapular blade represents 65% of the total length of the bone. In posterior view, the lateral margin of the blade is convex, and its medial margin is concave. In lateral view, the blade is straight, with distally concave and proximally subparallel anterior and posterior borders (Fig. 11A). Anteroposteriorly, the minimal width of the blade equals approximately 45% of the maximal anteroposterior extension of the proximal end of the scapula, and 24% of the dorsoventral length of the bone. Transversely, the blade is 40 mm wide at mid-length, that is 38% of the transverse width of the scapula at the level of the glenoid (Table 4). In transverse section, the blade has a suboval shape, with a slightly convex lateral margin and a flat medial margin. The lateral and medial surfaces of the blade merge to form anterior and posterior bulges. Besides this blunt edge, no real anterior and posterior surfaces are visible on the blade of the scapula. The lateral surface of the blade is smooth, apart from two small posterodorsal and anterodorsal ridges, which are extending on the distal part of the blade and which probably delimit the area of origin of the muscle *deltoideus scapularis* (Remes, 2008:figs.7-12) (Fig. 11A). The medial surface of the blade is flat and smooth. A blunt ridge, located on its posteroventral part, is poorly visible (Fig. 11B).

The proximal part of the scapula seems more extended anteroposteriorly than the distal part, even though it is impossible to declare with certainty. It equals half (53%) of the total length of the bone. In lateral view, the proximal extremity is subrectangular, its anteroposterior extension being clearly superior to its dorsoventral height. On the lateral surface of the proximal extremity, the acromion fossa extends for two thirds of the extremity length. The acromion fossa is anteroposteriorly longer than high, its height being of, approximately, 120 mm. It is a shallow fossa, with a marked anterior margin and a very light wrinkle outlining its anterodorsal border. The acromion is poorly developed anteroposteriorly, its extension (from the anterior border of the acromion to the anterior border of the scapular blade) equals 50% of the anteroposterior length of the blade (at mid-length). The height of the anterior margin of the acromion represents 19% of the entire length of the scapula (Table 4). The dorsal border of the acromion is oblique and extends from the anterior margin of the blade, following a gently slope, to merge with the anterior border of the acromion, without visible angle. In lateral view, the dorsal margin of the acromion is at approximately 40 ° to the main (dorsoventral) axis of the scapula. In lateral and medial views, the anterior border of the acromion is also slightly oblique. Its ventral extremity is a bit more anterior than its dorsal extremity (Fig. 11). In anterior view, the anterior margin of the acromion follows the anterior border of the scapula. The ventral part of the acromion is extremely thin transversely, it is the thinnest part of the bone. The glenoid is on the posterior border of the scapula proximal extremity. Conversely to the acromion, the glenoid is the largest part of the bone, transversely (Table 4). The glenoid cavity has a slightly coarse texture. The latter is particularly visible on the medial surface of the scapula, where the bone surface appears to be better preserved. In posterior view, the glenoid cavity is oval, dorsoventrally higher than transversely wide. In lateral view, the posterodorsal corner of the glenoid cavity is sharp and projects quite far posteriorly. A similar degree of projection is observed in *Antetonitrus*, *Lufengosaurus* or

Sefapanosaurus. On the ventral margin of the scapula, the contact area for the coracoid is sigmoid in lateral and medial views. In *Kholumolumo*, we also observe a rounded projection, located anteroventrally with respect to the glenoid, on the ventral border of the scapula (Fig. 11). This structure is also visible, although less pronounced, in *Antetonitrus*.

Anterior Member

Left Humerus [MNHN.F.LES379]—The left humerus is complete and well-preserved. It does not exhibit any distortion and the bone surface is relatively well-preserved, aside from the more abraded proximal and distal extremities. The proximolateral margin of the humerus and its distolateral corner are incomplete. On the posterior surface of the bone, the bone surface is cracked and slightly depressed in some places. The humerus also shows several fissures on its diaphysis (Fig. 12). The humerus is 685 mm long and is not particularly robust for its size. The deltopectoral crest has a limited anterior projection. The proximal and distal extremities are clearly extended with respect to the diaphysis, giving the humerus an hourglass shape in anterior and posterior views (Table 5). The proximal half of the humerus has been rotated of approximately 30 ° clockwise relative to its distal half.

The proximal part of the humerus has a concave anterior surface and a relatively flat posterior surface, with light lateral and medial concavities. The head of the humerus is thick and shows a convex dorsal margin (Fig. 12A-D). It bears a strong bulge anteroposteriorly thicker than the rest of the proximal articular surface. On this bulge, the bone surface is rough. In proximal view, the thickest part of the humeral head is located on its medial half. The lateral third of the humeral head is two to three times thinner than its medial part. In proximal view, the anterior margin of the humerus is flat to slightly concave, whereas its posterior margin is convex (Fig. 12E). The deltopectoral crest arises from the lateral border of the humerus. It extends anteriorly on approximately 5 cm and is projecting at nearly 90 ° of the anterior

surface of the humerus in proximal view. In anterior view, the main axis of the deltopectoral crest is oriented strictly dorsoventrally. The length of the deltopectoral crest (measured from the dorsalmost point in its alignment) equals 48% of the total length of the humerus. The distal margin of the deltopectoral crest bears a coarse bulge which appears straight in anterior view (Fig. 12A). In lateral view, the distal border of the deltopectoral crest is convex. The crest arises very gradually from the proximal end of the humerus. Proximally, the crest reaches a plateau, after a few centimeters, where its distal margin becomes straight in lateral or medial view. Distally, the deltopectoral crest ends quite abruptly at the level of the diaphysis. In lateral view, the distal dorsoventral axis of the crest is at approximately 130 ° of its ventral margin merging with the diaphysis (Fig. 12B).

The humerus diaphysis is not much extended with respect to the entire length of the bone. It is relatively thin; its transverse width equals approximately 30% of the maximum proximal extension of the humerus and 40% of the distal one. In anterior and posterior views, the medial and lateral borders of the diaphysis are both concave (Fig. 12A, C). In lateral and medial views, the anterior and posterior borders of the diaphysis are curved and subparallels, the anterior being concave and the posterior convex (Fig. 12B, D). In transverse section, the diaphysis is subcircular.

In posterior view, the distal half of the humerus is subtriangular. It is transversely extended, and its transverse width equals approximately 70% of the proximal width (Table 5). The ventral margin of the distal extremity is slightly concave in anterior and posterior views. The anterior surface of the distal extremity exhibits a well-marked median cuboid fossa (Fig. 12A). The posterior surface is also concave on its median part because of the presence of the olecranon fossa, but this fossa is still shallower than the cuboid fossa (Fig. 12C). The distal condyles of the humerus are preserved, but their posterior surface is abraded. In anterior view, the condyles appear poorly developed, as it is usually the case in prosauropod dinosaurs. The

anteroposterior thickness of the distal medial condyle is very close to the anteroposterior thickness of the proximal end of the humerus (Table 5). In distal view, the cuboid and olecranon fossae are well visible and demarcate, on both sides, the ovoid condyles. There is a small lack on the posteroventral part of the lateral condyle. Despite this lack, the ulnar (lateral) condyle seems to be a little more extended transversely than the radial (medial) condyle (Fig. 12F).

Right Ulna [MNHN.F.LES159]—The right, complete, *Kholumolumo* ulna is well-preserved. The only small missing part of the bone is located anteriorly, on the distal extremity. The proximal and distal articular surfaces of the ulna are complete, even though a bit abraded. The bone surface is, for the most part, rather well-preserved. The surface layer of the bone is still removed in some small patches on the lateral surface of the ulna. The bone shows multiple fractures on the entire length of the diaphysis (Fig. 13). For the following description, the ulna is positioned with the long axis of its distal extremity horizontal and oriented anteroposteriorly. The radial fossa is oriented anteriorly to anterolaterally and the two processes surrounding it are projecting anterolaterally and anteromedially.

The maximum length of the ulna is 390 mm (Table 5). The Maphutseng bone bed having delivered rests from several disarticulated specimens, it is not possible to associate this ulna to a particular humerus and, therefore, to calculate a length ratio. The ulna is a robust bone, with proximal and distal extremities extended both anteroposteriorly and transversely with respect to the diaphysis, the proximal extremity being more extended than the distal one (Table 5). The main axes of the extremities of the ulna are not parallel, but oriented following an angle of approximately 40 °. The ulna has a morphology very similar to that of the other basal sauropodomorphs, but appears less stout than some forms, like *Antetonitrus*, in which the ulna is shorter and stockier. The anteroposterior extension of the proximal extremity of the ulna equals 36% of the total length of the bone. In proximal view, the articular surface has a

subtriangular outline (Fig.13E), close to what is observed in *Antetonitrus* or *Melanorosaurus* (NM QR3314 and SAM-PK-3449). The posteromedial border of the proximal extremity is concave and its lateral border is convex. The anterolateral margin of the proximal extremity bears a concavity, the radial fossa, which is shallower than the posteromedial concavity. The radial fossa is less marked than in *Aardonyx*, *Melanorosaurus* (SAM-PK-3449) or *Sefapanosaurus*. It is bordered by both the anterolateral and anteromedial processes of the ulna. The anteromedial process is, like in many prosauropod dinosaurs, oval. Therefore, its distal extremity appears rounded. The process is well developed and exhibits a quite important width relative to its length. In *Antetonitrus* and *Sefapanosaurus*, the anteromedial process is much thinner. The anterolateral process is not much developed and is less protruding than in most basal sauropodomorph genera. On its posterior part, the proximal extremity of the ulna bears a rounded projection, of which the posterior margin is convex in proximal view. Ahead of this projection, the olecranon is visible, in a little more posterior position than the anterolateral process. The olecranon is not much developed, but remains visible in medial and lateral views. The dorsalmost point of the olecranon is some 3 cm above the lowest point of the proximal surface of the bone, on the anteromedial process surface (Fig. 13B).

The diaphysis is much less stout than that of *Antetonitrus*, which has an ulna of equivalent size. The transverse section of the diaphysis is elliptical. The anteroposterior extension of the diaphysis equals 35% of the one of the proximal extremity and 45% of the extension of the distal extremity (Table 5). In lateral and medial views, the proximal portion of the diaphysis is narrowing distally. The diaphysis appears waisted around two thirds of the length of the bone, and then widens distally. Therefore, the diaphysis has an anteroposterior length of 125 mm on the proximal part of the bone, but is merely 56 mm at its, more distal, thinnest point. The anterior and posterior margins of the diaphysis are concave. In anterior and posterior views,

the lateral border of the ulna diaphysis is sigmoid and its medial border is slightly concave. The medial surface of the diaphysis is concave on its proximal half and flat on the distal half (Fig. 13D). The lateral surface of the ulna diaphysis is slightly convex on the proximal portion of the bone and flat on the distal part.

The anteroposterior extension of the distal extremity of the ulna equals 85% of that of the proximal extremity. It is also equivalent to 28% of the entire length of the ulna (Table 5). The distal articular surface is simple and convex. The anterior surface of the distal extremity seems to bear a tuber, but the bone being broken, the structure cannot be observed in its entirety. The articular surface is subrectangular in distal view. The long axis of the distal extremity is oriented anteroposteriorly. The medial and lateral margins are straight, and the anterior and posterior borders appear convex (Fig. 13F).

Right Radius [MNHN.F.LES147]—The right radius is complete and well-preserved. The only damaged part of the bone is its proximal extremity, of which two margins are broken. The bone surface of the radius is well-preserved, even though it is not entirely prepared on the extremities of the bone. The diaphysis of the radius is cracked in two different spots (Fig. 14).

The radius is straight and relatively thin. Its proximal extremity is transversely extended. In lateral view, it also appears slightly anteroposteriorly extended with respect to the extension of the diaphysis. In proximal view, the extremity is not complete, but was, in all likelihood, oval. The transverse width of the proximal articular surface equals approximately 1.2 times its anteroposterior expansion (Table 5). The anterior border of the proximal extremity is straight, its posterior border is slightly convex and its lateral border convex. The lateral part of the proximal articular surface seems to be slightly shorter anteroposteriorly than the medial part (Fig. 14E). In anterior and posterior views, the lateral part of the proximal articular surface has a convex margin, more developed dorsally than the medial part of the surface. The medial

part of the proximal articular surface is slightly concave for the radial condyle of the humerus (Fig. 14A, C).

The diaphysis of the radius represents approximately three quarters of the entire length of the bone. In transverse section it is elliptical, the transverse width being superior to the anteroposterior expansion. The transverse width of the diaphysis equals approximately 45% of the transverse width of the radius proximal extremity and 55% of that of the distal extremity (Table 5). In anterior and posterior views, the diaphysis is straight. Its lateral and medial margins are subparallel and exhibit a slight concavity (Fig. 14A, C). In lateral and medial views, the diaphysis appears slightly curved with a straight anterior border and a slightly concave posterior border. The diaphysis starts widening both transversely and anteroposteriorly 8 cm above the distal extremity (Fig. 14B, D). On the distal part of the diaphysis, the lateral area of the radius bears a flat and rough tuber, situated 4 cm above the distal margin of the bone, which probably matches the contact point with the ulna.

The distal extremity of the radius is extended both transversely and anteroposteriorly with respect to the diaphysis. As it is usually the case in basal sauropodomorphs, the ventral margin of the distal extremity projects much further on the medial side than on the lateral side. In anterior and posterior views, the distal margin of the radius therefore appears slanted. The distal articular surface is flat. In distal view, the distal extremity is subcircular, its transverse width is slightly superior to its anteroposterior extension (Table 5). The posterior margin is the only one roughly straight in distal view, the other borders appear convex (Fig. 14F).

Manus—We were only able to identify with certainty four metacarpals (the metacarpal V was the only one not recovered) and two phalanges of *Kholumolumo* manus (the phalanges I.1 and IV.2) in the collected material. Given that the elements of the metacarpus have been found disarticulated, and belong to several individuals, they cannot be compared in size. Overall, the metacarpals are well-preserved, even though they exhibit some fractures. Their bone surface is eroded in some places and the proximal part of the metacarpal IV is incomplete (Fig. 15).

The first right metacarpal (MNHN.F.LES26) is, as in all basal sauropodomorphs, slightly longer than wide (Table 5). It is a very robust bone, quadrangular in shape. In dorsal view, the proximal margin is slightly concave, and the medial and lateral margins are strongly concave. In lateral view, the proximal border of the metacarpal I is straight, and its dorsal and ventral borders are strongly concave. A marked concavity on the proximolateral surface of the metacarpal allows the articulation with metacarpal II, which is located, not in the alignment of metacarpal I, but slightly anteriorly to the latter, as in most basal sauropodomorph dinosaurs. In proximal view, the articular surface of the metacarpal I appears subrectangular. The torsion between the bone proximal and distal extremities is slightly marked. The distal condyles are large and dorsoventrally well developed. The distal lateral condyle is projecting much more anteriorly than the medial (Fig. 15).

The second left metacarpal (MNHN.F.LES92) is an elongated element, of which the proximal transverse width equals 54% of its entire length (Table 5). This value supports the important difference of morphology of the proximal articular surfaces. Indeed, in proximal view, the proximal articular surface of metacarpal II is subrectangular with a long-axis oriented dorsomedially to ventrolaterally. In dorsal view, the metacarpal II is hourglass-like with concave lateral and medial borders. The transverse proximal width equals 1.7 times the minimum width of the metacarpal and is equivalent to its distal transverse width. In medial

view, the proximal margin of metacarpal II appears straight, whereas its ventral and dorsal margins are concave. The distal condyles are dorsoventrally less developed than the proximal extremity of the bone (Fig. 15).

The third metacarpal (MNHN.F.LES93) is also elongated and, compared to the second metacarpal, presents a thinner diaphysis with respect to its proximal and distal extremities. Thus, the transverse width of the metacarpal III proximal extremity equals 47% of the entire length of the bone and represents 2.5 times the minimum width of the diaphysis, as well as 1.2 times the transverse width of the distal extremity (Table 5). In dorsal view, the medial and lateral borders of the bone are concave. In medial view, the proximomedial area of the bone is slightly coarse on the contact surface for metacarpal II. The dorsal and ventral margins of the bone are concave. The proximal extremity of the third metacarpal shows a relatively flat surface and, in lateral view, is clearly more developed dorsoventrally than the distal extremity. The lateroventral surface of the bone bears a concavity in which metacarpal IV articulates. In proximal view, the articular surface of metacarpal III is subrectangular and dorsoventrally high (Fig. 15).

The fourth metacarpal (MNHN.F.LES76) is incomplete. In dorsal view, the medial and lateral borders of the bone are concave. The proximal extremity is broken, but seems to extend more transversely than the distal one. With respect to metacarpals II and III, the distal extremity of metacarpal IV is less developed than its diaphysis both transversely and dorsoventrally. In medial view, the beginning of a slight proximomedial concavity where metacarpal III articulates can be guessed. The dorsal and ventral borders of the bone are slightly concave (Fig. 15). A proximomedian prominence is visible on the metacarpals II to IV.

The first phalanx of digit I (MNHN.F.LES29) is one of the few elements of the manus, with the metacarpals, that we were able to identify with certainty. It is a short and stout bone, of which the maximum length and width are roughly equivalent. The proximal articular surface

of phalanx I-1 bears two concavities separated by a bulge, where the distal condyles of metacarpal I. The lateral concavity is considerably more marked than the medial one. Phalanx I-1 presents intercondylar dorsal and ventral processes, the ventral being the more developed. The diaphysis is very short, almost absent. It has undergone a torsion of approximately 40 °. In medial view, the dorsal and ventral margins of the bone are strongly concave. Distally, the ginglymus is more extended ventrally than dorsally. The distal condyles are rather large and bear clearly visible collateral fossae (Fig. 15).

The second phalanx of the manual digit IV (MNHN.F.LES101, LES105) have been identified based on its small size and on the asymmetry of its proximal and distal articular surfaces. The proximal articular surface is trapezoidal in outline and its width is almost equal to its height. The distal condyles are deeply divided with shallow collateral pits and extend ventrally.

Pelvic Girdle

Right Ilium [MNHN.F.LES375a]—The right ilium is complete, although very cracked. Its bone surface is very damaged, not to say, completely removed. A bone fragment of several centimeters is missing on the supracetabular crest, in the posterodorsal area of the pubic peduncle. Another fragment is missing at the junction between the posterodorsal border of the ischial peduncle and the ventral border of the postacetabular process (Fig. 16). The ilium is robust, large and typical, in morphology, of what is usually observed in prosauropod dinosaurs. It is 590 mm long, from the extremity of the preacetabular process to the one of the postacetabular process. The minimum anteroposterior length of the ilium is above the acetabulum and equals approximately 60% of the maximum length of the bone. The maximum height of the ilium is 370 mm (Table 6).

The dorsal border of the ilium is sigmoid in lateral view. The dorsalmost point is practically at the center of the anteroposterior axis of the ilium, above the anterior margin of the ischial

peduncle. The lowest point of the dorsal margin is at the level of the preacetabular process (Fig. 16A). In dorsal view, the medial border of the ilion is convex and its lateral border is concave (Fig.16C). Transversely, the iliac blade is 3 to 4 cm wide, measured on its dorsal border. The thinnest part of the blade is at the level of the concavity occupying the central part of the iliac blade and extending ventrally until a point close to the acetabulum. Some basal sauropodomorphs, like *Lufengosaurus* or *Riojasaurus*, show the same concavity on their ilium, located much more dorsally. Above the acetabulum, the iliac blade height equals approximately half of the entire height of the ilium. It is less extended dorsoventrally than in *Meroktenos*. The medial surface of the iliac blade is flat, both ventrally and dorsally, but presents a marked concavity on its central part, where the insertion of the sacral vertebrae is located (Fig. 16B).

The preacetabular process is suboval with a rounded extremity in lateral view. It is the most common shape in prosauropod dinosaurs, although in some genera, like *Adeopapposaurus* or *Anchisaurus*, the extremity is sharper. Here the process is as high as long, its height representing approximately 90% of its length. The length of the preacetabular process equals 18% of the ilium entire length and 53% that of the postacetabular process (Table 6). The lateral surface of the preacetabular process is flat and its medial surface concave. In lateral view, the dorsal and ventral margins are slightly convex and meet at the rounded extremity. The preacetabular process is oriented at approximately 50 ° of the pubic peduncle, and its distal margin is posterior to the anterior projection of the latter (Fig. 16A, B).

The postacetabular process is subtriangular with a rounded distal extremity. In several genera like *Jingshanosaurus*, *Lessemsaurus* or *Yunnanosaurus*, the process has a subrectangular shape. Its minimum height (at the level of the extremity) equals approximately 55% of its maximum height. It is longer than the preacetabular process and represents 34% of the ilium length (Table 6). The lateral surface of the postacetabular process is convex on its dorsal part

and flat on its ventral part. The medial surface is flat to very slightly concave. In lateral view, the dorsal margin of the postacetabular process is slightly concave, its ventral margin is straight and oblique, following an angle of approximately 45 °, relative to the horizontal. As in most sauropodomorphs else than *Eoraptor*, *Panphagia* or *Saturnalia*, there is no brevis crest and, by extension, no visible brevis fossa on the ventral surface of the postacetabular process (Fig. 16D).

The acetabulum is completely open, in contrast of what can be observed in *Chromogisaurus*, *Panphagia* or *Saturnalia*, and shows similar proportions than in most prosauropod genera. The acetabulum is semicircular and slightly longer than high (Fig. 16A-B). It presents an intermediate structure between the very low and elongated acetabulum of some basal forms as *Eoraptor* or *Panphagia* and those, narrower, observed in *Lessemsaurus* or *Sarahsaurus*. The supracetabular crest rises quite abruptly on the dorsal area of the pubic peduncle and runs along the dorsal border of the acetabulum (Fig. 16A). It extends posteriorly until the base of the ischial peduncle, where it merges gradually with the lateral bone surface. The supracetabular crest is eroded, but does not seem to have been laterally developed. It is approximately 2 cm at its widest point, that is to say on the dorsal area of the pubic peduncle. The acetabular wall is very wide transversely, a bit wider at the base of the pubic peduncle than at the one of the ischial peduncle. The anterior and anterodorsal surfaces of the wall are concave. More posteriorly, in the area where the supracetabular crest loses thickness, the acetabular wall gets flatter. It is completely flat at the level of the ischial peduncle. As in many sauropodomorph dinosaurs, the acetabular wall is oriented ventrolaterally, particularly on its posterior part.

The pubic peduncle extends anteroventrally on 195 mm. It is trapezoidal, robust, and clearly longer than the ischial peduncle. In lateral view, its anterior and distal margins appear straight. Its posterior margin is concave both laterally and medially (Fig. 16A). In distal view,

the pubic peduncle has a subtriangular shape, with a strongly convex anterior border and a concave posterior border. The posteromedial corner of the articular surface bears a projection which, probably due to erosion, appears slightly rounded. Taking this projection into account, the transverse width of the articular surface of the pubic peduncle equals approximately 75% of its maximum anteroposterior length (Table 6).

The ischial peduncle is projecting ventrally and slightly posteriorly on approximately 110 mm. It is stout and relatively developed and represents a little more than half the length of the pubic peduncle (Table 6). This morphology is widespread among basal sauropodomorphs, as opposed to that of sauropod dinosaurs, in which the ischial peduncle usually shows an extreme reduction (Upchurch et al., 2004). The ischial peduncle, despite its broken posterodorsal margin, appears subrectangular. In lateral view, its anterior margin is straight and its incomplete posterior border is slightly concave. This concavity induces a posterior projection of the posteroventral corner of the peduncle (Fig. 16A-B). This morphological trait is observed in many prosauropod genera, in a more or less marked manner. It is in *Plateosaurus* (Moser, 2003) and *Riojasaurus* that the projection is the most visible. In distal view, the ischial peduncle is almost square, the length and the width of the articular surface being nearly equivalent (Table 6). The anterior and medial margins of the peduncle are straight, whereas its posterior and lateral margins are slightly convex (Fig. 16D).

Left Pubis [MNHN.F.LES378]—For the need of the description, the pubis is described with its long axis oriented horizontally. Following this orientation, the flat surfaces of the pubic apron are oriented strictly dorsally and ventrally, and the iliac peduncle is oriented posteriorly. In vivo, the pubes were oriented at a slant angle with respect to the longitudinal axis of the animal, with the surface of the pubic apron oriented anterodorsally. The left pubis of *Kholumolumo* is practically complete, but very badly preserved. The bone exhibits numerous fractures, a part of the obturator plate is missing and the medial border of the pubic apron is not entirely preserved (Fig. 17). The extreme fragility of the pubic apron prevented us from taking photos in lateral or medial views; nevertheless, one illustration is available in the work of Gauffre (1996, annexe 2). The pubis, in spite of its robust aspect, is elongated and has a total length of 665 mm (Table 6). In dorsal and ventral views, the pubis is subrectangular with a straight lateral margin, which has a slight concavity on the proximal part of the bone (Fig. 17). This morphology is very similar to the one of *Meroktenos* or *Melanorosaurus* (NM QR1551) and is different from specimens in which a marked concavity is visible on the lateral border at the distal extremity of the pubis, and from specimens in which even the central part of the lateral border is concave, as in *Coloradisaurus* or *Lessemsaurus*.

The pubis obturator plate is incomplete, but still retains a visible obturator foramen, iliac and ischial peduncles, as well as the acetabular area. It is 215 mm long, 32% of the total length of the pubis, and its maximum width under the obturator foramen equals 37% of the total length of the bone (Table 6). The iliac peduncle is much more developed than the ischial peduncle. Its main axis is oriented dorsolaterally to ventromedially. There is no dorsal marked protrusion visible on the dorsolateral area of the obturator plate. The iliac peduncle is twice as long as large (Table 6). Its articular surface is flat and appears suboval with convex borders in proximal view. The pubic component of the acetabulum is complete and is 75 mm long,

following its main axis. It is located in the continuity of the iliac peduncle and is oriented dorsolaterally to ventromedially. It is short and thin. Its proximal surface is slightly concave. In dorsal view, the pubic component of the acetabulum is at right angles to the ischial peduncle (Fig. 17A). The ischial peduncle is subcomplete, it lacks some centimeters on its most distal part. It has a length almost equivalent to that of the iliac peduncle (Table 6). The articular surface of the ischial peduncle is oriented medially to ventromedially. The subtriangular ischial peduncle is considerably thinner than the iliac peduncle. The maximum width of the peduncle is on its proximal extremity, and is tapering to the distal tip (Fig. 17B). The obturator foramen is located on the medial side of the obturator plate, a few centimeters anteriorly to the proximal border of the pubis. Its borders appear a bit damaged, but it is almost complete, the only bone fragment missing is on the anteromedial margin of the foramen. In dorsal and ventral views, the obturator foramen has a subrectangular shape. The approximate anteroposterior length of the obturator foramen is 80 mm, that is 37% of the length of the obturator plate, and his width equals 63 mm. In dorsal view, the lateral borders of the obturator plate and the pubic apron are aligned. Regarding the medial margin of the pubis, the junction between the obturator plate and the pubic apron is lacking.

The pubic apron extends, distally to the obturator plate, on 450 mm, that is almost 70% of the entire length of the bone. The blade reaches a maximum width of 148 mm a few centimeters prior to the distal extremity (Table 6). On the center of the blade, the medial margin of the pubic apron is approximately 10 mm high, which is dorsoventrally thinner than the 35 mm lateral margin. The dorsal and ventral surfaces of the pubic apron are flat, no bulge nor ridge is visible. In dorsal and ventral views, the lateral and medial borders are straight and subparallel (Fig.17A). This morphology is similar to what is observed in *Antetonitrus*, *Melanorosaurus* (NM QR1551) or *Meroktenos*. In lateral view, the dorsal margin of the pubic apron is slightly concave and the ventral margin slightly convex (annexe 2).

In dorsal or ventral views, the distal extremity of the pubis is not laterally widened, unlike in *Yunnanosaurus*. Therefore, the transverse width of the distal extremity is almost equivalent to that of the one taken at the center of the pubic apron. It equals approximately 23% of the pubis total length (Table 6). In lateral or medial views, however, the club-shaped distal extremity gets dorsoventrally wider. Its dorsoventral height is twice the height of the pubic apron, measured on the lateral margin of the latter. In lateral view, the dorsal expansion of the distal extremity is faint. Most of the dorsoventral expansion of the extremity comes from a marked ventral projection, quite like what is observed in *Coloradisaurus*. In lateral view, the distal margin of the pubis appears strongly convex. In ventral and dorsal views, the distal margin of the pubis is also convex, although to a lesser extent. In distal view, the distal extremity has a suboval shape and convex borders.

Left Ischium [MNHN.F.LES152]—For the need of the description, we consider here that the ischium pubic peduncle is oriented strictly anteriorly and that the iliac peduncle is oriented anterodorsally.

There is only the proximal part of a left ischium of *Kholumolumo* preserved. It is rather badly preserved and presents several fractures. The bone surface is badly preserved too. The ischial component of the acetabulum is medially damaged (Fig. 18).

The proximal part os the ischium is transversely thin and dorsoventrally expanded. It is usually the thinnest part of the bone which represents, in prosauropod dinosaurs, approximately 30% of the ischium total length. The proximal extremity as it has been preserved, that is broken at the base of the ischium diaphysis, is almost as high dorsoventrally than anteroposteriorly long (Table 6). This ischial plate bears the pubic peduncle, the acetabular area and the iliac peduncle. In lateral view, the dorsal border of the proximal part is strongly convex, the anterior border shows a concavity due to the acetabulum, and the ventral

border is incomplete. The lateral surface of the bone is flat posteriorly to the pubic peduncle, slightly concave in the area surrounding the acetabulum component, and slightly convex behind the iliac peduncle (Fig. 18B). The medial surface of the bone presents a dorsal convexity just behind the iliac peduncle and a marked concavity on the rest of the surface (Fig. 18A). The pubic peduncle is located on the anterior part of the proximal extremity of the ischium (Fig. 18). It is dorsoventrally elongated and, in anterior view, subtriangular and very similar in shape to the ischial peduncle of the pubis with which it is articulating. The maximum width of the pubic peduncle if located on its dorsal part, and tapers ventrally. This maximum transverse width equals approximately 32% of the maximum length of the pubic peduncle (Table 6). Posteriorly to the pubic peduncle, the ischium ventral margin is damaged and broken. It is therefore impossible to determine if a ventral obturator notch was present between the pubic peduncle and the ischium diaphysis, as it is the case in *Lufengosaurus*, *Massospondylus* or *Ruehleia*. The ischial component of the acetabulum constitutes a deep notch between the pubic peduncle and the iliac peduncle. It is approximately 5 cm deep, with respect to the articular surface of the pubic peduncle, but 2 cm deep with respect to the one of the iliac peduncle (Fig. 18). It represents approximately 45% of the length of both the pubic and iliac peduncles, and shows almost the same extension as the pubic component of the acetabulum (70 and 75 mm, respectively) (Table 6). The iliac peduncle is located in the dorsal area of the ischium proximal extremity. It is approximately the same length as the pubic peduncle, but its maximum transverse width is more important. The latter equals roughly 44% of the maximum length of the peduncle (Table 6). In dorsal view, the iliac peduncle shows a suboval outline, with slightly convex lateral and medial margins (Fig. 18C). Distally to the iliac peduncle, the posterodorsal border of the ischium proximal extremity shows a marked concavity merging with the diaphysis of the bone.

Posterior Member

Right Femur [MNHN.F.LES394]—Several femora, more or less complete, are part of the material referred to *Kholumolumo*. The following description is based on a right, complete, and relatively well-preserved, femur. The most damaged area of the femur is its laterodistal corner, where a bone fragment has been torn off. Several centimeters thick bone fragments are also missing on the anterior surface of the diaphysis, which is covered with numerous cracks. The bone surface is not very well preserved, particularly on the anterior surface of the bone (Fig.19).

The femur is 755 mm long and is relatively stout. Its robustness index is 2.36, that is quite close to those of some specimens like *Massospondylus*, *Melanorosaurus* (NM QR1551) and *Plateosaurus* (Table 7). In anterior and posterior views, the femur has a slightly sigmoid shape (Fig. 19A, C). In lateral and medial views, the femur is curved at the level of its distal extremity. On the first three quarters of its length, the anterior and posterior margins of the femur are straight. On its distal extremity, the anterior margin is convex and the posterior one is concave (Fig. 19B, D). The femoral head has undergone a rotation of approximately 30 ° relatively to the transverse axis of the distal condyles.

In anterior and posterior views, the femoral head is rounded and projects at approximately 90 ° with respect to the main axis of the bone. The head of the femur is higher dorsoventrally than transversely elongated. In proximal view, it is oval, all its margins are convex and its transverse length equals twice its anteroposterior width (Table 7). The long transverse axis of the head is oriented strictly transversely (Fig. 19E).

The femur diaphysis is subcircular and more robust than in most other basal sauropodomorphs that have a similar morphology. It has an eccentricity of 1.16. The diaphysis is slightly thinner transversely on its center than on its proximal and distal extremities (Fig. 19A). The lesser trochanter is located on the anterior surface of the femur, in

the proximal area of the diaphysis. It is a low ridge extending proximodistally, at the center of the transverse axis of the diaphysis. In comparison, *Lessemsaurus* or *Riojasaurus* display very high lesser trochanters. The lesser trochanter is not visible in posterior view. Its proximal extremity is lower than the ventral margin of the femoral head. The lateral border of the lesser trochanter is higher and better defined than the medial border (Fig. 19A). On the posterior surface of the diaphysis, the fourth trochanter is quite developed. Its proximal extremity is located 280 mm under the proximal margin of the bone and is 145 mm long, that is 19% of the entire length of the femur (Table 7). The fourth trochanter extends beyond the median point of the femur proximodistal axis. In posterior view, it is straight, as in *Coloradisaurus*, *Lessemsaurus* or *Melanorosaurus* (NM QR1551). The proximal extremity of the fourth trochanter is slightly curved medially with respect to the rest of the structure. This extremity is located in the medial quarter of the diaphysis transverse axis. The distal extremity of the fourth trochanter is in the mediocentral quarter of the diaphysis (Fig. 19C). In lateral view, the fourth trochanter is asymmetrical and subrectangular. Its proximal margin rises gradually from the diaphysis, whereas its distal margin is steep and straight (Fig. 19B). In between, the apical border of the trochanter is straight. It is, however, oblique with respect to the long axis of the femur, because its proximal height is more important than its distal one. Regarding the shape, the closest fourth trochanter is observed in *Riojasaurus*, even if in the latter, the apical margin of the trochanter is subparallel to the femur main axis instead of being oblique. In cross-section, the fourth trochanter of *Kholumolumo* is subtriangular in its proximal part and suboval in its distal part.

The distal extremity of the femur is incomplete. Its transverse width equals approximately 1.5 times that of the center of the diaphysis (Table 7). In anterior view, the bad preservation of the fossil prevents us from checking the presence of an extensor groove (Fig. 19A). In posterior and distal views, a marked popliteal fossa is visible between the distal condyles (Fig. 19C, F).

The femur distal condyles are rounded. In medial view, the medial condyle has a strongly convex posterior border and a straight to slightly convex ventral border (Fig. 19D). The tibiofibular crest is rather marked and well visible in lateral view. The transverse width of the distal extremity of the femur is superior to its anteroposterior extension (Table 7). The medial condyle appears to be approximately the same size as the lateral and fibular condyles put together, even though we cannot say it with certainty because of the deformation (Fig. 19F).

Right Tibia [MNHN.F.LES381m]—The *Kholumolumo* tibia is complete, but not particularly well-preserved. Its bone surface is damaged and depressed in some areas, particularly on the lateral surface of the bone. The tibia diaphysis is covered in numerous fractures and cracks. The proximal and distal extremities of the bone are not completely prepared and the posteromedial corner of the proximal articular surface is broken (Fig. 20). The tibia exhibits a short and stocky morphology. It is straight, with widened proximal and distal extremities in anterior and posterior views (Fig. 20A, C). The proximal extremity also appears slightly extended in lateral and medial views (Fig. 20B, D). It is clearly more robust than the distal extremity, and is not in the same axis as the latter due to a torsion at the level of the diaphysis.

The proximal articular surface of the tibia seems flat and bears, as in all the prosauropod dinosaurs, a cnemial crest as well as two condyles. In proximal view, without considering the cnemial crest, the articular surface is subcircular. Considering the cnemial crest, the surface is suboval and appears 1.6 times more extended anteroposteriorly than tranversely (Table 7). In *Kholumolumo*, the long axis of the proximal articular surface is oriented anteroposteriorly and slightly laterally. In proximal view, the anterior margin of the proximal articular surface is strongly convex. The lateral margin is sigmoid as a result of the depression adjacent to the cnemial crest. The posterior and medial margins are convex (Fig. 20E). The cnemial crest is oriented anterolaterally and measures on its most proximal part 50 mm, that is 24% of the

total anteroposterior length of the articular surface (Table 7). In lateral view, the dorsalmost point of the cnemial crest is near its proximal extremity. On the anterior part of the bone, the cnemial crest is not well defined. Nonetheless, it seems to extend on 10 to 15 cm proximodistally, on which it is losing height. The depression visible in proximal view is also exposed in lateral view, and separates the cnemial crest from the proximal lateral condyle. The latter, which is oval, clearly appears in proximal view and seems to extend on almost all the length of the surface, posteriorly to the cnemial crest. The lateral condyle represents approximately 65% of the anteroposterior length of the proximal surface. In proximal view, the proximal medial condyle is extending as posteriorly as the lateral condyle, but its anterior extension is more limited. The intercondylar groove, which usually defines the two condyles, is not visible in proximal view (Fig. 20E). In medial and lateral views, the medial condyle seems to be projecting less dorsally than the lateral one. In anterior and posterior views, the medial and lateral margins of the tibia proximal extremity are convex and, more ventrally, slightly concave at the level of the transition with the diaphysis.

The tibia diaphysis is large and stocky. It is cylindrical with parallel margins in anterior and posterior views (Fig. 20A, C). In medial and lateral views, the diaphysis borders are getting closer distally. Hence, the anteroposterior extension of the diaphysis is reduced from 120 mm proximally to 90 mm near the distal extremity of the bone (Fig. 20B, D). At mid-length, the cross-section of the tibia is oval, the anteroposterior extension of the bone being superior to its transverse width (Table 7).

The distal extremity of the tibia is approximately the same transverse width as its proximal extremity, and therefore appears transversely extended. However, its anteroposterior extension is considerably inferior to that of the proximal extremity, given that the distal extremity exhibits practically the same extension as the diaphysis in medial and lateral views. The distal extremity is 2.3 times larger transversely and 1.2 times more extended

anteroposteriorly than the diaphysis (Table 7). As in all sauropodomorph dinosaurs, the distal processes of the tibia are projecting laterally. On this *Kholumolumo* specimen, their distal extremities are slightly weathered. Le processus postérodistal s'étend plus ventralement que l'antérodistal. En vue antérieure, le processus antérodistal dissimule en grande partie le postérodistal (Fig. 20A) et en vue postérieure, l'inverse se produit (Fig. 20C). Les deux processus ont une forme subtriangulaire avec un bord dorsolatéral droit. The distal articular surface of the tibia is flat to sightly convex. In distal view, it appears suboval with convex medial and posterior margins, a slightly concave anterior border, and a strongly concave lateral margin due to the presence of distal processes. The anteroposterior extension of the distal surface equals 78% of its transverse width (Table 7). The maximum anteroposterior extension of the distal extremity is located at the center of the articular surface. Despite all this, the lateral margin is more extended anteroposteriorly than the medial one. The anteromedial corner of the distal extremity is rounded, it forms an angle of approximately 100 ° (Fig. 20F).

Right Fibula [MNHN.F.LES374]—The right fibula is subcomplete. The proximal extremity is incomplete, the anteroproximal and posteroproximal corners are broken. The distal extremity of the fibula is also damaged, its lateral surface being eroded and the posterodistal corner being broken. The bone diaphysis shows seven fractures and some cracks. The bone surface is relatively well-preserved, even though it has been removed in some places (Fig. 21). The fibula is 575 mm long, it is elongated and relatively thin (Table 7). The main axis of the bone exhibits a torsion of approximately 20 °.

The proximal extremity of the fibula is incomplete, but still remains the most anteroposteriorly extended part of the bone. In medial and lateral views, it is subtriangular (Fig. 21B, D). The lateral surface of the proximal extremity is slightly convex, and its medial surface is slightly concave. The latter exhibits a rough texture, due to the articulation surface

for the tibia. On the medial surface, a poorly defined proximomedial tubercle, which is only a few millimeters high, is visible. This structure is also observed in *Aardonyx*, *Antetonitrus*, *Coloradisaurus* or *Ruehleia*. In proximal view, the articular surface is crescentic. Its transverse width equals 33% of its anteroposterior extension. The lateral border of the articular surface is convex in proximal view, and its medial border is concave (Fig. 21E). The proximal articular surface is smooth and slightly convex in lateral view.

The diaphysis is straight with subparallel margins in medial and lateral views. The anteroposterior extension of the fibula diaphysis decreases distally, going from 58 mm underneath the proximal extremity, to 38 mm above the distal extremity (Fig. 21B). In anterior and posterior views, the margins of the diaphysis are also subparallel, even though the lateral one appears slightly convex and the medial one slightly concave. The diaphysis tapers slightly between the proximal extremity and the distal one (Fig. 21A). At mid-length, the cross-section of the fibula is elliptical, with a long axis directed anteroposteriorly (Table 7). In the anterolateral area of the diaphysis, at approximately twenty centimeters distally to the proximal extremity of the bone, a poorly defined bulge probably corresponding to the fibular trochanter is present. On the medial surface of the diaphysis, two longitudinal concavities are visible. The most proximal one is at approximately twenty centimeters of the proximal border of the fibula. It is about 5 cm long proximodistally and is surrounded by a posterior bulge. The second concavity appears under the preceding one, and extends on more or less 10 cm. It is bordered by a bulge posteriorly and a ridge anteriorly (Fig. 21D).

The distal extremity of the fibula exhibits a subtriangular shape in lateral view. It is less extended anteroposteriorly than the proximal extremity and should represent approximately 70% of the latter. With respect to the anteroposterior extension at mid-diaphysis, the distal extremity is practically twice more extended (Table 7). The medial surface of the distal extremity bears an anterior shallow concavity, posteriorly surrounded by a small bulge. The

distal articular surface of the fibula articulates with the calcaneum and astragalus and appears flat to slightly convex in lateral and medial views (Fig. 21B, D). In distal view, the extremity is oval, and its transverse width equals approximately 50% of its anteroposterior extension (Fig. 21F).

Pes—The pes of *Kholumolumo* is known by several metatarsals and phalanges. A complete right pes is stored in Cape Town (obs. pers., 2014). Unfortunately, the MNHN material only comprises a very incomplete pes (MNHN.F.LES381), as well as isolated metatarsals and phalanges, coming from several individuals. The phalanges are not easily identifiable, we will therefore propose in what follows a description of the metatarsus only. The metatarsals are subcomplete and present some cracks. The quality of preservation differs from bone to bone. On the whole, however, the bone surface is rather badly preserved (Fig. 22).

As in all basal sauropodomorphs, the metatarsals articulate via the proximolateral surface of the most medial element recovering partially the proximomedial area of the following metatarsal. *Kholumolumo* metatarsus is one of the stockiest among prosauropod dinosaurs. It is, more or less, as robust as the metatarsus of *Antetonitrus* or *Melanorosaurus* (NM QR1551 & NM QR3314), but still remains more elongated than the one of *Blikanasaurus*. Thus, the ratio of the proximal transverse width on the length of the metatarsal I is 47% in *Kholumolumo* and 87% in *Blikanasaurus*.

The left metatarsal I of *Kholumolumo* (MNHN.F.LES89), despite its robust appearance, remains longer than wide (Table 7). In dorsal view, the proximal margin of the metatarsal I is straight, its lateral and medial borders are concave and its distal margin is convex. In lateral view, its dorsal and ventral margins are concave. The proximal articular surface of the metatarsal I is eroded and appears flat to slightly convex. In proximal view, the extremity is subquadrangular with relatively straight borders. The diaphysis of metatarsal I shows a

strongly elliptical cross-section and convex margins. The minimum width of the diaphysis equals 66% of the proximal width of the bone. The distal extremity of metatarsal I bears two distal condyles, one of which (the medial one) is broken. It, however, seems that the condyles were asymmetrical, the lateral projecting more distally than the medial. The lateral part of the distal lateral condyle is damaged and does not exhibit a collateral ligament fossa. On the distal lateral condyle, the ginglymus is not more developed ventrally than dorsally. Ventrally, a marked groove separates the two distal condyles (Fig. 22).

The left metatarsal II (MNHN.F.LES81) is subcomplete. Its proximal extremity is incomplete and its distal extremity is eroded, however, the total length of the bone seems to have been preserved. In dorsal view, the lateral and medial borders of the metatarsal II are slightly concave, while its distal margin is convex. In lateral view, the dorsal and ventral borders of metatarsal II are concave. The diaphysis of metatarsal II is straight with concave margins. The cross-section is elliptical, being more extended transversally than dorsoventrally. At the level of the distal extremity, both distal condyles are separated by a small distal depression and a shallow ventral groove. The collateral fossa is not visible on the medial side of the metatarsal, and is shallow on its lateral side. In medial view, the ginglymus appears more extended ventrally than dorsally (Fig. 22).

The metatarsal III is usually the longest element of the metatarsus. On the left metatarsal III of *Kholumolumo* (MNHN.F.LES82), the proximal width of the bone equals 36% of its entire length (Table 7). In dorsal view, the lateral and medial borders of the metatarsal are concave. On the proximomedial part of the bone, we can see the articulation facet receiving the metatarsal II. In medial view, the proximal part of the bone is more extended dorsoventrally than its distal part. The proximal area is damaged, especially on the edges. The proximal articular surface is concave, and in proximal view it appears subtriangular with an oblique long axis. The metatarsal III diaphysis is straight with concave margins and an elliptical

cross-section. Distally, the distal condyles are not well developed and separated by a slight groove. The collateral fossa is not visible on the medial side of the bone and is shallow on its lateral side. On the dorsal surface of the metatarsal III, posteriorly to the distal condyles, a small crescentic fossa is visible (Fig. 22). This fossa is also visible in other genera, like *Coloradisaurus* or *Mussaurus*.

The metatarsal IV is usually a bit longer than the metatarsal II. Here, the transverse width of the proximal extremity of the left metatarsal IV (MNHN.F.LES381c) equals 44% of the entire length of the bone (Table 7). In dorsal view, the proximal extremity is much more extended transversely than the distal one. The lateral and medial borders of the metatarsal IV are concave, the lateral being more concave than the medial one. In medial view, the dorsal and ventral margins are concave too. The proximal and distal extremities show the same dorsoventral extension. The proximomedial area of the metatarsal IV presents an articulation facet receiving the metatarsal III, bordered by a thin dorsal ridge which merges with the proximal articular surface of the bone. The latter is flat. In proximal view, it exhibits a subtriangular outline with a long transverse axis and a concave ventral margin. The diaphysis has concave margins, it is straight, and is transversely extending towards the proximal extremity of the metatarsal. The minimum transverse width of the diaphysis is a few centimeters away from the distal extremity of the bone. The cross-section of the diaphysis is strongly elliptical. In dorsal view, the distal extremity of the metatarsal IV is very slightly asymmetrical, the medial distal condyle projecting a little more distally than the lateral one. The two distal condyles are separated by a groove, as observed in the preceding metatarsals. The medial distal condyle does not bear a visible collateral fossa, while the distal lateral condyle exhibits a marked one (Fig. 22).

The metatarsal V is a vestigial element, and consequently, the shortest element of the metatarsus. The metatarsal V of *Kholumolumo* (MNHN.F.LES77) is strongly asymmetrical,

unlike in *Adeopapposaurus*, *Coloradisaurus* or *Mussaurus*. Based on the comparison with other asymmetrical metatarsals V, we suppose that this is a left element. The metatarsal V is stout and almost as wide as long, its proximal width representing 83% of its length (Table 7). In lateral view, the dorsal and ventral margins of the bone are concave and the dorsoventral extension of both extremities is almost the same. In medial view, the distal extremity is more developed dorsoventrally than the proximal one. In dorsal view, the metatarsal V exhibits concave medial and lateral margins, the medial one being much more concave than the lateral. The proximal articular surface of the bone is slightly damaged but appears slightly convex. In proximal view, it is subtriangular. The diaphysis of the bone is very short. Distally, the metatarsal V extremity equals 37% of its proximal extremity in width. The distal extremity is convex and shows no condyles nor collateral fossae (Fig. 22).

ANATOMICAL COMPARISONS

Among basal sauropodomorphs, twelve genera other than *Kholumolumo* are known from the Late Triassic of southwestern Gondwana (southern Africa and South America). Of these, *Euskelosaurus*, which is currently considered a nomen dubium by most authors (Yates, 2004), is not included in the following comparisons. Given their very dissimilar anatomy, the small and gracile forms such as *Eoraptor* (Sereno et al., 2013), *Pampadromeus* (Cabreira et al., 2011), *Saturnalia* (Langer et al., 1999) and the like are not taken into account in this amount.

Comparison with Large Basal Sauropodomorphs from the Upper Triassic of Southern Africa

The main differences between *Blikanasaurus* and *Kholumolumo* are located on the tibia. The excavation of the proximal part and the curvature of the posterior edge of the tibia of

Blikanasaurus are not considered here, both being presumably pathological (Galton and Van Heerden, 1998:164). In *Blikanasaurus*, the shaft of the tibia is triangular in cross-section, whereas it is oval in *Kholumolumo*. In lateral view, the tibia of *Blikanasaurus* is more curved, with a proximal extremity more extended anteroposteriorly relatively to the shaft. The distal articular surface of the fibula is asymmetrical in lateral view in *Blikanasaurus*, whereas it is subsymmetrical in *Kholumolumo*. Finally, the metatarsals of *Blikanasaurus* are stockier (with a superior width/length ratio at midshaft), especially the metatarsals II and III.

In *Eucnemesaurus*, the posterior tubercle and the lesser trochanter of the femur are much more developed than in *Kholumolumo*. The rounded fourth trochanter is part of the generic diagnosis of *Eucnemesaurus* (McPhee et al., 2015). It is rounded and subsymmetrical in profile, whereas it is both angular and asymmetrical in *Kholumolumo*. Furthermore, a fourth trochanter with a curved and oblique long axis is diagnostic of *E. fortis* (Yates, 2007a:96). In *Kholumolumo*, it appears straight in posterior view.

The syntype series of *Melanorosaurus readi* originally included several elements of the members, pelvis, as well as some vertebrae (Haughton, 1924). Unfortunately, some of these pieces are currently lost. The femur and the proximal half of a humerus were found in a higher stratigraphic layer than the remaining type materials. They are thus excluded from the syntype series. The tibia (SAM-PK-3449) of *M. readi* shows a more curved diaphysis in lateral view and its posterodistal process extends further distally (relatively to the anterodistal process) than in *Kholumolumo*. In proximal view, the cnemial crest is less developed in *M. readi* than in *Kholumolumo*. Considering the ulnae, the olecranon is more developed proximally and the radial fossa is deeper in *M. readi* than in *Kholumolumo*.

The material referred to *Melanorosaurus readi* catalogued under the accession number NM QR1551 includes vertebrae (mostly caudals), some bones from the pectoral and pelvic girdles and many bones from both members (Van Heerden and Galton, 1997). The centrum of the

posterior cervical vertebrae is much anteroposteriorly longer than dorsoventrally high in NM QR1551, whereas it is almost as long as high in *Kholumolumo*. The neural arch is dorsoventrally lower: its height is inferior to what is observed in *Kholumolumo* relatively to the total height of the vertebra. The scapula is stouter in *Kholumolumo* than in *M. readi*. In the latter, the blade appears longer relative to the total length of the bone, and its lateral borders are straight and subparallel in lateral view. Conversely, the lateral borders are curved in *Kholumolumo*. The articular surface of the proximal end of the ulna of *M. readi* is triangular in proximal view, with the anteromedial and anterolateral processes subequal in length. In *Kholumolumo* the articular surface is more pear-shaped, with an anteromedial process much more developed than the anterolateral one. The postacetabular process of the ilium of *M. readi* is anteroposteriorly elongated and exhibits a subrectangular extremity, while the extremity is shorter and more rounded in *Kholumolumo*. The dorsal margin of the ilium is straight in lateral view of *M. readi*, but sigmoid in *Kholumolumo*. In dorsal view, the dorsal border of the iliac blade is much thinner, at its central point, in NM QR1551. The lateral margin of the pubis is more curved throughout its length in anterior view in *M. readi* than in *Kholumolumo*. Finally, the femur of *M. readi* differs from that of *Kholumolumo* in various ways: in anterior view, the main axis of the femur is straight and its femoral head is projecting less medially. On the anterior surface, the lesser trochanter of *M. readi* is laterally located and more developed with a marked proximal extremity. On the posterior surface, the fourth trochanter is located more medially than in *Kholumolumo* and, in lateral view, it is low and rounded. In distal view, the articular surface is wider transversely than anteroposteriorly long in *M. readi*, whereas it is almost as wide as long in *Kholumolumo*.

The second specimen referred to *Melanorosaurus readi* NM QR3314 is represented by a poorly preserved but articulated skeleton. On the skull, the postorbital of NM QR3314 presents a marked step between its anterior and posterior processes in lateral view, step not

visible in *Kholumolumo*. In dorsal view, the posterior process of the postorbital is laterally convex in NM QR3314, but appears straight in *Kholumolumo*. The radial fossa of the ulna of NM QR3314 is deeper and the anterolateral process is more developed than in *Kholumolumo*. Also, the posteromedial corner of the proximal articular surface appears more elongated and sharper than in *Kholumolumo*.

The genus *Meroktenos* is known from an incomplete skeleton, including a femur and two elements of the pelvis. The material referred to *Meroktenos* strongly differs from *Kholumolumo* in terms of size and proportions. A comprehensive comparison between the two taxa is available in the original publication of *Meroktenos thabanensis* (Peyre de Fabrègues and Allain 2016:21).

The material referred to *Plateosauravus* (Van Heerden, 1979) might be among the most resembling *Kholumolumo*. On the anterior dorsal vertebra of *Plateosauravus* (SAM-PK-3345a) the postzygapophyses are at the same level as the prezygapophyses. In *Kholumolumo*, the articular surface of the postzygapophyses are more dorsally located than the prezygapophyses. In *Plateosauravus*, the anterior border of the neural spine is posterior to the anterior margin of the diapophyses, whereas it is anterior to the anterior margin of the diapophyses in *Kholumolumo*. The humeri of *Plateosauravus* (SAM-PK-3350 and 3342) are a bit stockier and their humeral head is less marked than in *Kholumolumo*. The ilium of *Plateosauravus* (SAM-PK-3609) is more elongated than the one of *Kholumolumo* (H/L ratio = 0.53 versus 0.63, respectively). Its dorsal margin appears straight in lateral view and the postacetabular process is subrectangular in *Plateosauravus*. In *Kholumolumo*, the dorsal margin is sigmoid and the postacetabular process is more rounded.

Comparison with Massive Basal Sauropodomorphs from the Upper Triassic of Southern America

Several cranial (Apaldetti et al., 2014) and postcranial elements of *Coloradisaurus* (Apaldetti et al., 2013) can be compared with the material referred to *Kholumolumo*. In *Coloradisaurus*, the posterior process of the postorbital is thicker and shorter, the scapula is much slender with a gracile outline, the deltopectoral crest of the humerus projects more anteriorly and is more rectangular in lateral view. On the pubis, the lateral border of the bone is strongly concave in *Coloradisaurus*, whereas it is straight in *Kholumolumo*. In lateral view, the distal extremity of the pubic apron is more developed anteroposteriorly in *Coloradisaurus*. The femur is straight in posterior view with a fourth trochanter located in the proximal half and rounded in lateral view. In *Kholumolumo*, it is slightly sigmoid in posterior view, with a fourth trochanter more distally located and subrectangular. The tibia is much stockier in *Kholumolumo*. Finally, the metatarsal V of *Kholumolumo* is strongly asymmetrical, unlike in *Coloradisaurus* in which it is subsymmetrical.

Lessemsaurus is known by numerous postcranial elements (Pol and Powell, 2007). The acromion process of the scapula of *Lessemsaurus* is subrectangular, when it is rounded in *Kolumolumo.* The posterodorsal corner of the scapular blade projects much more posteriorly compared to *Kholumolumo*. The distal and proximal ends of the humerus are more expanded transversely, relatively to the shaft, in *Lessemsaurus*. In *Kholumolumo*, the humeral head also presents a distinctive bump in anterior view which is not visible in *Lessemsaurus*. There are several main discrepancies in the pelvic girdle. The postacetabular process of the ilium is subrectangular in *Lessemsaurus*, whereas it is subtriangular with a rounded distal extremity in *Kholumolumo*. The acetabulum is higher and narrower in *Lessemsaurus*. In dorsal view, the pubis exhibits a strongly concave lateral border in *Lessemsaurus*. In *Kholumolumo*, the lateral border is straight with a slight concavity on the proximal part of the bone. The lesser trochanter of the femur appears high and well-developed in *Lessemsaurus*, whereas it is very low in *Kholumolumo*. The fourth trochanter of *Lessemsaurus* is located near the medial

margin of the diaphysis in posterior view, whereas it is at the center of the diaphysis in *Kholumolumo*. Finally, the distal extremity of the tibia is much more extended relatively to its width at midshaft in *Lessemsaurus*, in lateral view.

Quite a few postcranial elements are known from *Mussaurus* (Otero and Pol, 2013). The postzygapophyses of the anterior dorsal vertebrae are larger and project more laterally in *Kholumolumo* than in *Mussaurus*. In posterior view, the postzygapophyses are very high compared to the position of the diapophyses in *Kholumolumo*, whereas they are practically at the same height in *Mussaurus*. The scapulae differ a lot from each other. The scapula of *Mussaurus* is slender and gracile, while the one of *Kholumolumo* is stout and large. In *Mussaurus*, the ratio of the minimal transverse width at midshaft of the scapula relatively to its maximum transverse width on the proximal extremity is much inferior. The metacarpal I of *Mussaurus* is longer than large, while it is almost as long as large in *Kholumolumo*. The phalanx I.1 of the manus exhibits discreet condyles in dorsal and ventral views, while they are bulging and bulbous in *Kholumolumo*. The ilia referred to *Mussaurus* are incomplete but their ventral part is preserved (Otero and Pol, 2013). In lateral view, the ventral margin of the postacetabular process is straight and the ischial peduncle appears subtriangular in *Mussaurus*. In *Kholumolumo*, the ventral margin of the postacetabular process is oblique and the ischial peduncle is subrectangular. The lateral margin of the pubic apron of *Mussaurus* is slightly concave, whereas it is straight in *Kholumolumo*. In *Mussaurus*, the femur is less sigmoid in anterior and posterior views. In anterior view, the lesser trochanter is more developed and more laterally located. In lateral view, the fourth trochanter is less developed and is much shorter proximodistally. In posterior view, the fourth trochanter is more medially located. In distal view, the extensor and popliteal fossae are more marked. Finally, the metatarsal I is longer and more gracile in *Mussaurus* than in *Kholumolumo*, while the proportions of the other metatarsals do not vary much.

Riojasaurus preserves most of its cranial and postcranial elements (Bonaparte, 1971). The skull material having not been studied first-hand, the comparison between the two postorbitals has not been performed. The height of the neural arch of the most posterior cervical vertebra of *Riojasaurus* is much inferior to the height of the centrum, conversely to what is observed in *Kholumolumo*. The diapophysis is less developed both anteroposteriorly and laterally in *Riojasaurus*. The posterior margin of the proximal articular surface of the humerus of *Riojasaurus* bears a distinct tubercle, which is not present in *Kholumolumo*. The deltopectoral crest is sigmoid and thick in *Riojasaurus*, while it is straight and thinner in *Kholumolumo*. The diaphysis appears much shorter, relatively to the total proximodistal length of the humerus, in *Riojasaurus*. The proportions of the ilium are slightly different: in *Riojasaurus* the acetabulum is higher, relatively to the total height of the ilium than in *Kholumolumo*. The preacetabular process is sharp in *Riojasaurus*, whereas it is rounded in *Kholumolumo*. On the pubis, the obturator foramen is smaller in *Riojasaurus*. The pubic apron is transversely wider, relatively to the maximum transverse width of the pubis, in *Riojasaurus*. The femur of *Riojasaurus* is straight in anterior view, whereas in *Kholumolumo* it is slightly sigmoid. The lesser trochanter is more developed and protruding in *Riojasaurus*. In posterior view, the fourth trochanter is oblique in *Riojasaurus*, whereas it is straight in Kholumolumo. In distal view, the lateral condyle of the femur is more developed in *Riojasaurus* and the depression between the fibular and lateral condyles is much more marked than in *Kholumolumo*. The tibia of *Riojasaurus* has a slenderer morphology than the tibia of *Kholumolumo*. In lateral and medial views, the proximal end of the bone is more developed anteroposteriorly in *Riojasaurus* than in *Kholumolumo*. In distal view, the anteroposterior length of the lateral margin is inferior to the same length measured on the medial margin in *Riojasaurus*, whereas the opposite is observed in *Kholumolumo*.

Although a considerable number of new basal sauropodomorph taxa have been described over the past 15 years in southern Africa, it seems that the material from Maphutseng cannot be referred to any known taxon. Even if detailed nomenclatural and taxonomic revisions, allied with clear diagnoses based on associated material and works on the intraspecific variation are required for numerous southern gondwanan taxa (e.g. *Massospondylus*, *Euskelosaurus*, *Melanorosaurus*), the type material of *Kholumolumo ellenbergerorum* is diagnostic (see above) and the erection of a new genus and species is justified.

RESULTS

Characterization of the Maphutseng Bone Bed

The Maphutseng locality is the only basal sauropodomorph bonebed ever discovered in southern Africa. Nearly 470 pieces have been collected in 1959, 1963 and 1970 at Maphutseng, but only 225 pieces are currently housed in the MNHN collections in Paris. This is undoubtedly a consequence of the attribution, on the field, of several numbers to fragments of the same bone (see the introduction for more details). Among the 225 identifiable bones and fragments, several fragments fit together, leading to 212 fossilized remains. Of the 212, 99% (210) are considered to belong to *Kholumolumo ellenbergerorum*, classifying this a monotaxic bone bed (Eberth et al., 2007). The remaining two are two large teeth of a rauisuchian. Based on the number of right radii present in the collections, the minimum number of individuals (MNI) in the bone bed can be estimated at 5. Given that the 1955 and 1956 excavations yielded nearly 650 bones, the number of *Kholumolumo* individuals preserved in the Maphutseng bone bed is probably twice as large.

The Maphutseng bone bed is distinct from most of the *Plateaosaurus* bonebeds of the Late Triassic of Europe which preserved articulated skeletons and are interpreted as mire traps

(Sander, 1992), except for the Ellingen locality (Moser 2004). Miring can not definitively be excluded for the *Kholumolumo* specimens of Maphutseng, as the presence of small bones (distal caudal vertebrae and distal phalanges), vertebrae and ribs suggests very little scattering within the assemblage. Skull material is very rare, but it could be a sampling bias on the field. However, all the skeletons are disarticulated indicating post-mortem displacement and more likely a bone accumulation area. The latter interpretation is more consistent with the meandearing river environment with associated floodplain areas depicted for the lower Elliot Formation (Bordy et al., 2004).

Phylogenetic Analysis

Here, we include *Kholumolumo* to a comprehensive cladistic analysis of basal sauropodomorphs. We amended the data matrix from Apaldetti et al. (2018) to carry out the phylogenetic analysis. The original matrix consists of 372 characters and 63 terminal taxa, including *Kholumolumo*, which was scored based on all the available material. We carried out three consecutive parsimony analyses, all performed with Winclada (Nixon, 2002) running over NONA (Goloboff, 1993), using a heuristic search with a random stepwise-addition of 100 replicates and an unconstrained search strategy of multiple TBR + TBR branch swapping. The first analysis includes all the original taxa and resulted in a 1491 steps consensus tree (Supplementary Data Figure 2S). In the second one, we pruned three taxa a priori: *Barapasaurus*, *Isanosaurus* and *Gongxianosaurus*. *Gongxianosaurus*, given the uncertainty surrounding its anatomy. *Isanosaurus* because of the uncertainty about the age of the material. Indeed, a part of the Nam Phong Formation, where was collected the type material of *Isanosaurus*, has been recently dated as Late Jurassic on the basis of its palynoflora (Racey, 2009; Racey and Goodall, 2009). It is very likely that *Isanosaurus* is Late Jurassic in age and that its basal position in sauropodomorph phylogeny is only the reflect of the incompleteness

of the known material for this taxon. This second analysis resulted in a 1472 steps consensus tree (Supplementary Data Figure 3S).

For the third analysis, we removed from the sampling all the taxa presenting more than 70% of missing data, leaving only 47 taxonomic units. The analysis resulted in 24 most parsimonious trees (length=1402 steps, CI=0.30, RI=0.61). Based on this analysis, we produced a strict consensus tree (length=1451 steps; Fig. 23) where *Lessemsaurus*, *Antetonitrus* and the Sauropoda (sensu Salgado, Coria & Calvo, 1997; Peyre de Fabrègues et al., 2015) pertain to the same clade, *Antetonitrus* being the sister group of Sauropoda. The Massospondylidae (*Adeopapposaurus*, *Coloradisaurus*, *Leyesaurus*, *Lufengosaurus* and *Massospondylus*) is the clade recovered in the most "apical" (i.e., close to Sauropoda) position. The Plateosauridae (*Unaysaurus*, *Plateosaurus*) are also recovered. In between, *Kholumolumo* is retrieved as sister group of *Sarahsaurus*, within a clade also comprising *Xingxiulong*. This clade is diagnosed by the following unambiguous synapomorphies: epipophyses not overhanging the rear margin of the postzygapophyses in the cervical vertebrae (character 137, state 0), transversely expanded plate-like summits of posterior dorsal neural spines (character 174, state 1), length of first caudal centrum inferior to its height (character 183, state 1), anteroposterior width of the lateral side of the distal articular surface of the tibia as wide as the anteroposterior width of its medial side (character 307, state 0), transverse width of the calcaneum less than 30% of the transverse width of the astragalus (character 324, state 1).

The clade comprising *Kholumolumo* and *Sarahsaurus* is diagnosed by the following unambiguous synapomorphies: centra of the anterior cervical vertebrae approximately 1.25 times higher than wide (1) (character 130, state 1), flattened epipophyses (character 136, state 1), strongly convex dorsal margin of the ilium (character 245, state 1), preacetabular process of the ilium blunt and rectangular (character 247, state 0), length of the ischial peduncle of the

ilium much shorter than pubic peduncle (character 254, state 1), anterior margin of the pubic apron smoothly confluent with the anterior margin of the iliac pedicel in lateral view (character 261, state 0), lesser trochanter forming just a scar upon the femoral surface (character 287, state 0), transverse width of the distal tibia subequal to its anteroposterior length (character 306, state 0), anteromedial corner of the distal articular surface of the tibia forming a right angle (character 310, state 0).

As a result, *Kholumolumo* is nested among the basal sauropodomorphs with an ancestral morphotype and a bipedal bauplan and, despite its large size, is not recovered close to "sauropod-like" forms like *Antetonitrus* or *Lessemsaurus*.

DISCUSSION

Phylogenetic Relationships and Paleobiogeography

The phylogenetic tree (Fig. 23) exhibits a particular topology consisting of *Sarahsaurus* and *Xingxiulong*, two Jurassic taxa, in the same clade as *Kholumolumo*. The latest study of *Sarahsaurus* (Marsh and Rowe, 2018) showed the North American taxon with more or less the same affinities as in this paper. It was recovered among Massospondylidae in two phylogenetic trees out of three, the authors having considered three different datasets (Marsh and Rowe, 2018:figs. 47–49). In the only dataset, also including *Xingxiulong* (Marsh and Rowe, 2018:fig. 49), the latter appears just before Massospondylidae, closer to the base of the tree. However, in the phylogenetic analysis published with the original description of *Xingxiulong* (Wang et al., 2017), the Chinese taxon does not show the same phylogenetic affinities. It is not close to the Massospondylidae, but sister taxon of *Jingshanosaurus* and rather at the base of the Sauropodiformes (Wang et al., 2017:fig. 5). This phylogenetic result led the authors to assume an Asian origin for the Sauropodiformes clade. Our phylogenetic analysis does not corroborate this hypothesis, *Xingxiulong*, *Sarahsaurus* and *Kholumolumo*

being not recovered among Sauropodiformes. It is the first time that one clade includes taxa from China, North America and Africa. It was suggested that *Sarahsaurus*'s lineage most likely originated and dispersed from Gondwana between the end of the Norian and the Pliensbachian (Marsh and Rowe, 2018). The affinities with *Kholumolumo* could be explained by such an occurrence. An initial concentration of the sauropodomorph populations in Gondwana could have resulted in a geographic dispersal during the Late Triassic and vicariance during the Early Jurassic, with new taxa arising from the Triassic forms, including in North America and China.

Size and Body Mass Estimation

We used the relation between the femur length and the overall body length in *Plateosaurus engelhardti* which evaluates the body length to ten times the femur length (Sander and Klein, 2005) to estimate the size of *Kholumolumo*. Using the longest femur found in Maphutseng (Table 7), we estimate the body length of the largest *Kholumolumo* specimen around 9 meters long (Table 8). Compared to other Norian basal sauropodomorphs, it is the genus with the most important size just before *Lessemsaurus* (PVL 4822:8.4 m).

It has been established that there is a correlation between the long-bones circumference and the weight in dinosaurs (Anderson et al., 1985). In quadrupeds, the circumferences of the femur and humerus of one species are correlated to its body mass (Campione and Evans, 2012). In bipeds, the equation is linking only the circumference of the femur to the body mass (Campione et al., 2014). The stance is therefore crucial to estimate the body mass of a given genus, but uncertainties remain concerning the stance of numerous basal sauropodomorphs (Bonnan and Senter, 2007; Bonnan and Yates, 2007; Otero et al., 2017; McPhee et al., 2018). Hence, we propose different estimations of the body mass of *Kholumolumo ellenbergerorum* using both the quadrupedal and bipedal equations (Benson et al., 2018:16), as well as the

regression equations given by Apaldetti et al. (2018) (Table 8). Based on the largest femur available (MNHN.F.LES371), the bipedal equation gives a body mass of 1754 kg for *Kholumolumo*. Other prosauropod specimens known from the Late Triassic range from 438 kg (*Coloradisaurus*) to 1963 kg (*Lessemsaurus*) (Table 8). The quadrupedal equation requires the circumferences of the humerus and femur of a same individual. The remains from Maphutseng coming from several individuals, we chose to calculate the body mass based on the biggest humerus (MNHN.F.LES379) and femur (MNHN.F.LES371) available, the proportions of which are consistent. The quadrupedal equation gives a result of 3334 kg for *Kholumolumo*, that is roughly double the calculated weight with the bipedal equation. The same result is observed in other taxa, except *Lessemsaurus* for which the body mass is roughly equivalent regardless of the equation used. The body mass ranges between 757 kg (*Coloradisaurus*) and 3334 kg (*Kholumolumo*). In that case, *Kholumolumo* is heavier than *Lessemsaurus* (Table 8).

The correlation between the size of the girdle elements and the body mass among Sauropodomorpha (Apaldetti et al., 2018) give an even more significant estimation of the weight of basal sauropodomorphs. Using the maximum length of the scapula (MNHN.F.LES386) and ilium (MNHN.F.LES375a) of *Kholumolumo* we obtain, respectively, 3864 kg and 3963 kg. *Unaysaurus*, of which the scapula is known, is the smallest specimen (88 kg) from the Late Triassic. It is followed by *Coloradisaurus* (307 kg). In both cases, *Kholumolumo* is one of the largest basal sauropodomorphs, with *Lessemsaurus* 1. The recently described *Lessemsaurus* 2 (CRILAR) appears to be the heaviest (Table 8). Considering a larger temporal scale, *Kholumolumo* is still one of the biggest basal sauropodomorphs, being only lighter than the Jurassic taxa *Antetonitrus* (Apaldetti et al., 2018) and *Ledumahadi* (McPhee et al., 2018).

Three equations out of four give an estimated body weight of more than 3000 kg for *Kholumolumo*. Therefore, *Kholumolumo* was among the heaviest terrestrial animals in gondwanan wildlife at the end of the Triassic. However, the significant gap between the results of the bipedal and quadrupedal equations is a prime example of the uncertainties surrounding the weight estimates in fossil organisms, particularly in groups such as Sauropodomorpha, including bipedal and quadrupedal animals, as well as transitional forms. These results should therefore be interpreted cautiously. In any case, *Kholumolumo* appears to be the biggest known basal sauropodomorph in the Triassic of Southern Africa. It is, however, not linked to the origin of Sauropoda, as supported by the proportions and anatomy of its anterior and posterior members and by its phylogenetic position.

CONCLUSIONS

The complete anatomical description of the Late Triassic *Kholumolumo ellenbergerorum*, discovered in Lesotho in 1955 and hosted in the collections of the MNHN during more than 50 years, is provided here. The remains, pertaining to at least five different specimens, form a virtually subcomplete skeleton, one of the most complete in the lower Elliot Formation. The only parts not maintained in the collections are the skull (with the exception of the postorbital), the coracoids and the complete ischium. The 210 bones unveiled in the Maphutseng bone bed present an exclusive morphology as well as a unique combination of characters and are therefore attributed to a new genus and new species.
The phylogenetic reconstruction replaces the new genus between two well-known clades of basal sauropodomorphs: Plateosauridae and Massospondylidae. The exact position of the Triassic *Kholumolumo* is intriguing, as it is recovered within the same clade as *Xingxiulong*, a Jurassic form from China and *Sarahsaurus*, another Jurassic form from North America. This

topology might be a testimony of the prosauropods biogeographic history by illustrating the effects of Late Triassic geographic dispersals and Early Jurassic vicariance.

The total body length of *Kholumolumo* is estimated at 9 meters. Based on the long-bones circumference and the size of the girdle elements, we calculated a body mass ranging between 1754 kg and 3963 kg, making of *Kholumolumo* one of the heaviest terrestrial animals at the end of the Triassic.

ACKNOWLEDGEMENTS

We thank (reviewer 1), and (reviewer 2)...

Access to specimens was provided by B. Zipfel and S. Jirah at the Evolutionary Studies Institute of Johannesburg, N. Ntheri, W. Molehe, M. Chaka, E. Butler and T. Peyper at the National Museum of Bloemfontein and Z. Erasmus and R. Smith at the Iziko South African Museum of Cape Town. Access to Ellenberger archives was allowed by the Ellenberger family, who donated the work documents, and by S. Jiquel at the ISEM of Montpellier. Many thanks at each and every one of them.

We thank B. Battail for providing details about the field campaigns and anterior publications and for his photographies, J. Falconnet for the storing of most of the material and for his comprehensive database, and V. Barriel for her occasional assistance and attentiveness.

We are also grateful to C. Bouillet and Y. Despres for the preparation of the material, and to L. Cazes for photography of the all the elements.

LITERATURE CITED

Anderson, J. F., A. Hall-Martin, and D. A. Russell. 1985. Long-bone circumference and weight in mammals, birds and dinosaurs. Journal of Zoology 207:53–61.

Apaldetti, C., D. Pol, and A. M. Yates. 2013. The postcranial anatomy *of Coloradisaurus brevis* (Dinosauria: Sauropodomorpha) from the Late Triassic of Argentina and its phylogenetic implications. Palaeontology 56:277–301.

Apaldetti, C., R. N. Martínez, I. A. Cerda, D. Pol, and O. Alcober. 2018. An early trend towards gigantism in Triassic sauropodomorph dinosaurs. Nature Ecology and Evolution 2:1227.

Apaldetti, C., R. N. Martínez, D. Pol, and T. Souter. 2014. Redescription of the skull of *Coloradisaurus brevis* (Dinosauria, Sauropodomorpha) from the Late Triassic Los Colorados Formation of the Ischigualasto-Villa Union Basin, northwestern Argentina. Journal of Vertebrate Paleontology 34:1113–1132.

Barrett, P. M., P. Upchurch, X.-D. Zhou, and X.-L. Wang. 2007. The skull of *Yunnanosaurus huangi* Young, 1942 (Dinosauria: Prosauropoda) from the Lower Lufeng Formation (Lower Jurassic) of Yunnan, China. Zoological Journal of the Linnean Society 150:319–341.

Benson, R. B., G. Hunt, M. T. Carrano, and N. Campione. 2018. Cope's rule and the adaptive landscape of dinosaur body size evolution. Palaeontology 61:13–48.

Bonnan, M. F., and P. Senter. 2007. Were the basal sauropodomorph dinosaurs *Plateosaurus* and *Massospondylus* habitual quadrupeds? Special Papers in Palaeontology 77:139–155.

Bonnan, M. F., and A. M. Yates. 2007. A new description of the forelimb of the basal sauropodomorph *Melanorosaurus*: implications for the evolution of pronation, manus shape and quadrupedalism in sauropod dinosaurs. Special Papers in Palaeontology 77:157–168.

Bordy, E. M., P. J. Hancox, and B. S. Rubidge. 2004. Basin development during the deposition of the Elliot Formation (Late Triassic–Early Jurassic), Karoo Supergroup, South Africa. South African Journal of Geology 107:397–412.

Cabreira, S. F., C. L. Schultz, J. S. Bittencourt, M. B. Soares, D. C. Fortier, L. R. Silva, and M. C. Langer. 2011. New stem-sauropodomorph (Dinosauria, Saurischia) from the Triassic of Brazil. Naturwissenschaften 98:1035–1040.

Campione, N. E., and D. C. Evans. 2012. A universal scaling relationship between body mass and proximal limb bone dimensions in quadrupedal terrestrial tetrapods. BMC Biology, 10:60–81.

Campione, N. E., D. C. Evans, C. M. Brown, and M. T. Carrano. 2014. Body mass estimation in non-avian bipeds using a theoretical conversion to quadruped stylopodial proportions. Methods in Ecology and Evolution, 5:913–923.

Charig, A. J., J. Attridge, and A. W. Crompton. 1965. On the origin of the sauropods and the classification of the Saurischia. Proceedings of the Linnean Society of London 176:197–221.

Chure, D., B. B. Britt, J. A. Whitlock and J. A. Wilson. 2010. First complete sauropod dinosaur skull from the Cretaceous of the Americas and the evolution of sauropod dentition. Naturwissenschaften 97:379–391.

Department of Mines and Geology of Lesotho. 1982. Geological map of Lesotho, Maseru, Lesotho. 1:250,000. Government of the United Kingdom (Directorate of Overseas Surveys) for the Government of Lesotho. UNDP Exploration for Minerals Project, D.O.S. series:Les Geol 250 (DOS 621/1).

Eberth, D. A., M. Shannon and B. G. Noland 2007. A Bonebeds Database : Classification, Biases, and Patterns of Occurrence; pp. 103–131 in R. R. Rogers, D. A. Eberth and A.

R. Fiorillo (eds.), Bonebeds : Genesis, analysis, and paleobiological significance, University of Chicago Press, Chicago.

Ellenberger, P. 1955. Note préliminaire sur les pistes et restes osseux de vertébrés du Basutoland (Afrique du Sud). Comptes Rendus de l'Académie des Sciences 240:889–891.

Ellenberger, P. 1970. Les niveaux paléontologiques de première apparition des mammifères primordiaux en Afrique du Sud et leur ichnologie : établissement de zones stratigraphiques détaillées dans le Stormberg du Lesotho (Afrique du Sud) (Trias supérieur à Jurassique); pp. 343–370 in S. H. Haughton (ed.), IUGS Commission on Stratigraphy: Proceedings and Papers of the 2nd Gondwana Symposium, Pretoria, July to August 1970.

Ellenberger, F., and P. Ellenberger. 1956a. Quelques précisions sur la série du Stormberg au Basutoland (Afrique du Sud). Comptes Rendus de l'Académie des Sciences 242:799–801.

Ellenberger, F., and P. Ellenberger. 1956b. Le gisement de dinosauriens de Maphutseng. Compte Rendu Sommaire de la Société Géologique de France 8:99–101.

Ellenberger, F., and P. Ellenberger. 1960. Sur une nouvelle dalle à pistes de vertébrés découverte au Basutoland (Afrique du Sud). Compte Rendu Sommaire de la Société Géologique de France 9:236–237.

Ellenberger, F., and L. Ginsburg. 1966. Le gisement de dinosauriens triasiques de Maphutseng (Basutoland) et l'origine des sauropodes. Comptes Rendus de l'Académie des Sciences 262:444–447.

Ellenberger, F., P. Ellenberger, and L. Ginsburg. 1970. Les dinosaures du Trias et du Lias en France et en Afrique du Sud, d'après les pistes qu'ils ont laissées. Bulletin de la Société Géologique de France 12:151–159.

Ellenberger, F., P. Ellenberger, J. Fabre, L. Ginsburg, and C. Mendrez. 1964. The Stormberg Series of Basutoland (South Africa); pp. 320–330 in R. K. Sundaram (ed.), International Geological Congress: Proceedings of the 22nd International Geological Congress, New Delhi, 14–22 December 1964.

Galton, P. M. 1999. Sex, sacra and *Sellosaurus gracilis* (Saurischia, Sauropodomorpha, Upper Triassic, Germany) - or why the character "two sacral vertebrae" is plesiomorphic for Dinosauria. Neues Jahrbuch für Geologie und Paläontologie-Abhandlungen 213:19–56.

Galton, P. M., and J. Van Heerden. 1998. Anatomy of the prosauropod dinosaur *Blikanasaurus cromptoni* (Upper Triassic, South Africa), with notes on the other tetrapods from the lower Elliot Formation. Paläontologische Zeitschrift 72:163–177.

Galton, P. M., and P. Upchurch. 2004. Prosauropoda; pp. 232–258 in D. B. Weishampel, P. Dodson, and H. Osmólska (eds.), The Dinosauria 2nd ed. University of California Press, Berkeley, California.

Gauffre, F.-X. 1993. Biochronostratigraphy of the lower Elliot Formation (southern Africa) and preliminary results on the Maphutseng dinosaur (Saurischia : Prosauropoda) from the same Formation of Lesotho. New Mexico Museum of Natural History and Science Bulletin 3:147–149.

Gauffre, F.-X. 1996. Phylogénie des dinosaures prosauropodes et étude d'un nouveau prosauropode du Trias supérieur d'Afrique australe. Dissertation, Muséum National d'Histoire Naturelle, Paris, France, 156 pp.

Van Gend, J., E. Bordy, R. Tucker, and B. McPhee. 2015. Maphutseng fossil heritage: stratigraphic context of the dinosaur trackways and bone bed in the Upper Triassic–Lower Jurassic Elliot Formation (Karoo Supergroup, Lesotho); pp. 67–68 in H. Saber, A. Lagnaoui, and A. Belahmira (eds.), ICCI: Proceeding of abstracts of the First International Congress on Continental Ichnology, El Jadida, 21–25 April 2015.

Goloboff, P.A. 1993. NONA 2.0. Published by the author, Tucumán, Argentina.

Haughton, S. H. 1924. Fauna and stratigraphy of the Stormberg series. Annals of the South African Museum 12:323–497.

Van Heerden, J. 1979. The morphology and taxonomy of *Euskelosaurus* (Reptilia: Saurischia; Late Triassic) from South Africa. Navorsinge van die Nasionale Museum 4:21–84.

Van Heerden, J., and P. M. Galton. 1997. The affinities of *Melanorosaurus* – a Late Triassic prosauropod dinosaur from South Africa. Neues Jahrbuch für Geologie und Paläontologie 1:39–55.

Huxley, T. H. 1866. On the remains of large dinosaurian reptiles from the Stormberg mountains, South Africa. Geological Magazine 3:563–564.

Johnson, M. R., C. J. Van Vauuren, W. F. Hegenberger, R. Key, and U. Shoko. 1996. Stratigraphy of the Karoo Supergroup in southern Africa: an overview. Journal of African Earth Sciences 23:3–15.

Kitching, J. W., and M. A. Raath. 1984. Fossils from the Elliot and Clarens Formations (Karoo sequence) of the Northeastern Cape, Orange Free State and Lesotho, and a suggested biozonation based on tetrapods. Palaeontologia Africana 25:111–125.

Knoll, F. 2004. Review of the tetrapod fauna of the “Lower Stormberg Group” of the main Karoo Basin (southern Africa): implication for the age of the lower Elliot Formation. Bulletin de la Société Géologique de France 175:73–83.

Langer, M. C., F. Abdala, M. Richter, and M. J. Benton. 1999. A sauropodomorph dinosaur from the Upper Triassic (Carnian) of southern Brazil. Comptes Rendus de l’Académie des Sciences, Sciences de la terre et des planètes 329:511–517.

Marsh, A. D., and T. B. Rowe. 2018. Anatomy and systematics of the sauropodomorph *Sarahsaurus aurifontanalis* from the Early Jurassic Kayenta Formation. PLoS ONE 13: e0204007.

McPhee, B. W., R. B. Benson, J. Botha-Brink, E. M. Bordy, and J. N. Choiniere. 2018. A giant dinosaur from the earliest Jurassic of South Africa and the transition to quadrupedality in early sauropodomorphs. Current Biology 28:3143–3151.

McPhee, B. W., E. M. Bordy, L. Sciscio, and J. N. Choiniere. 2017. The sauropodomorph biostratigraphy of the Elliot Formation of southern Africa: Tracking the evolution of Sauropodomorpha across the Triassic–Jurassic boundary. Acta Palaeontologica Polonica 62:441–465.

McPhee, B. W., J. Choiniere, A. M. Yates, and P. A. Viglietti. 2015. A second species of *Eucnemesaurus* Van Hoepen, 1920 (Dinosauria, Sauropodomorpha): new information on the diversity and evolution of the sauropodomorph fauna of South Africa's lower Elliot Formation (latest Triassic). Journal of Vertebrate Paleontology 35:e980504.

McPhee, B. W., A. M. Yates, J. N. Choiniere, and F. Abdala. 2014. The complete anatomy and phylogenetic relationships of *Antetonitrus ingenipes* (Sauropodiformes, Dinosauria): implications for the origins of Sauropoda. Zoological Journal of the Linnean Society 171:151–205.

Moser, M. 2003. *Plateosaurus engelhardti* Meyer, 1837 (Dinosauria: Sauropodomorpha) aus dem Feuerletten (Mittelkeuper; Obertrias) von Bayern. Zitteliana B 24:3–186.

Nixon, K. C. 2002. WinClada 1.00.08. Published by the author, Ithaca, New York, USA.

Otero, A., and D. Pol. 2013. Postcranial anatomy and phylogenetic relationships of *Mussaurus patagonicus* (Dinosauria, Sauropodomorpha). Journal of Vertebrate Paleontology 33:1138–1168.

Otero, A., V. Allen, D. Pol, and J. R. Hutchinson. 2017. Forelimb muscle and joint actions in Archosauria: insights from *Crocodylus johnstoni* (Pseudosuchia) and *Mussaurus patagonicus* (Sauropodomorpha). PeerJ 5:e3976.

Peyre de Fabrègues, C., and R. Allain. 2016. New material and revision of *Melanorosaurus thabanensis*, a basal sauropodomorph from the Upper Triassic of Lesotho. PeerJ 4:e1639.

Peyre de Fabrègues, C., R. Allain, and V. Barriel. 2015. Root causes of phylogenetic incongruence observed within basal sauropodomorph interrelationships. *Zoological Journal of the Linnean Society* 175:569–586.

Pol, D., and J. E. Powell. 2007. New information on *Lessemsaurus sauropoides* (Dinosauria: Sauropodomorpha) from the Upper Triassic of Argentina. Special Papers in Palaeontology 77:223–243.

Pol, D., A. Garrido, and I. A. Cerda. 2011. A new sauropodomorph dinosaur from the Early Jurassic of Patagonia and the origin and evolution of the sauropod-type sacrum. PLoS ONE 6:e14572.

Racey, A. 2009. Mesozoic red bed sequences from SE Asia and the significance of the Khorat Group of NE Thailand; pp. 41–67 in E. Buffetaut, G. Cuny, J. Le loeuff, and V. Suteethorn (eds.), Late Palaeozoic and Mesozoic Ecosystems in SE Asia, Geological Society Special Publications, London, England.

Racey, A., and J. G. S. Goodall. 2009. Palynology and stratigraphy of the Mesozoic Khorat Group red bed sequences from Thailand; pp. 69–83 in E. Buffetaut, G. Cuny, J. Le loeuff, and V. Suteethorn (eds.), Late Palaeozoic and Mesozoic Ecosystems in SE Asia, Geological Society Special Publications, London, England.

Remes, K. 2008. Evolution of the pectoral girdle and forelimb in Sauropodomorpha (Dinosauria, Saurischia): osteology, myology and function. Dissertation, Ludwig-Maximilians Universität, München, Germany, 355 pp.

De Ricqlès, A. J., K. Padian, and J. R. Horner. 2003. On the bone histology of some Triassic pseudosuchian archosaurs and related taxa. Annales de Paléontologie 89:67–101.

Rowe, T. B., H.-D. Sues, and R. R. Reisz. 2010. Dispersal and diversity in the earliest north american sauropodomorph dinosaurs, with a description of a new taxon. Proceedings of the Royal Society of London B 278:1044–1053.

Salgado, L., R. A. Coria, and J. O. Calvo. 1997. Evolution of titanosaurid sauropods. I: phylogenetic analysis based on the postcranial evidence. *Ameghiniana* 34:3–32.

Sander, P. M. 1992. The Norian *Plateosaurus* bonebeds of central Europe and their taphonomy. Palaeogeography, Palaeoclimatology, Palaeoecology, 93:255–299.

Sander, P. M., and N. Klein. 2005. Developmental plasticity in the life history of a prosauropod dinosaur. Science 310:1800–1802.

Sekiya, T. 2010. A new prosauropod dinosaur from the Early Jurassic Lower Lufeng Formation in Lufeng, Yunnan. Global Geology 29:6–15.

Sereno, P. C., R. N. Martínez, and O. A. Alcober. 2013. Osteology of *Eoraptor lunensis* (Dinosauria, Sauropodomorpha). Journal of Vertebrate Paleontology 32:83–179.

SACS (South African Committee for Stratigraphy). 1980. Stratigraphy of South Africa. Part I: Lithostratigraphy of the Republic of South Africa, South West Africa/Namibia and the Republics of Bophuthatswana, Transkei and Venda. Government Printer, Pretoria, South Africa, 690pp.

Sciscio, L., M. de Kock, E. Bordy, and F. Knoll. 2017. Magnetostratigraphy across the Triassic-Jurassic boundary in the main Karoo Basin. Gondwana Research 51:177–192.

Upchurch, P., P. M. Barrett, and P. Dodson. 2004. Sauropoda; pp. 259–322 in D. B. Weishampel, P. Dodson, and H. Osmólska (eds.), The Dinosauria 2nd ed. University of California Press, Berkeley, California.

Wang, Y.-M., H.-L. You, and T. Wang. 2017. A new basal sauropodiform dinosaur from the Lower Jurassic of Yunnan Province. Scientific Reports 7:41881.

Wilson, J. A. 2012. New vertebral laminae and patterns of serial variation in vertebral laminae of sauropod dinosaurs. Contributions from the Museum of Paleontology, University of Michigan 32:91–110.

Yates, A. M. 2004. The death of a dinosaur: dismembering *Euskelosaurus*. Geoscience Africa 2004:715.

Yates, A. M. 2007a. Solving a dinosaurian puzzle: the identity of *Aliwalia rex* Galton. Historical Biology 19:93–123.

Yates, A. M. 2007b. The first complete skull of the Triassic dinosaur *Melanorosaurus* Haughton (Sauropodomorpha: Anchisauria). Special Papers in Palaeontology 77:9–55.

Yates, A. M. 2010. A revision of the problematic sauropodomorph dinosaurs from Manchester, Connecticut and the status of *Anchisaurus* Marsh. Palaeontology 53:739–752.

Zhang, Y., and D. Yang. 1994. A new complete osteology of Prosauropoda in Lufeng Basin, Yunnan, China. Yunnan Publishing House of Science and Technology, Kunming, China, 100 pp.

Submitted March DD, 2019; accepted Month DD, YYYY.

FIGURE CAPTIONS

FIGURE 1. Maphutseng bone bed location and excavation plan. **A**, Geological map drawn by F. Ellenberger situating the Maphutseng bone bed (“Gisement”, F) relative to the trackways (“Pistes”) and to the Protestant mission (“PEMS”) (Ellenberger archives, ISEM); **B**, Satellite view framed in a similar way than the drawing, showing the exact location of the Maphutseng bone bed (F) and the river as a reference (Image © 2018 DigitalGlobe); **C**, Excavation plan of

the 1955/56 and 1959 campaigns drawn by F. Ellenberger (Ellenberger archives, ISEM). The location of the 1963 and 1970 excavations were deduced thanks to a more comprehensive excavation plan figured in Gauffre (1996:fig. 21). [planned for page width]

FIGURE 2. Photographs of the excavations on the Maphutseng bone bed during the last campaign, in 1970. **A**, The excavation site. The photography was taken by P. Ellenberger. On the right side of the photography, from right to left: B. Battail and L. Ginsburg (Ellenberger archives, ISEM); **B**, Bones in situ. This photography was taken by B. Battail and illustrates perfectly the status of bone bed attributed to Maphutseng. From left to right and top to bottom appear: a caudal vertebra, a tibia, a right femur, an ischium, an ilium, a left femur, several metatarsals and phalanges. [planned for 2/3 width]

FIGURE 3. Geological map of Lesotho showing the five geological Formations outcropping and the Maphutseng bone bed as part of the Elliot Formation, based on the Geological map of Lesotho of the Department of Mines and Geology of Lesotho (1982). [planned for page width]

FIGURE 4. *Kholumolumo ellenbergerorum* postorbitals. Left postorbital (MNHN.F.LES153) in lateral (**A**) and medial (**B**) views; Right postorbital (MNHN.F.LES54) in lateral (**C**) and medial (**D**) views. **Abbreviations**: **apr**, anterior process; **cfr**, contact with frontal; **cpa**, contact with parietal; **csq**, contact with squamosal; **ppr**, posterior process; **ru**, orbital rugosity; **vpr**, ventral process. Scale bar equals 1 cm. [planned for page width]

FIGURE 5. *Kholumolumo ellenbergerorum* posterior cervical vertebra (C10?) (MNHN.F.LES169). **A**, right lateral view; **B**, left lateral view; **C**, posterior view; **D**, anterior

view; **E**, dorsal view; **F**, ventral view. **Abbreviations**: **di**, diapophysis; **hpo**, hyposphene; **hy**, hypapophysis; **nc**, neural canal; **ns**, neural spine; **poz**, postzygapophysis; **pp**, parapophysis; **prz**, prezygapophysis; **vk**, ventral keel. Scale bar equals 5 cm. [planned for page width]

FIGURE 6. *Kholumolumo ellenbergerorum* anterior dorsal (D1?) neural arch (MNHN.F.LES397). **A**, dorsal view; **B**, right lateral view; **C**, posterior view; **D**, anterior view. **Abbreviations**: **cdf**, centrodiapophyseal fossa; **cpol**, centropostzygapophyseal lamina; **cprl**, centroprezygapophyseal lamina; **di**, diapophysis; **hpo**, hyposphene; **nc**, neural canal; **ns**, neural spine; **pcdl**, posterocentrodiapophyseal lamina; **pocdf**, postzygapophyseal centrodiapophyseal fossa; **podl**, postzygodiapophyseal lamina; **poz**, postzygapophysis; **prcdf**, prezygapophyseal centrodiapophyseal fossa; **prdl**, prezygodiapophyseal lamina; **prz**, prezygapophysis. Scale bar equals 5 cm. [planned for page width]

FIGURE 7. *Kholumolumo ellenbergerorum* middle dorsal vertebra (D7-12?) (MNHN.F.LES32). **A**, right lateral view; **B**, anterior view; **C**, posterior view; **D**, anterior view. **Abbreviations**: **di**, diapophysis; **hpo**, hyposphene; **nc**, neural canal; **pcdl**, posterocentrodiapophyseal lamina; **pp**, parapophysis; **ppdl**, paradiapophyseal lamina; **prdl**, prezygodiapophyseal lamina; **prz**, prezygapophysis. Scale bar equals 5 cm. [planned for page width]

FIGURE 8. *Kholumolumo ellenbergerorum* primordial sacral vertebra (2?) (MNHN.F.LES155). **A**, posterior view; **B**, left lateral view; **C**, dorsal view. **Abbreviations**: **di**, diapophysis; **hpo**, hyposphene; **nc**, neural canal; **ns**, neural spine; **poz**, postzygapophysis; **sr**, sacral rib. Scale bar equals 10 cm. [planned for page width]

FIGURE 9. *Kholumolumo ellenbergerorum* anterior caudal vertebra (Ca1-5?) (MNHN.F.LES168). **A**, right lateral view; **B**, posterior view. **Abbreviations: nc**, neural canal; **ns**, neural spine; **poz**, postzygapophysis; **prz**, prezygapophysis. Scale bar equals 10 cm. [planned for 2/3 width]

FIGURE 10. *Kholumolumo ellenbergerorum* anterior caudal vertebra (Ca5-15?) (MNHN.F.LES376). **A**, anterior view; **B**, posterior view; **C**, left lateral view; **D**, dorsal view; **E**, ventral view. **Abbreviations: di**, diapophysis; **gr**, longitudinal groove; **nc**, neural canal; **ns**, neural spine; **poz**, postzygapophysis; **prz**, prezygapophysis. Scale bar equals 5 cm. [planned for page width]

FIGURE 11. *Kholumolumo ellenbergerorum* left scapula (MNHN.F.LES386). **A**, lateral view; **B**, medial view. **Abbreviations: ac**, acromion; **acf**, acromial fossa; **adr**, anterodorsal ridge; **gl**, glenoid; **nc**, neural canal; **ns**, neural spine; **pdr**, posterodorsal ridge; **rss**, ridge surrounding the attachment area of the muscle *serratus superficialis*; **sb**, scapular blade. Scale bar equals 10 cm. [planned for 2/3 width]

FIGURE 12. *Kholumolumo ellenbergerorum* left humerus (MNHN.F.LES379). **A**, anterior view; **B**, lateral view; **C**, posterior view; **D**, medial view; **E**, proximal view; **F**, distal view. **Abbreviations: cuf**, cuboid fossa; **dpc**, deltopectoral crest; **hh**, humerus head; **mt**, medial tuberosity; **olf**, olecranon fossa; **rc**, radial condyle; **uc**, ulnar condyle. The arrow indicates the anterior surface of the bone for E and F. Scale bar equals 10 cm. [planned for page width]

FIGURE 13. *Kholumolumo ellenbergerorum* right ulna (MNHN.F.LES159). **A**, anteromedial view; **B**, lateral view; **C**, posterolateral view; **D**, medial view; **E**, proximal view; **F**, distal

view. **Abbreviations: alp**, anterolateral process; **amp**, anteromedial process; **ol**, olecranon; **rf**, radial fossa. The arrow indicates the anterior surface of the bone for E and F. Scale bar equals 5 cm. [planned for page width]

FIGURE 14. *Kholumolumo ellenbergerorum* right radius (MNHN.F.LES147). **A**, anterior view; **B**, lateral view; **C**, posterior view; **D**, medial view; **E**, proximal view; **F**, distal view. The arrow indicates the anterior surface of the bone for E and F. Scale bar equals 5 cm. [planned for page width]

FIGURE 15. *Kholumolumo ellenbergerorum* elements of the manus (from top to bottom: metacarpals I to IV and phalange I-1. Respectively: MNHN.F.LES26, MNHN.F.LES92, MNHN.F.LES93, MNHN.F.LES76, MNHN.F.LES29). **A**, **F**, **K**, **P**, **T**, dorsal views; **B**, **G**, **L**, **Q**, **U**, ventral views; **C**, **H**, **M**, **R**, **V**, lateral views; **D**, **I**, **N**, **W**, proximal views; **E**, **J**, **O**, **S**, **X**, distal views. Scale bar equals 5 cm. [planned for page width]

FIGURE 16. *Kholumolumo ellenbergerorum* right ilium (MNHN.F.LES375a). **A**, lateral view; **B**, medial view; **C**, dorsal view; **D**, ventral view. **Abbreviations: ibl**, iliac blade; **isp**, ischial peduncle; **mwa**, medial wall of the acetabulum; **pop**, postacetabular process; **prp**, preacetabular process; **pup**, pubic peduncle; **sac**, supracetabular crest; **svi**, sacral vertebrae insertion. Scale bar equals 10 cm. [planned for 2/3 width]

FIGURE 17. *Kholumolumo ellenbergerorum* left pubis (MNHN.F.LES378). **A**, dorsal view; **B**, ventral view. **Abbreviations: ac**, acetabulum; **ilp**, iliac peduncle; **isp**, ischial peduncle; **of**, obturator foramen; **pa**, pubic apron; **pp**, pubic plate. Scale bar equals 10 cm. [planned for 2/3 width]

FIGURE 18. *Kholumolumo ellenbergerorum* incomplete left ischium (MNHN.F.LES152). A, medial view; **B**, lateral view; **C**, dorsal view. **Abbreviations: ac**, acetabulum; **ilp**, iliac peduncle; **pup**, pubic peduncle. Scale bar equals 10 cm. [planned for page width]

FIGURE 19. *Kholumolumo ellenbergerorum* right femur (MNHN.F.LES394). **A**, anterior view; **B**, lateral view; **C**, posterior view; **D**, medial view; **E**, proximal view; **F**, distal view. **Abbreviations: ef**, extensor fossa; **fc**, fibular condyle; **fh**, femoral head; **lc**, lateral condyle; **lt**, lesser trochanter; **mc**, medial condyle; **pf**, popliteal fossa; **4t**, fourth trochanter. The arrow indicates the anterior surface of the bone for E and F. Scale bar equals 10 cm. [planned for page width]

FIGURE 20. *Kholumolumo ellenbergerorum* right tibia (MNHN.F.LES381m). **A**, anterior view; **B**, lateral view; **C**, posterior view; **D**, medial view; **E**, proximal view; **F**, distal view. **Abbreviations: adp**, anterodistal process; **cnc**, cnemial crest; **lc**, lateral condyle; **lco**, lateral concavity; **mc**, medial condyle; **pdp**, posterodistal process. The arrow indicates the anterior surface of the bone for E and F. Scale bar equals 10 cm. [planned for page width]

FIGURE 21. *Kholumolumo ellenbergerorum* right fibula (MNHN.F.LES374). **A**, anterior view; **B**, lateral view; **C**, posterior view; **D**, medial view; **E**, proximal view; **F**, distal view. **Abbreviation: pmt**, proximomedial tubercle. The arrow indicates the anterior surface of the bone for E and F. Scale bar equals 10 cm. [planned for 2/3 width]

FIGURE 22. *Kholumolumo ellenbergerorum* elements of the pes (from top to bottom: metatarsals I to V. Respectively: MNHN.F.LES89, MNHN.F.LES81, MNHN.F.LES82,

MNHN.F.LES381c, MNHN.F.LES77). **A**, **F**, **K**, **P**, **T**, dorsal views; **B**, **G**, **L**, **Q**, **U**, ventral views; **C**, **H**, **M**, **R**, **V**, lateral views; **D**, **I**, **N**, **S**, **W**, proximal views; **E**, **J**, **O**, **S**, **X**, distal views. Scale bar equals 10 cm. [planned for page width]

FIGURE 23. Strict consensus tree (length=1451 steps) of the phylogenetic analysis conducted with 47 taxa and 372 characters and based on the matrix and scorings of Apaldetti et al., 2018 (except for *Kholumolumo*). The consensus is based on 24 MPTs of 1402 steps each. [planned for 2/3 width]

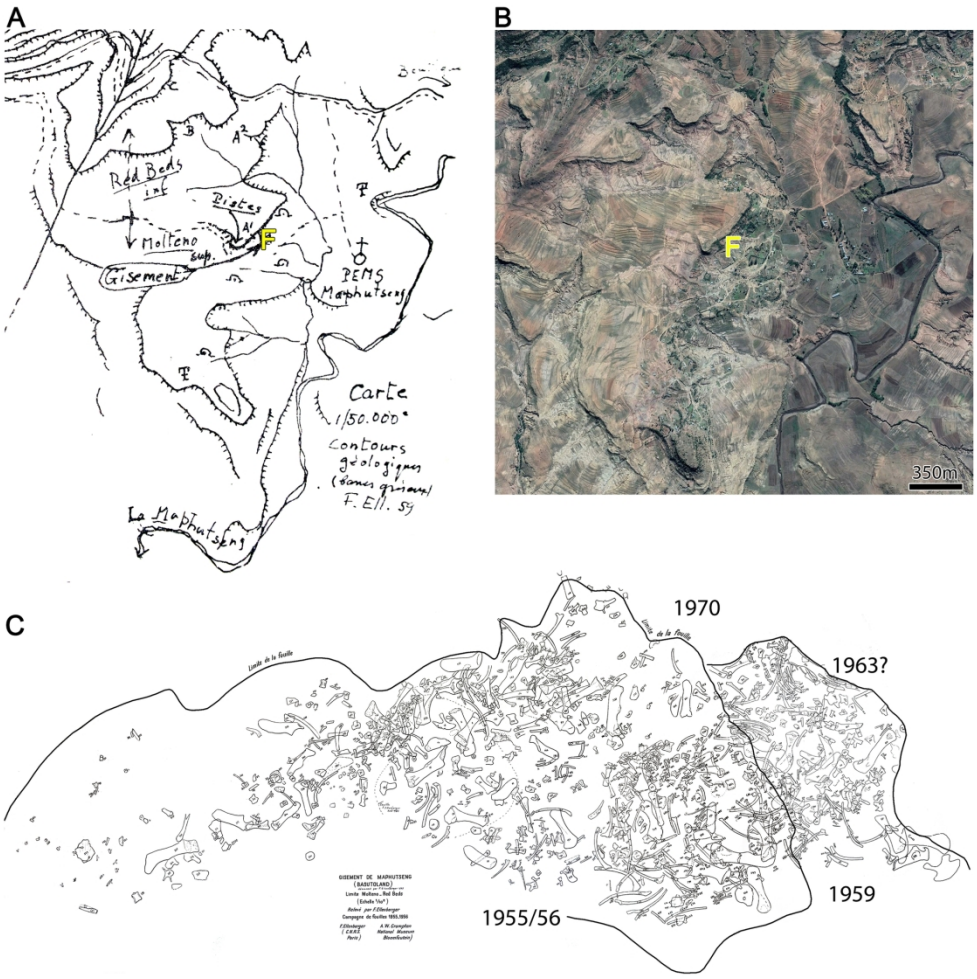

181x178mm (300 x 300 DPI)

121x159mm (300 x 300 DPI)

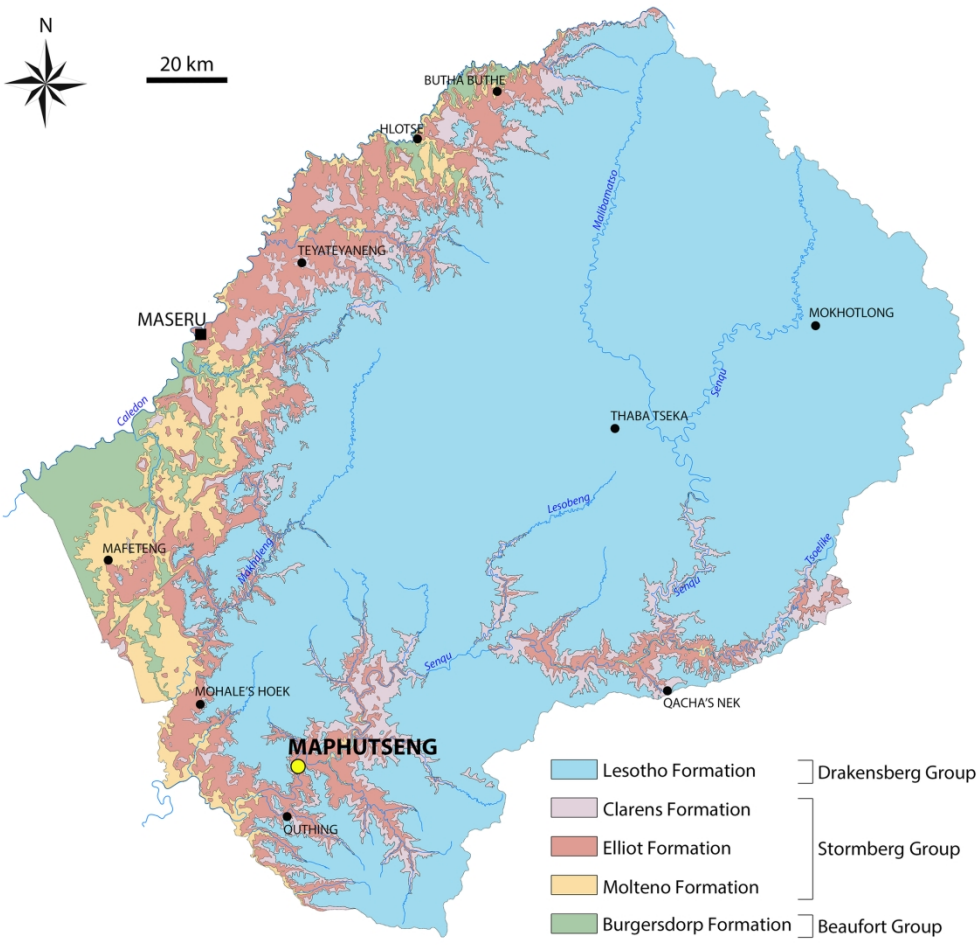

181x174mm (300 x 300 DPI)

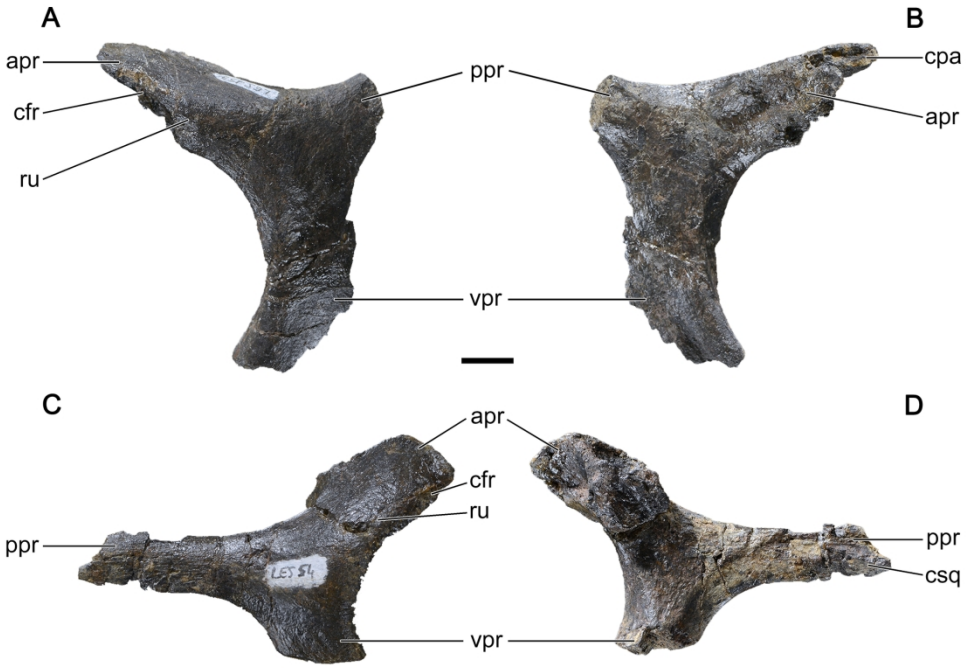

182x123mm (300 x 300 DPI)

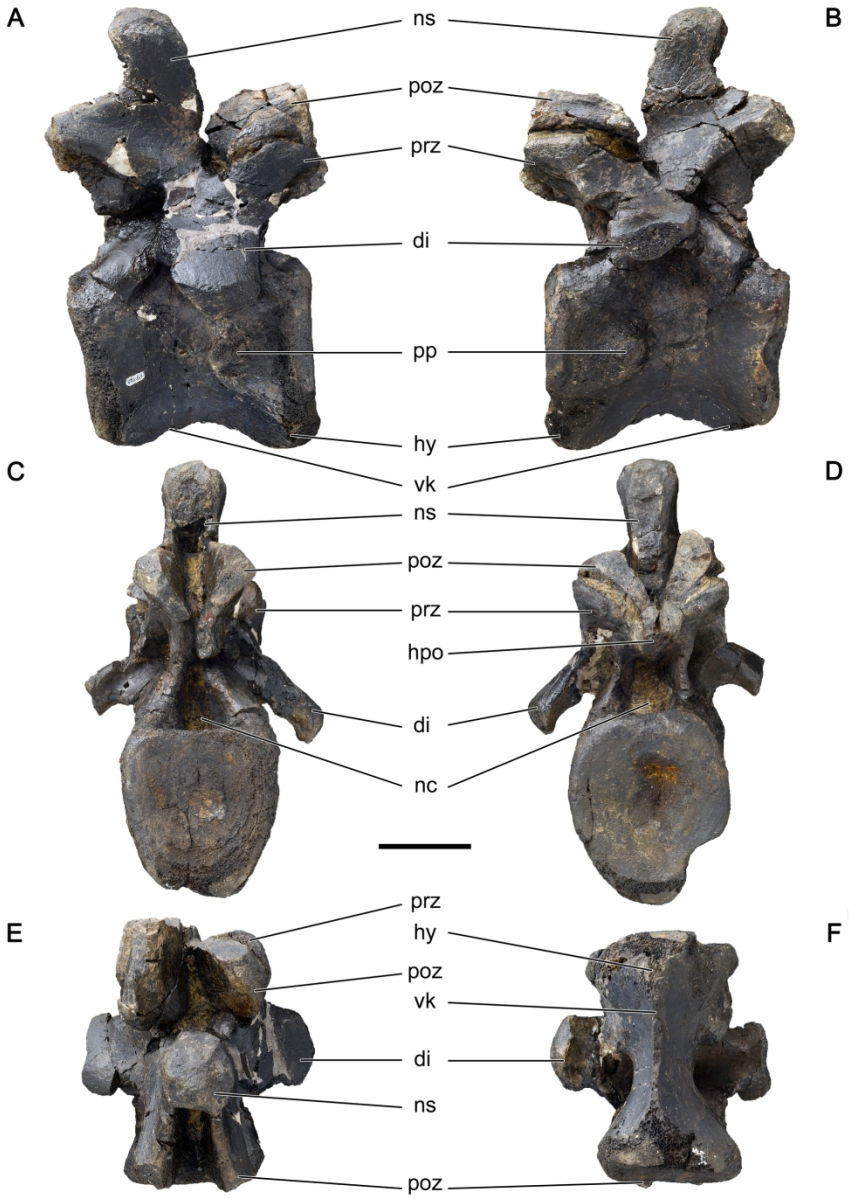

181x232mm (300 x 300 DPI)

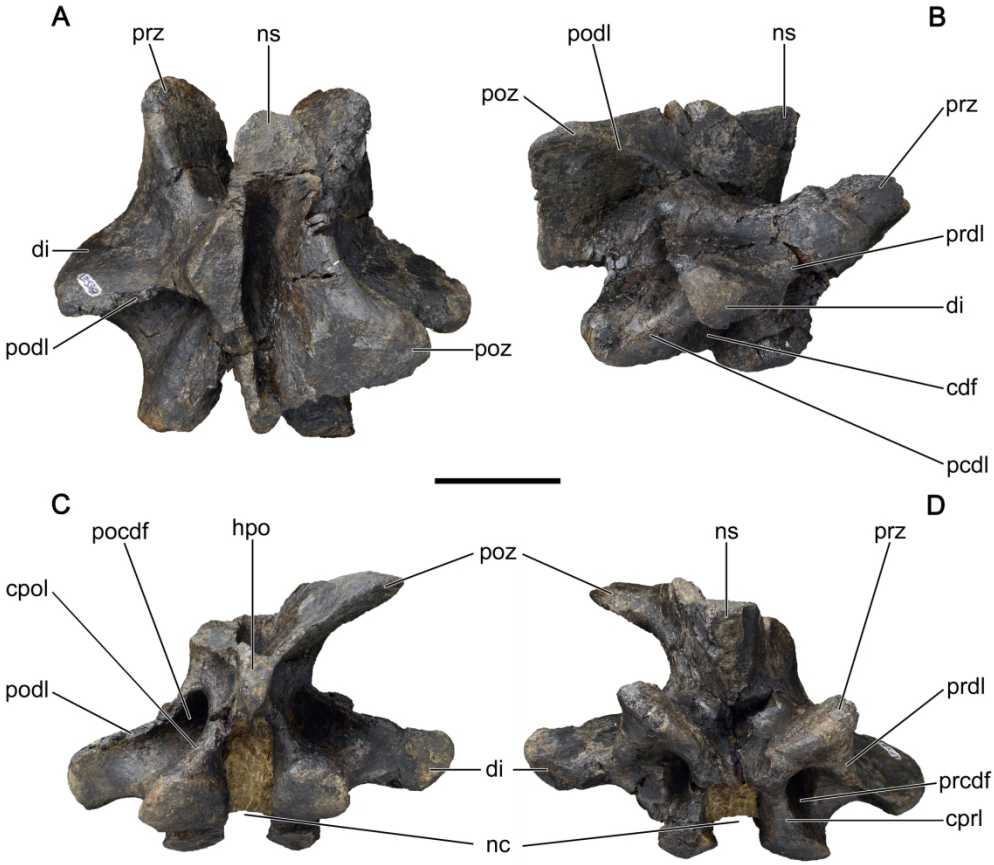

181x159mm (300 x 300 DPI)

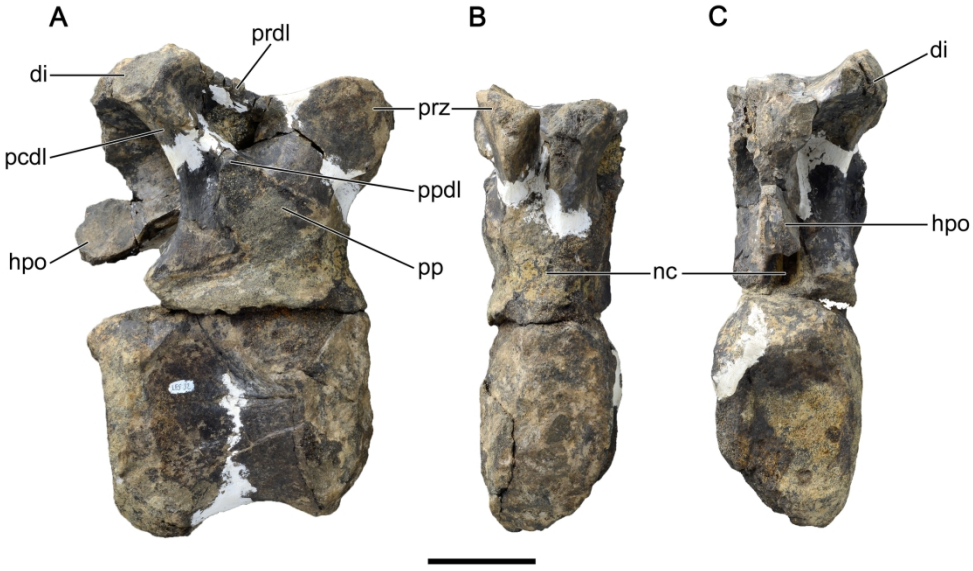

181x105mm (300 x 300 DPI)

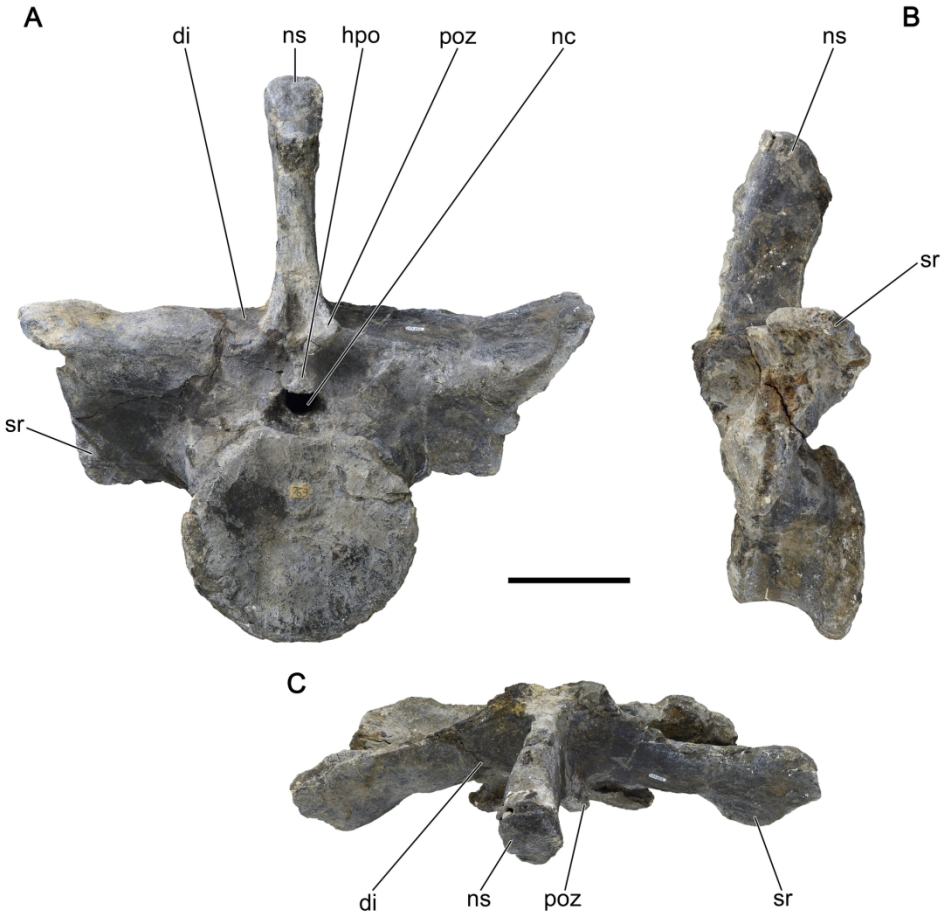

181x168mm (300 x 300 DPI)

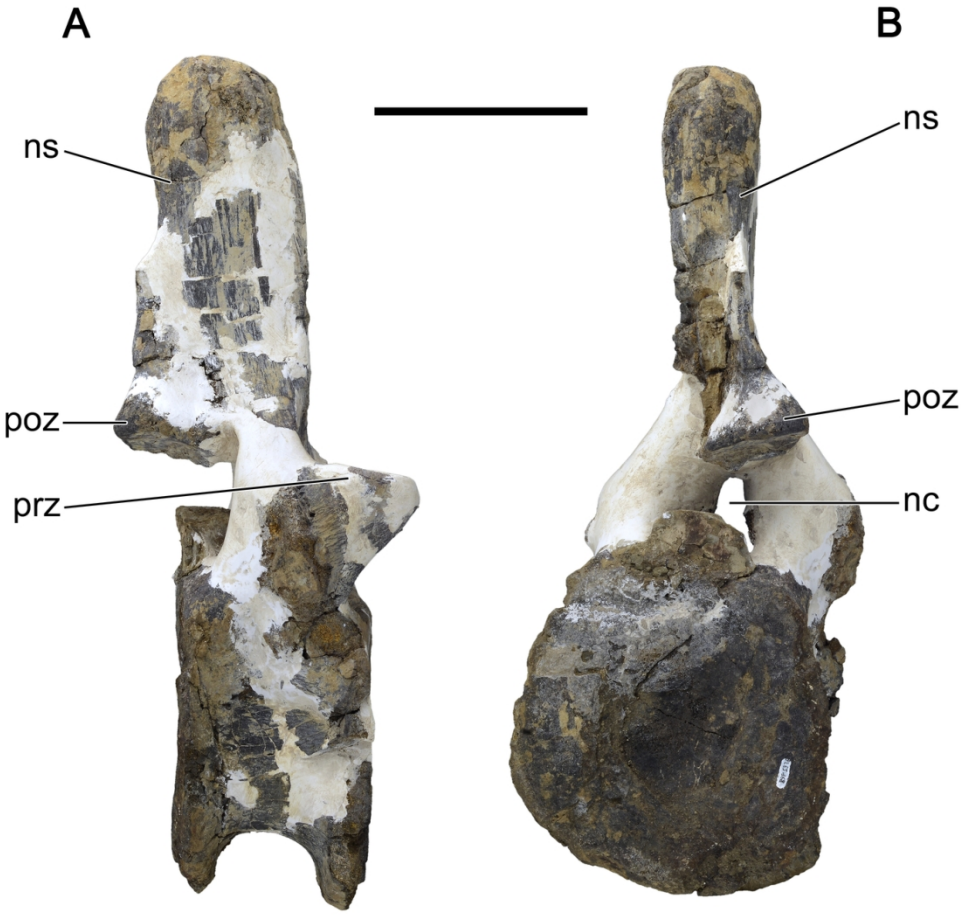

122x113mm (300 x 300 DPI)

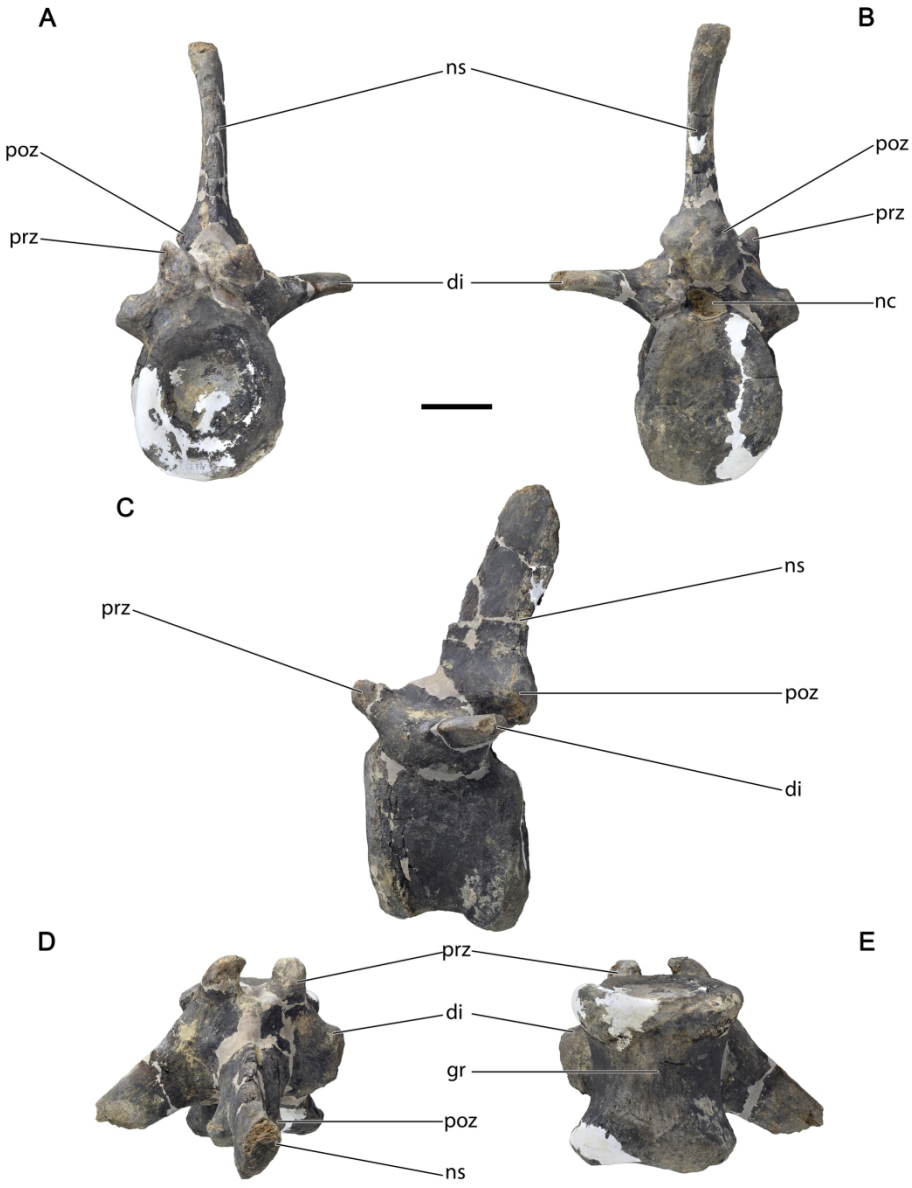

181x232mm (300 x 300 DPI)

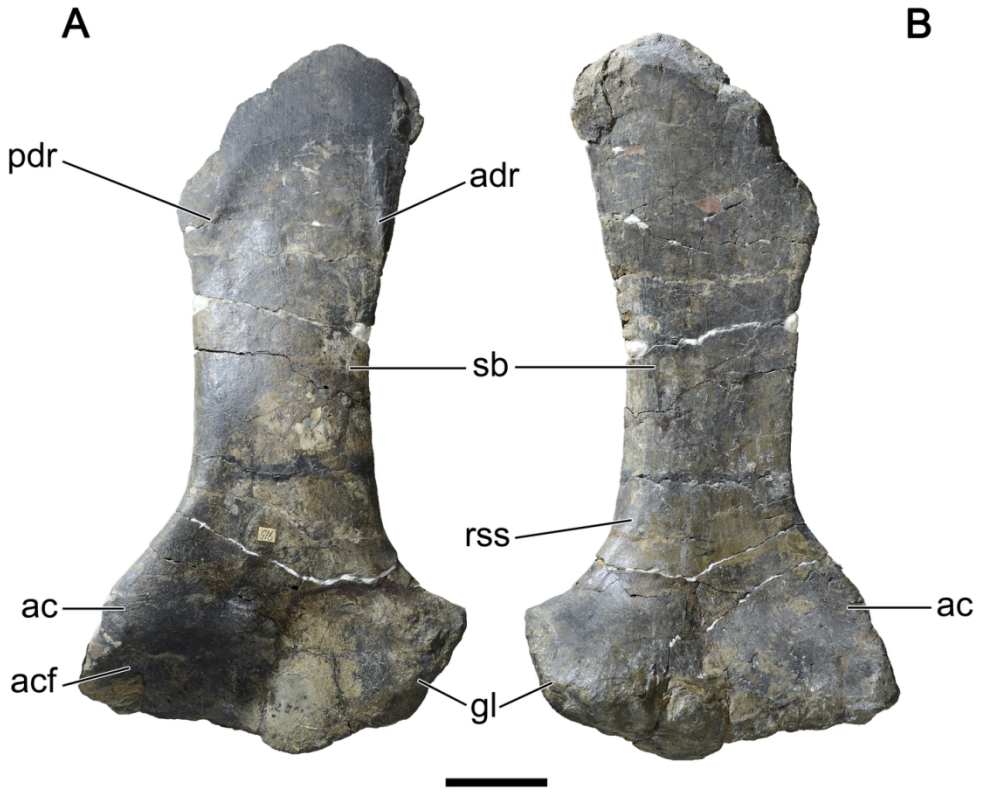

122x98mm (300 x 300 DPI)

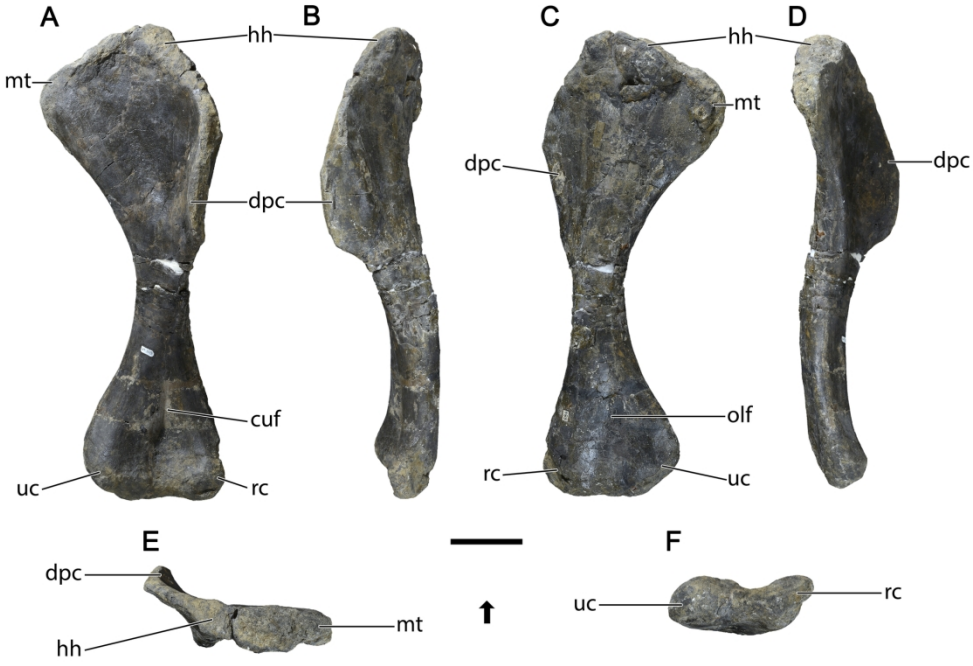

181x121mm (300 x 300 DPI)

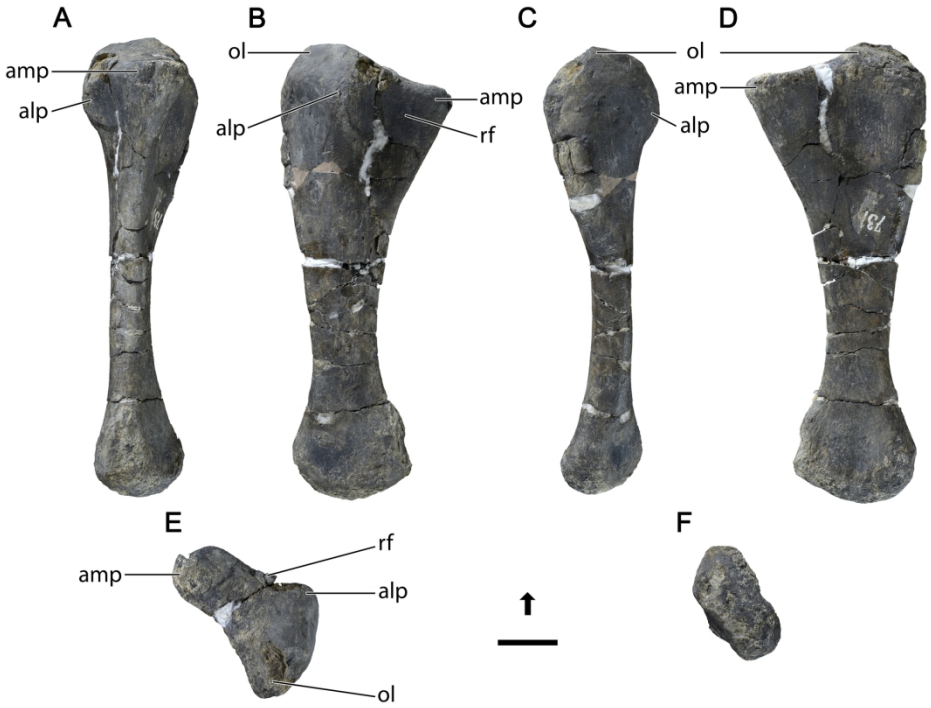

181x131mm (300 x 300 DPI)

181x131mm (300 x 300 DPI)

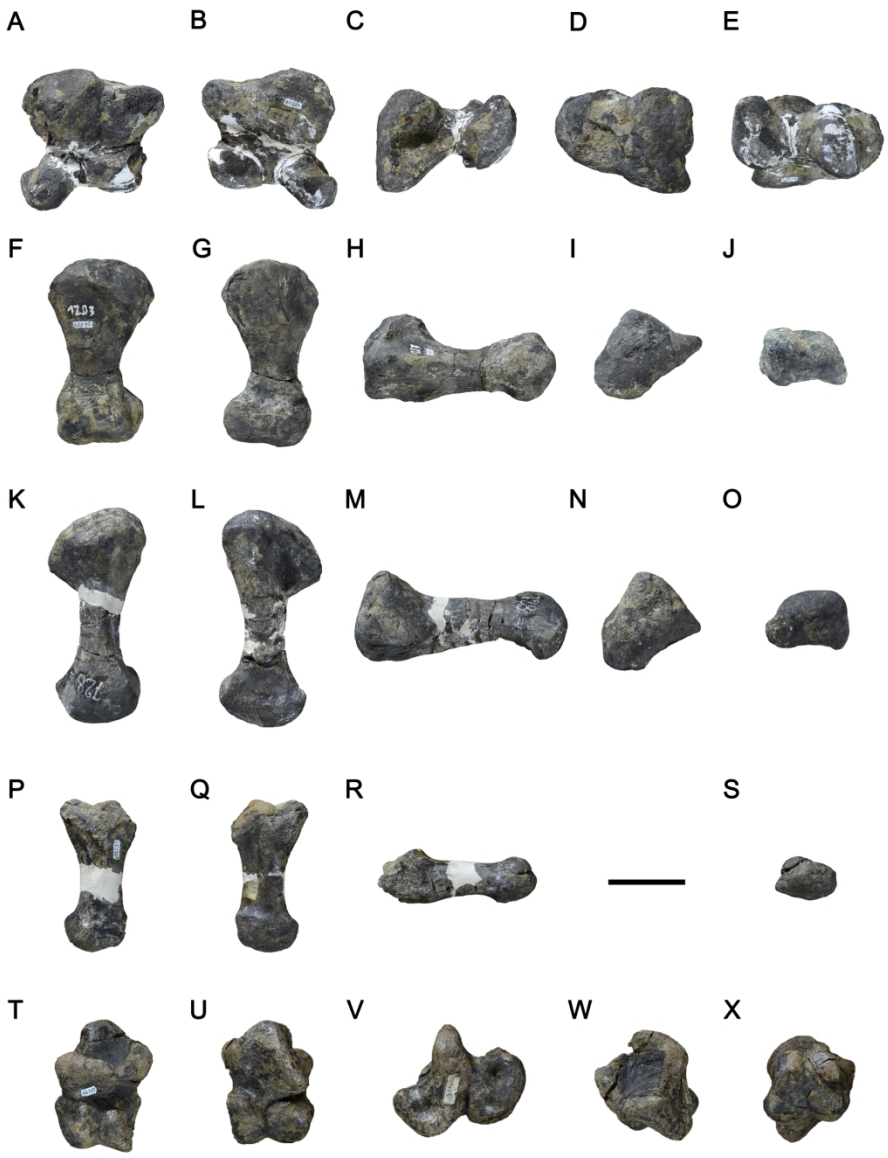

181x232mm (300 x 300 DPI)

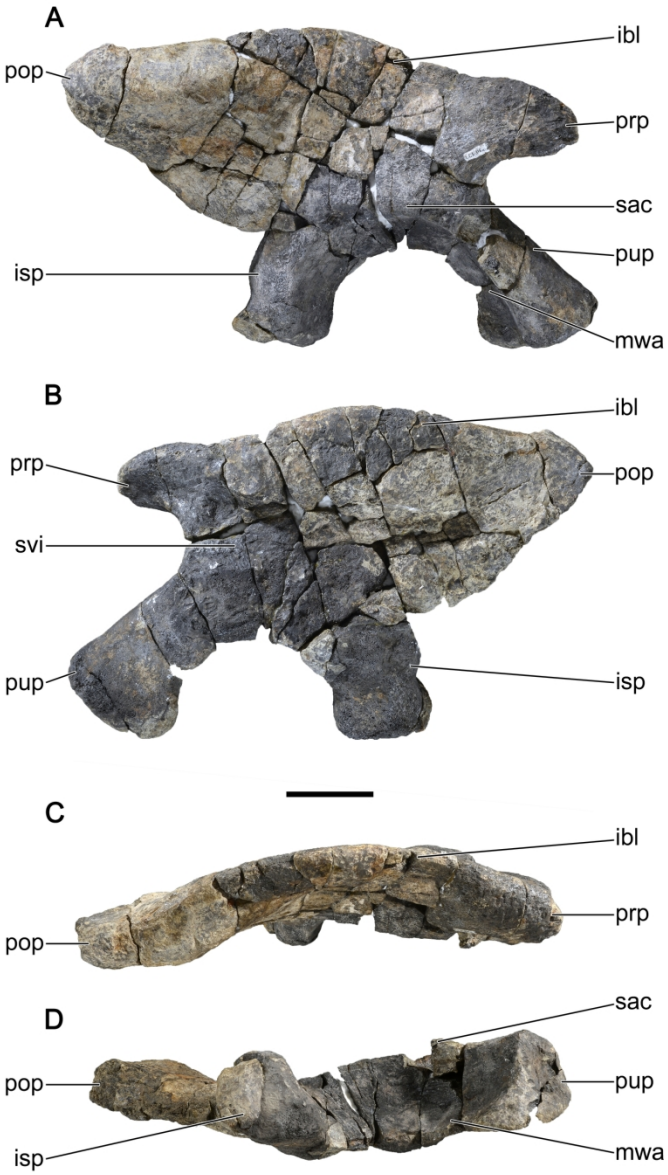

122x214mm (300 x 300 DPI)

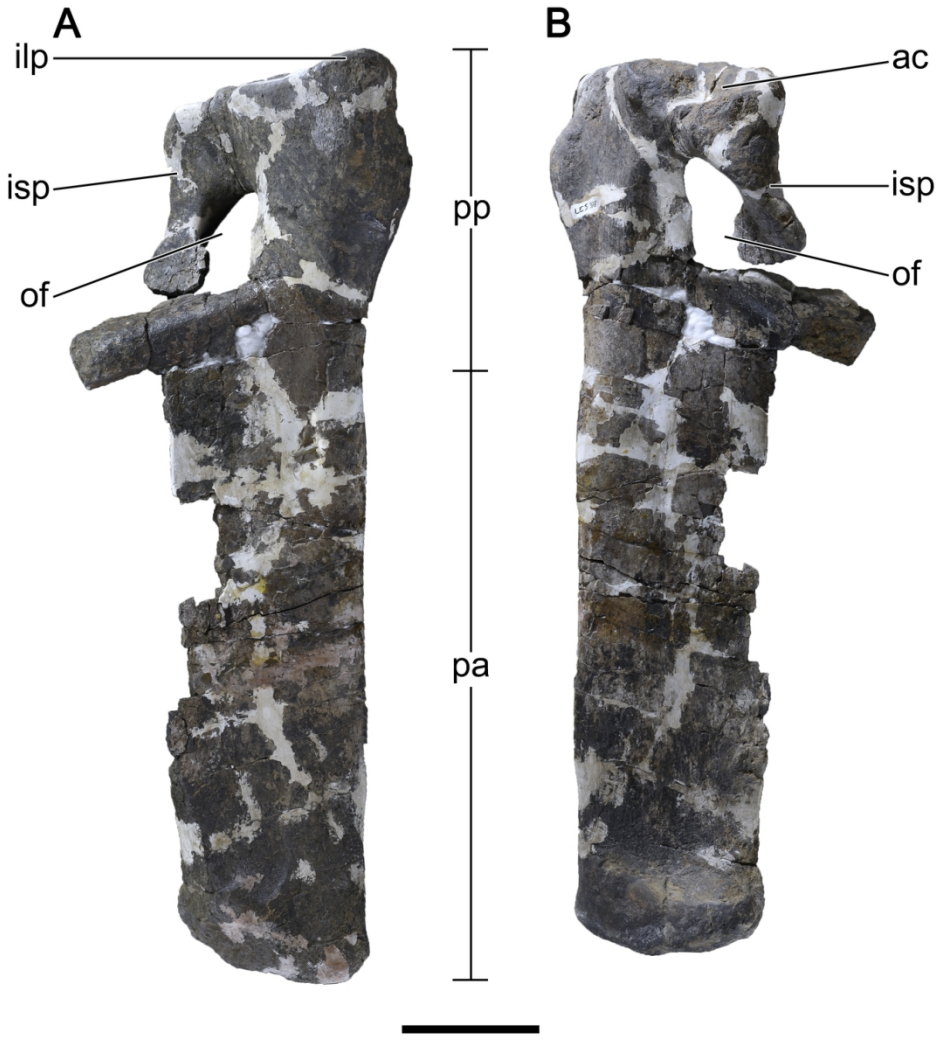

122x130mm (300 x 300 DPI)

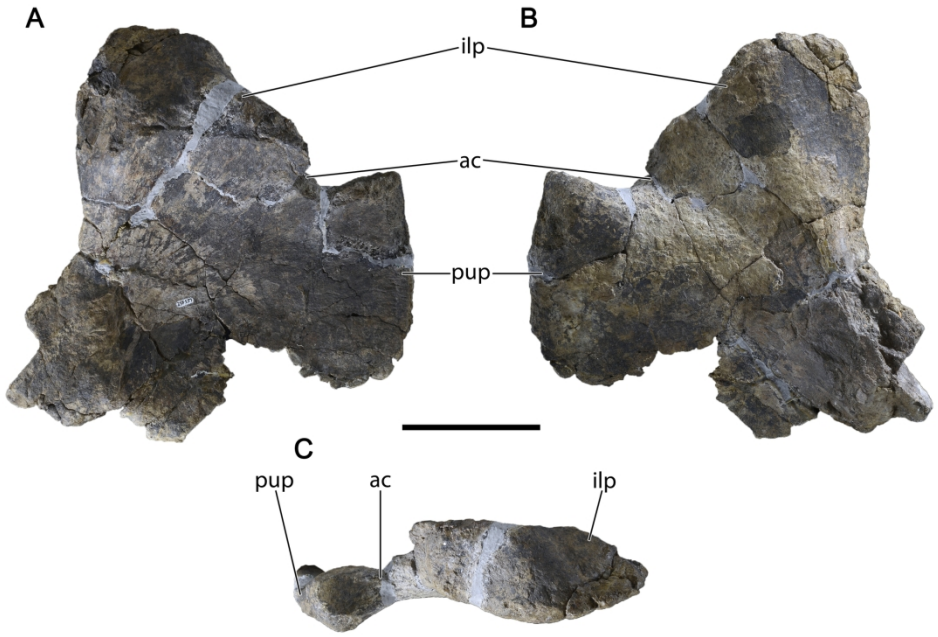

181x120mm (300 x 300 DPI)

181x149mm (300 x 300 DPI)

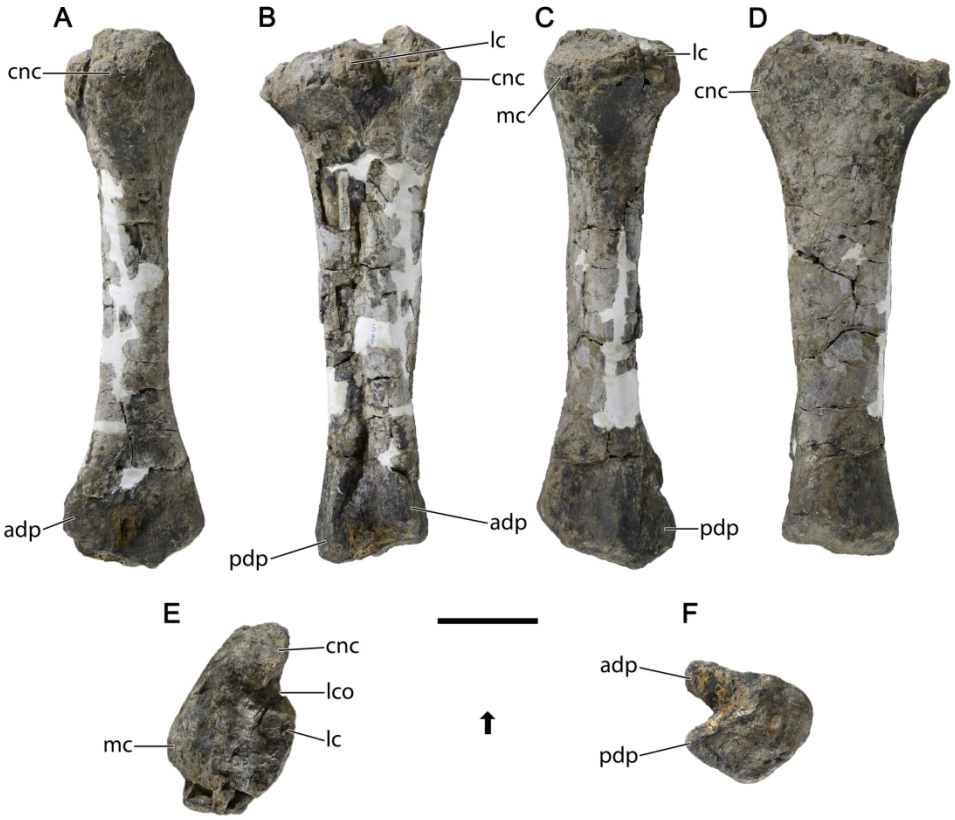

181x149mm (300 x 300 DPI)

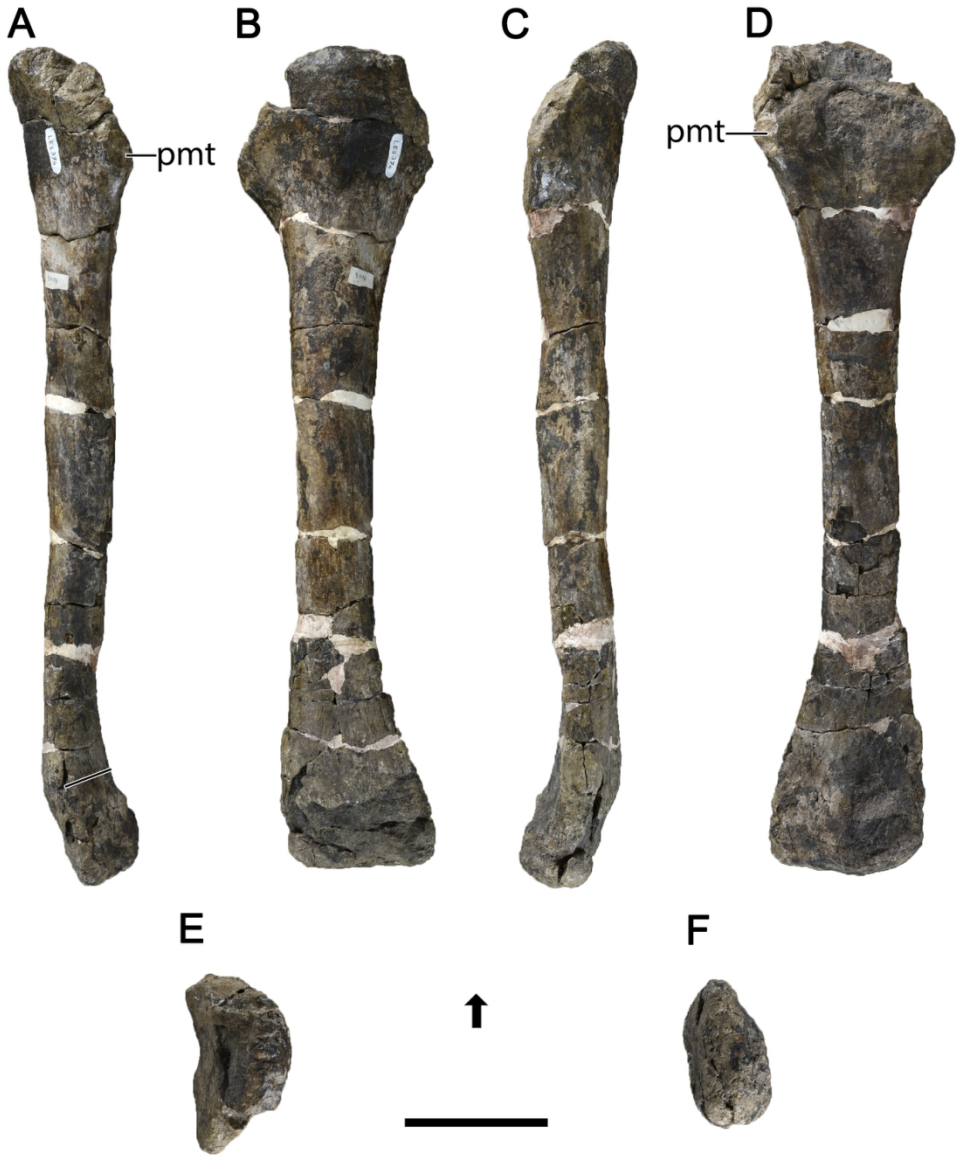

122x142mm (300 x 300 DPI)

181x232mm (300 x 300 DPI)

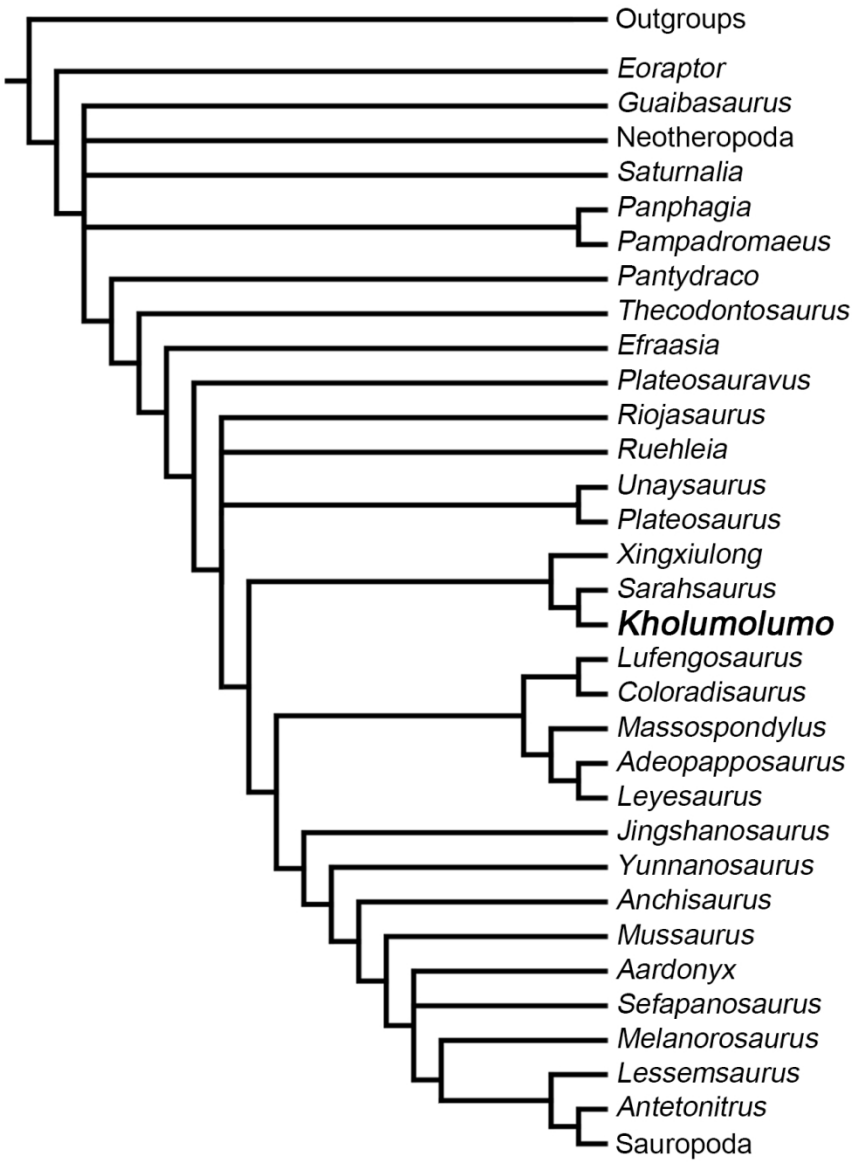
Outgroups
Eoraptor
Guaibasaurus
Neotheropoda
Saturnalia
Panphagia
Pampadromaeus
Pantydraco
Thecodontosaurus
Efraasia
Plateosauravus
Riojasaurus
Ruehleia
Unaysaurus
Plateosaurus
Xingxiulong
Sarahsaurus
Kholumolumo
Lufengosaurus
Coloradisaurus
Massospondylus
Adeopapposaurus
Leyesaurus
Jingshanosaurus
Yunnanosaurus
Anchisaurus
Mussaurus
Aardonyx
Sefapanosaurus
Melanorosaurus
Lessemsaurus
Antetonitrus
Sauropoda

TABLE 1. List of the five field campaigns in the Maphutseng bone bed, with the approximative number of attributed numbers on the field and the team involved in each campaign. In bold: MNHN researchers.

1955 August & September	1955 November 300 numbers attributed	1956 February 400 numbers attributed	1959 ? 200 numbers attributed	1963 Month? 100 numbers attributed	1970 September 300 numbers attributed
P. Ellenberger F. Ellenberger	P. Ellenberger F. Ellenberger A.W. Crompton R.F. Ewer	P. Ellenberger F. Ellenberger A.W. Crompton R.F. Ewer	P. Ellenberger F. Ellenberger H. Ellenberger **L. Ginsburg** **J. Fabre**	P. Ellenberger **L. Ginsburg** **J. Fabre** **C. Mendrez**	P. Ellenberger **L. Ginsburg** **J. Fabre** **B. Battail**

TABLE 2. Source of comparative data used in the anatomical descriptions. The underlined specimens were studied first-hand by the first author of this work.

Aardonyx celestae	BP/1/6254; Yates et al., 2010
Adeopapposaurus mognai	PVSJ 610; PVSJ 568; PVSJ 569; Martínez, 2009
Anchisaurus polyzelus	AM 41/109; YPM 208; YPM 1883; Galton, 1976; Fedak and Galton, 2007; Yates, 2010
Antetonitrus ingenipes	BP/1/4952; McPhee et al., 2014
Blikanasaurus cromptoni	SAM-PK-K403; Galton and Van Heerden, 1985, 1998
Camelotia borealis	Galton, 1998
Chromogisaurus novasi	PVSJ 845; Ezcurra, 2010; Martínez et al., 2013
Coloradisaurus brevis	PVL 3967; PVL 5904; Apaldetti et al., 2013, 2014
Efraasia minor	Galton, 1984; Yates, 2003
Eoraptor lunensis	PVSJ 512; Sereno et al., 2013
Eucnemesaurus entaxonis	McPhee et al., 2015
Jingshanosaurus xinwaensis	Zhang and Yang, 1994
Lamplughsaura dharmaramensis	Kutty et al., 2007
Leonerasaurus taquetrensis	MPEF-PV 1663; Pol et al., 2011
Lessemsaurus sauropoides	PVL 4822; Pol and Powell, 2007
Leyesaurus marayensis	PVSJ 706; Apaldetti et al., 2011
Lufengosaurus huenei	IVPP V15; Young, 1941; Barrett et al., 2005
Massospondylus carinatus	BP/1/4934; BP/1/5241; BP/1/4779; BP/1/5247; BP/1/4924; BP/1/4693; Sues et al., 2004; MNHN.F.LES15
Melanorosaurus readi	NM QR3314; NM QR1551; SAM-PK-3449; SAM-PK-3450
Meroktenos thabanensis	MNHN.F.LES16; MNHN.F.LES351
Mussaurus patagonicus	MLP 61-III-20-22; MLP 61-III-20-23; MLP 68-II-27-1; Pol and Powell, 2007; Otero and Pol, 2013
Pampadromaeus barberenai	Cabreira et al., 2011; Müller et al., 2016
Panphagia protos	PVSJ 874; Martínez and Alcober, 2009; Martínez et al., 2013
Plateosaurus longiceps	MB.R.1937; MB.R.4402; MB.R.4404; MB.R.4416
Pulanesaura eocollum	McPhee et al., 2015
Riojasaurus incertus	PVL 3808
Ruehleia bedheimensis	MB.R.4718; MB.R.4430; Galton, 2001
Sarahsaurus aurifontanalis	MCZ 8893; TMM 43646-2; Rowe et al., 2010
Saturnalia tupiniquim	MCP 3845-PV; MCP 3846-PV; Langer et al., 1999; Langer 2003; Langer et al., 2007
Sefapanosaurus zastronensis	BP/1/386; BP/1/7409–7455; Otero et al., 2015
Seitaad ruessi	Sertich and Loewen, 2010
Thecodontosaurus antiquus	Benton et al., 2000
Unaysaurus tolentinoi	UFSM11069; Leal et al., 2004
Xixiposaurus suni	Sekiya, 2010

TABLE 2. (Continued)

Yunnanosaurus huangi	IVPP V20; IVPP V505; Young, 1942; Barrett et al., 2007

TABLE 3. Selected measurements (mm) of the vertebrae of *Kholumolumo ellenbergerorum*. Abbreviations followinf the order of the table: **L**, maximum anteroposterior ventral length; **antW**, anterior width; **medW**, medial width; **postW**, posterior width; **antH**, anterior height; **postH**, posterior height; **naH**, neural arch height; **nsH**, maximum neural spine height; **nsL**, maximum neural spine length; **nsW**, maximum neural spine width measured at its distal end; **przD**, distance between the lateral borders of the prezygapophyses; **H**, total height; *****, deformation.

	CENTRUM						NEURAL ARCH					VERTEBRA
	L	antW	medW	postW	antH	postH	naH	nsH	nsL	nsW	przD	H
Cmid MNHN.F.LES338	?	65	30	?	78	?	?	?	?	?	?	?
Cmid MNHN.F.LES342	127	41*	20*	?	54*	?	?	?	?	?	?	?
C10? MNHN.F.LES169	132	90	34	85	105	92	150	46	39	37	88	255
D1? MNHN.F.LES397	?	?	?	?	?	?	>110	?	?	?	91	?
D2-3? MNHN.F.LES172	115	90*	33*	82*	117*	105*	?	?	?	?	?	?
D8-12? MNHN.F.LES32	120	63*	38*	71*	97*	108*	>120	?	?	?	68	>233
Sp2? MNHN.F.LES155	101	105	73	175	137	155	265	175	75	45	?	420
Ca1-5 MNHN.F.LES168	90	?	102	155	141	165	260	180	65	41	?	425
Ca5-15 MNHN.F.LES376	105	108	68	107	125	124	210	155	55	23	75	335
Ca15-25 MNHN.F.LES177	90	60	46	59	53	52	?	?	?	?	?	?
Ca25+ MNHN.F.LES35	65	35	25	34	34	29	?	?	?	?	?	?

TABLE 4. Selected measurements (mm) of the scapulae of *Kholumolumo ellenbergerorum*. Abbreviations following the order of the table: **L**, maximum dorsoventral length; **dW**, maximum distal width; **bW**, blade minimal anteroposterior width; **bT**, blade transversal thickness measured at midpoint on the posterior border; **pW**, maximum proximal width; **amxH**, acromion maximum height measured at the level of the point of divergence with the anterior border of the blade; **amnH**, acromion minimum height measured on its distal extremity; **aW**, acromion anteroposterior width measured at the level of the anterior border of the blade; **aT**, acromion transversal thickness; **nsW**, maximum neural spine width measured at its distal end; **gcT**, glenoid cavity maximum thickness.

			BLADE			ACROMION				
	L	dW	bW	bT	pW	amxH	amnH	aW	aT	gcT
Scapula (right) MNHN.F.LES133	?	?	?	35	?	?	?	?	?	?
Scapula (left) MNHN.F.LES134	?	?	132	34	?	?	?	?	?	?
Scapula (right) MNHN.F.LES135	?	?	164	35	?	?	?	?	?	?
Scapula (right) MNHN.F.LES158	?	?	76	34	?	?	?	?	?	?
Scapula (left) MNHN.F.LES386	720	?	172	30	385	265	140	85	40	106

TABLE 5. Selected measurements (mm) of the bones from the anterior member of *Kholumolumo ellenbergerorum*. Abbreviations following the table order: **L**, maximum proximodistal length; **dpcL**, deltopectoral crest dorsoventral length (measured from the proximal border of the humerus); **W**, maximum transverse width; **T**, maximum anteroposterior thickness; **C**, circumference of the diaphysis (measured beneath the deltopectoral crest on humeri); **>**, length measured given that one or both extremities of the bone are broken.

			PROXIMAL		DIAPHYSIS			DISTAL	
	L	dpcL	W	T	W	T	C	W	T
Humerus (left) MNHN.F.LES379	685	330	300	70	82	80	262	220	68
Humerus (right) MNHN.F.LES385	630	280	?	?	77	70	235	225	?
Humerus (right) MNHN.F.LES390	610	265	233	64	85	72	257	214	60
Ulna (right) MNHN.F.LES145	>305	-	?	?	50	44	-	54	?
Ulna (right) MNHN.F.LES156	370	-	120	150	53	50	-	50	100
Ulna (right) MNHN.F.LES159	390	-	126	142	52	48	-	56	108
Radius (left) MNHN.F.LES140	>264	-	112	65	47	45	-	?	?
Radius (right) MNHN.F.LES142	>235	-	?	?	42	39	-	?	58
Radius (left) MNHN.F.LES144	320	-	97	54	42	42	-	?	65
Radius (left) MNHN.F.LES147	320	-	99	58	46	38	-	85	64
Metacarpal I (right) MNHN.F.LES26	97	-	95	69	66	33	-	85	53
Metacarpal II (left) MNHN.F.LES92	125	-	68	60	32	27	-	60	38
Metacarpal III (right) MNHN.F.LES93	142	-	67	64	26	29	-	57	40
Metacarpal IV (right) MNHN.F.LES76	>103	-	?	?	28	21	-	43	27
Phalanx I.I (left) MNHN.F.LES29	94	-	65	-	-	-	-	-	-

TABLE 6. Selected measurements (mm) of the ilia, pubes and ischium *of Kholumolumo ellenbergerorum*. Abbreviations following the table order: **L**, maximum anteroposterior length; **La**, anteroposterior length above the acetabulum (at the level of the notch); **H**, maximum dorsoventral height; **Hibl**, maximum dorsoventral height of the iliac blade (measured on the lateral surface above the supracetabular crest); **Dac**, maximum diameter of the acetabulum (measured on the medial side); **Lprp**, length of the preacetabular process measured from its extremity to the level of the notch; **Lpop**, length of the postacetabular process measured from its extremity to the level of the notch of the ischial peduncle; **Lpup**, length of the pubic peduncle following its main axis; **Lepup**, anteroposterior length of the extremity of the pubic peduncle measured in ventral view; **Wepup**, transverse width of the extremity of the pubic peduncle measured in ventral view; **Lisp**, length of the ischial peduncle following its main axis; **Leisp**, anteroposterior length of the extremity of the ischial peduncle measured in ventral view; **Weisp**, transverse width of the extremity of the ischial peduncle measured in ventral view; **>**, length measured given that one or both extremities of the bone are broken; *****, deformation.

	L	La	H	Hibl	Dac	Lprp	Lpop	Lpup	Lepup	Wepup	Lisp	Leisp	Weisp
Ilium (right) MNHN.F.LES375a	610	390	385	205	180	95	200	185	155	117	110	117	122
Ilium (right) MNHN.F.LES396	550	360	350	180	177	85	160	160	113	90	75	102	105

	L	Lpp	Wpp	Hepp	Lilp	Lac	Lisp	Lpa	Wpa	Wde	Hde
Pubis (right) MNHN.F.LES373	660	180	?	>160	136	45	?	≈430	155	?	?
Pubis (left) MNHN.F.LES378	665	215	243	74*	160	75	>155	450	148	152	75

Ischium (left) MNHN.F.LES152	315	300	160	51	70	31	155	68

TABLE 7. Selected measurements (mm) of the femora, tibiae and fibulae of *Kholumolumo ellenbergerorum*. Abbreviations following the table order: **L**, maximum proximodistal length; **W**, maximum transverse width; **T**, maximum anteroposterior thickness; **C**, circumference of the diaphysis (measured beneath the fourth trochanter on femora, at midpoint on tibiae and fibulae); **dp**, distance between the proximalmost point of the fourth trochanter and the proximal extremity of the femur; **IR**, robustness index (L/C); **E**, eccentricity of the diaphysis (W/T); **>**, length measured given that one or both extremities of the bone are broken; *****, deformation.

	PROXIMAL			DIAPHYSIS			DISTAL		4th TROCH.		RATIOS	
	L	W	T	W	T	C	W	T	dp	L	IR	E
Femur (left) MNHN.F.LES371	860	235	140	102	109	333	198	195	300	165	2,58	0,94
Femur (right) MNHN.F.LES394	755	220	107	108	93	320	172	140	280	145	2,36	1,16
Tibia (left) MNHN.F.LES148	345	?	?	50	51	165	99	67	-	-		
Tibia (right) MNHN.F.LES167	>410	128	173	78	88	267	?	?	-	-		
Tibia (right) MNHN.F.LES381m	510	130	205	63	100	270	148	116	-	-		
Tibia (right) MNHN.F.LES387	580*	218*	110*	90*	85*	275*	156*	90*	-	-		
Tibia (left) MNHN.F.LES389	515	145	200	70	95	255	138	105	-	-		
Fibula (right) MNHN.F.LES149	>460	?	?	40	48	146	60	104	-	-		
Fibula (right) MNHN.F.LES150	>400	?	?	46	54	163	?	?	-	-		
Fibula (right) MNHN.F.LES374	575	40	>141	45	54	162	52	107	-	-		
Metatarsal I (left) MNHN.F.LES89	134	92	43	61	34	-	81	50	-	-	-	-
Metatarsal II (left) MNHN.F.LES81	180	?	?	48	35	-	70	47	-	-	-	-
Metatarsal III (left) MNHN.F.LES82	219	78	50	45	34	-	73	50	-	-	-	-
Metatarsal IV (left) MNHN.F.LES381c	228	100	40	43	27	-	55	50	-	-	-	-
Metatarsal V (left) MNHN.F.LES77	111	92	41	39	29	-	36	31	-	-	-	-

TABLE 8. Size and body mass estimations for *Kholumolumo ellenbergerorum* compared to those of other gondwanan basal sauropodomorphs from the Norian or Rhaetian. The parameters were defined by Campione & Evans, 2012 and the linear regression curve is from Apaldetti et al., 2018. Material used for *Kholumolumo* measurements: MNHN.F.LES371 (femur); MNHN.F.LES379 (humerus); MNHN.F.LES386 (scapula); MNHN.F.LES375a (ilium). Specimens considered for the comparison: *Coloradisaurus* PVL 5904; *Lessemsaurus* 1 PVL 4822; *Lessemsaurus* 2 CRILAR PV-303 (scapula), CRILAR PV-302 (ilium); *Melanorosaurus* NM QR 1551; *Plateosauravus* SAM PK 3602 (femur), SAM PK 3609 (ilium); *Riojasaurus* PVL 3808; *Ruehleia* MB.R.4718; *Unaysaurus* UFSM11069. All were measured first-hand, except *Unaysaurus*.

Genera	Size	Body mass			
	Size estimation (Sander and Klein, 2005)	Bipedal equation (Benson et al., 2018)	Quadrupedal equation (Benson et al., 2018)	Scapula equation (Apaldetti et al., 2018)	Ilium Equation (Apaldetti et al., 2018)
Kholumolumo	**8.6 m**	**1754 kg**	**3334 kg**	**3864 kg**	**3963 kg**
Coloradisaurus	5.0 m	438 kg	757 kg	307 kg	?
Lessemsaurus 1	8.4 m	1963 kg	2208 kg	1746 kg	2792 kg
Lessemsaurus 2	?	?	?	5268 kg	7165 kg
Melanorosaurus	6.2 m	946 kg	1603 kg	1396 kg	1656 kg
Plateosauravus	8.0 m	824 kg	?	?	2792 kg
Riojasaurus	6.1 m	1005 kg	1923 kg	?	1552 kg
Ruehleia	7.6 m	986 kg	?	?	2371 kg
Unaysaurus	?	?	?	88 kg	?

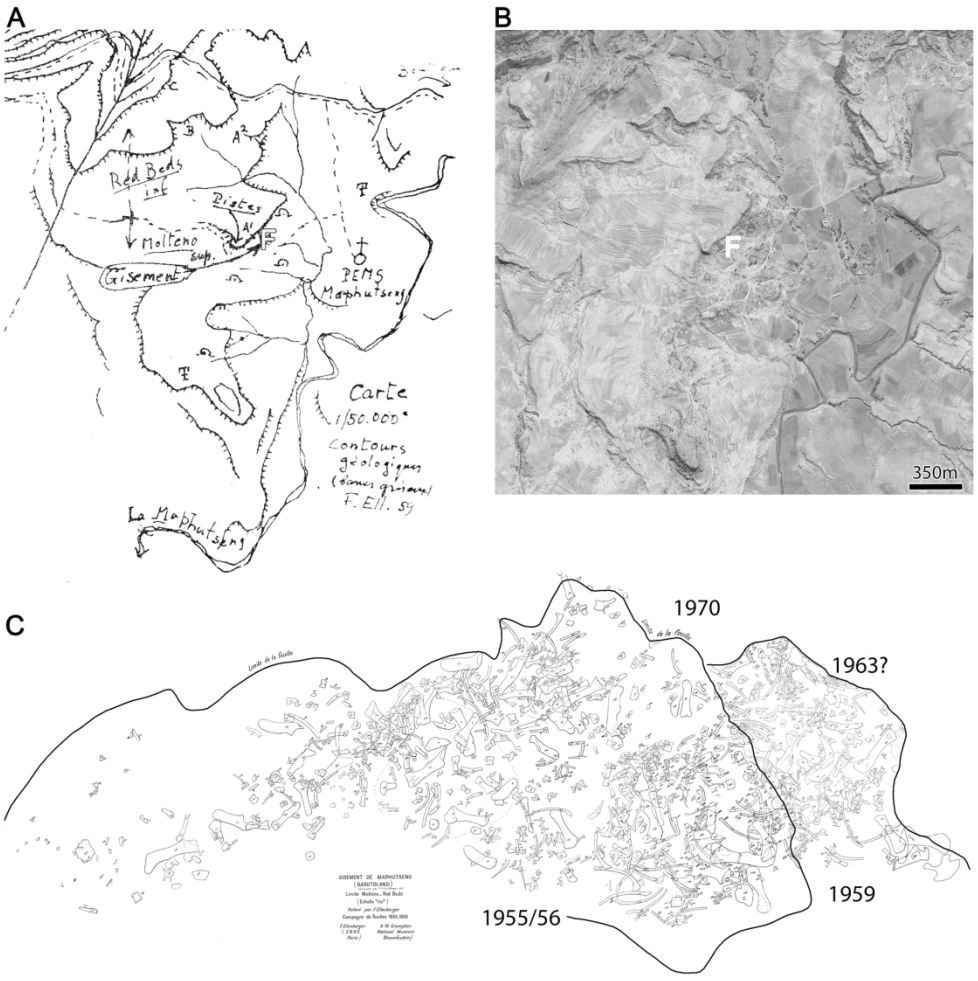

181x178mm (300 x 300 DPI)

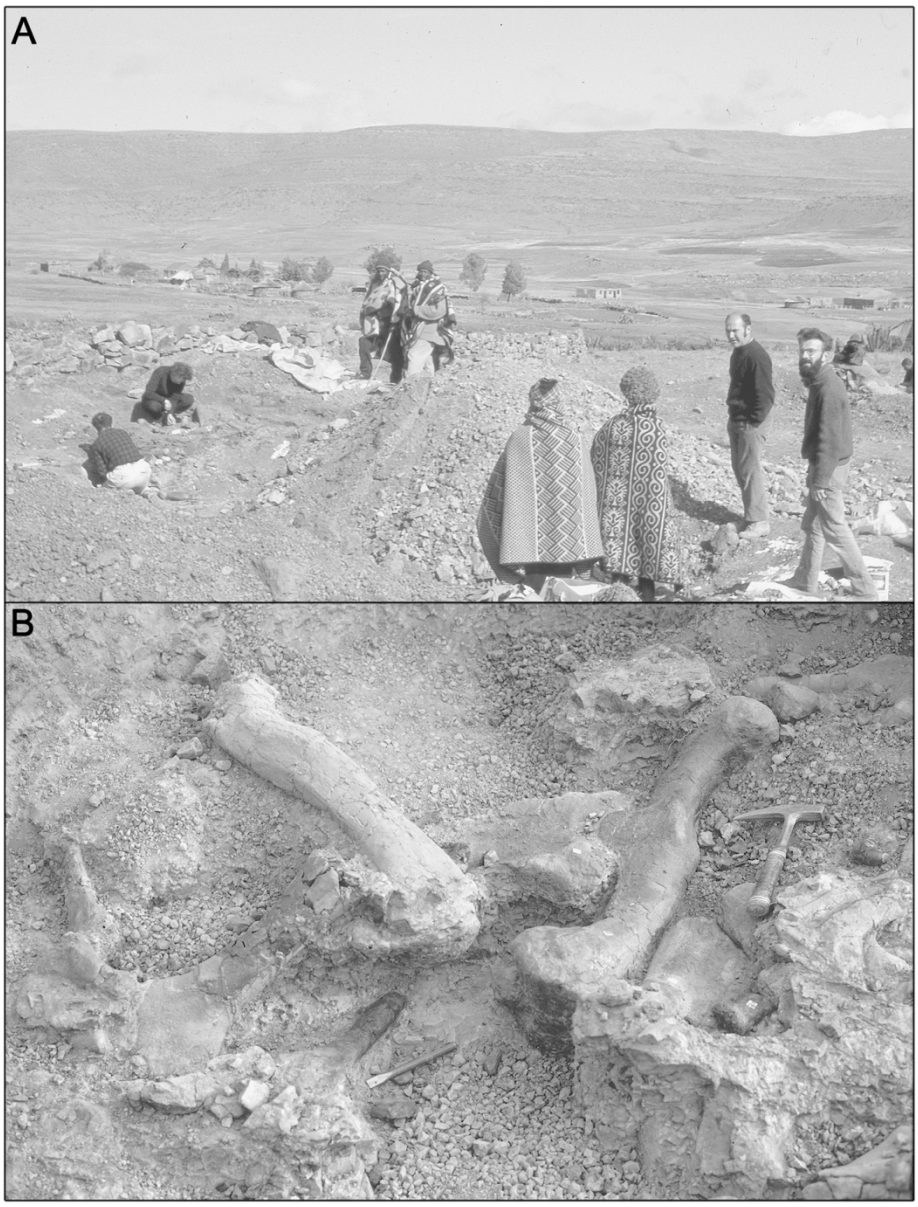

121x159mm (300 x 300 DPI)

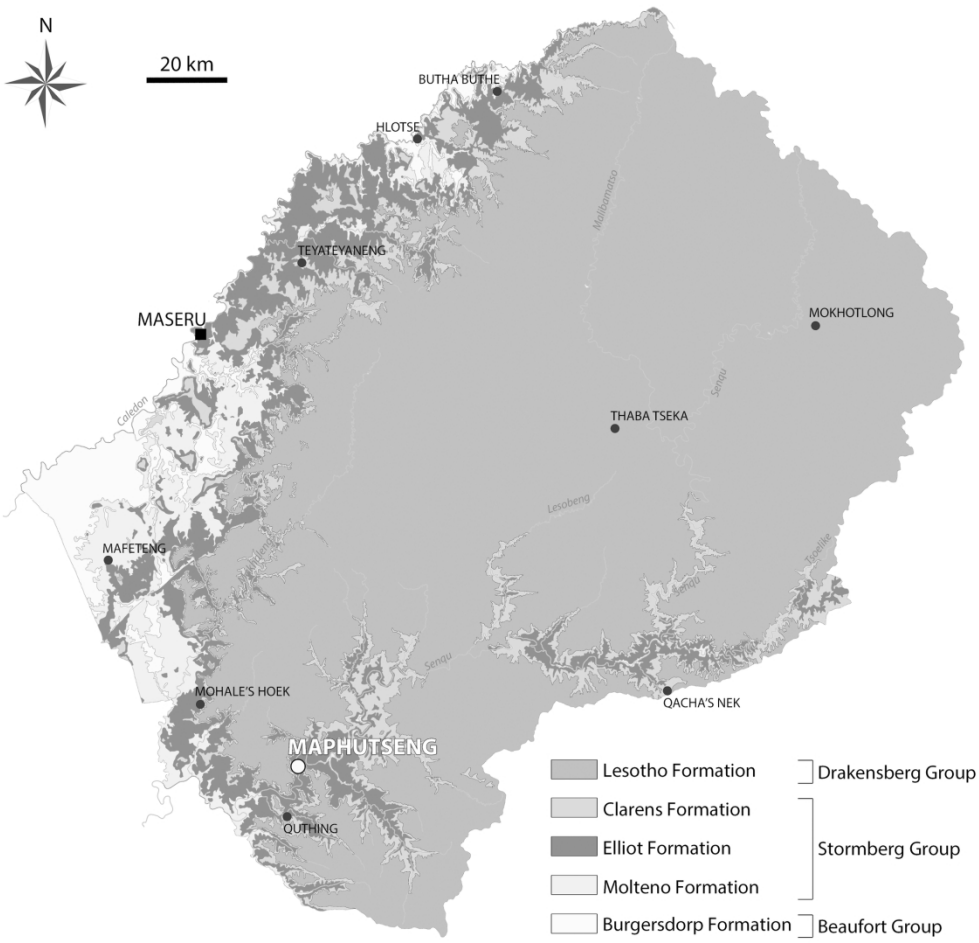

181x174mm (300 x 300 DPI)

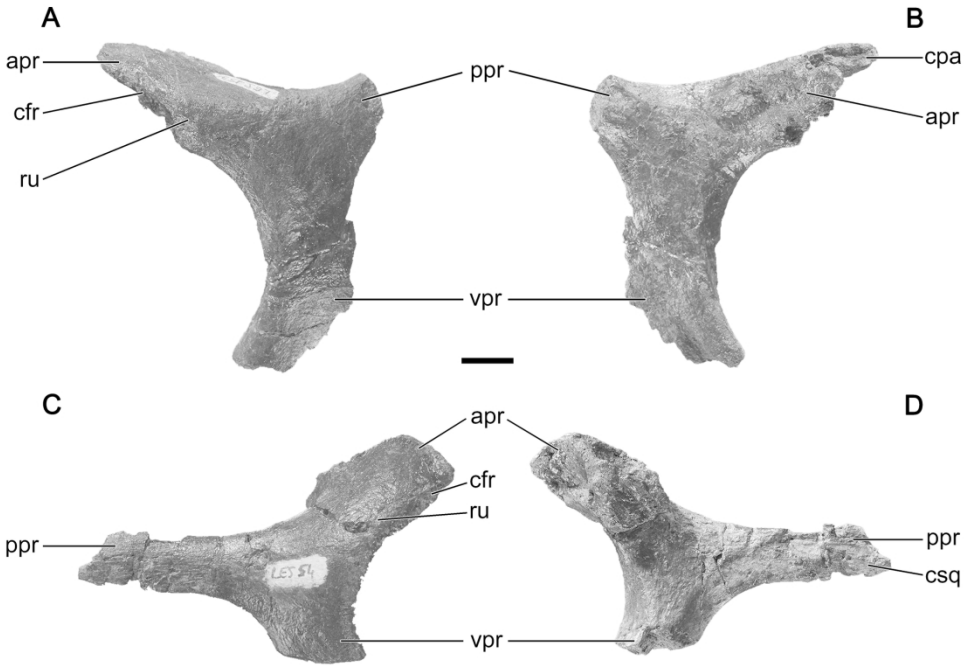

182x123mm (300 x 300 DPI)

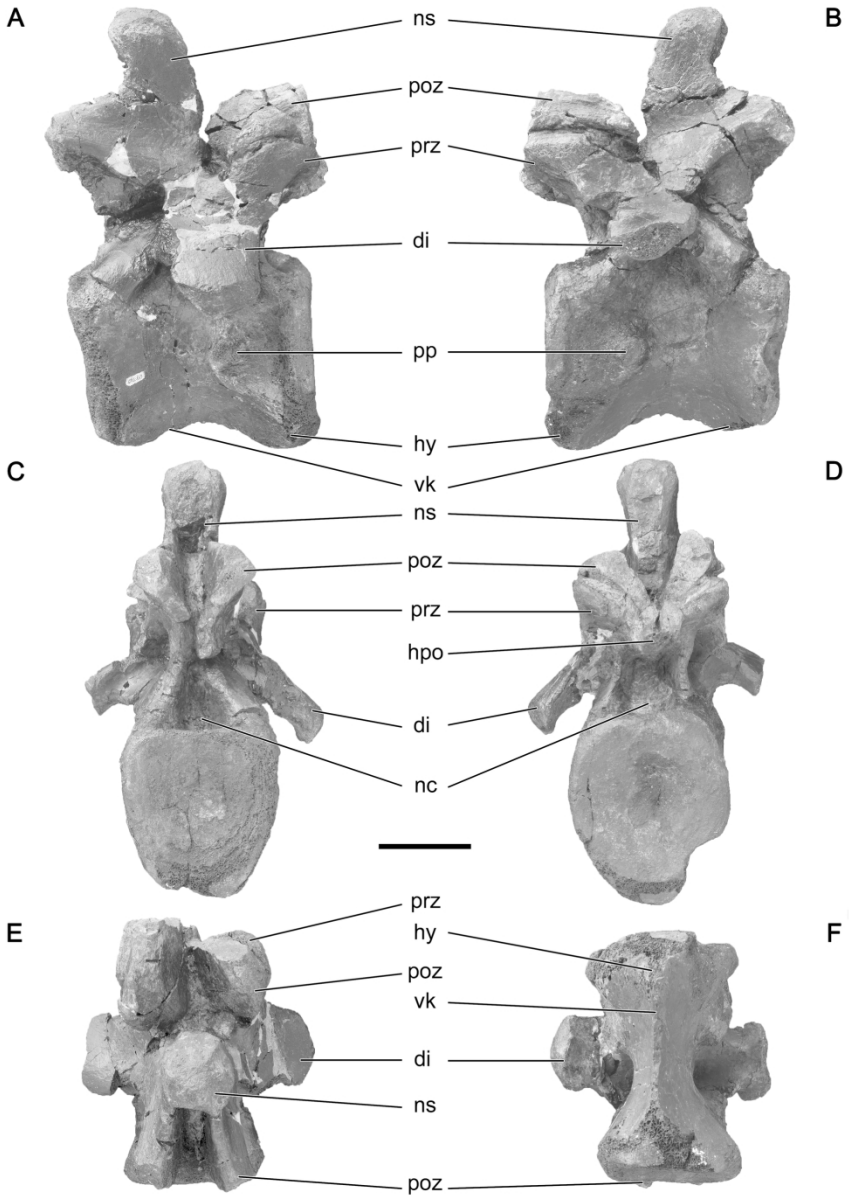

181x232mm (300 x 300 DPI)

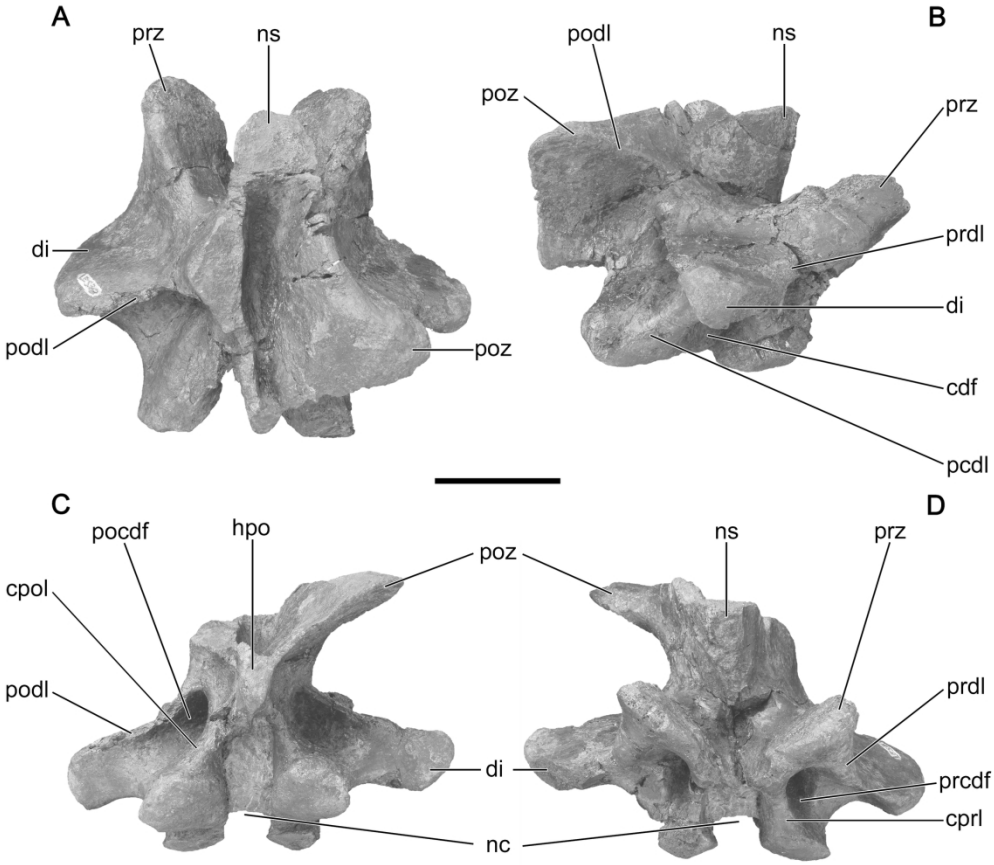

181x159mm (300 x 300 DPI)

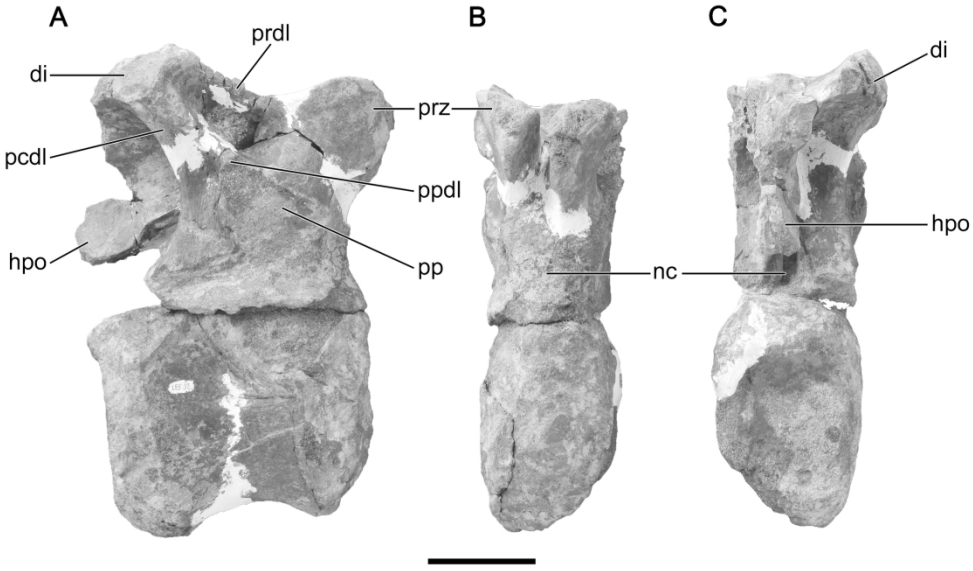

181x105mm (300 x 300 DPI)

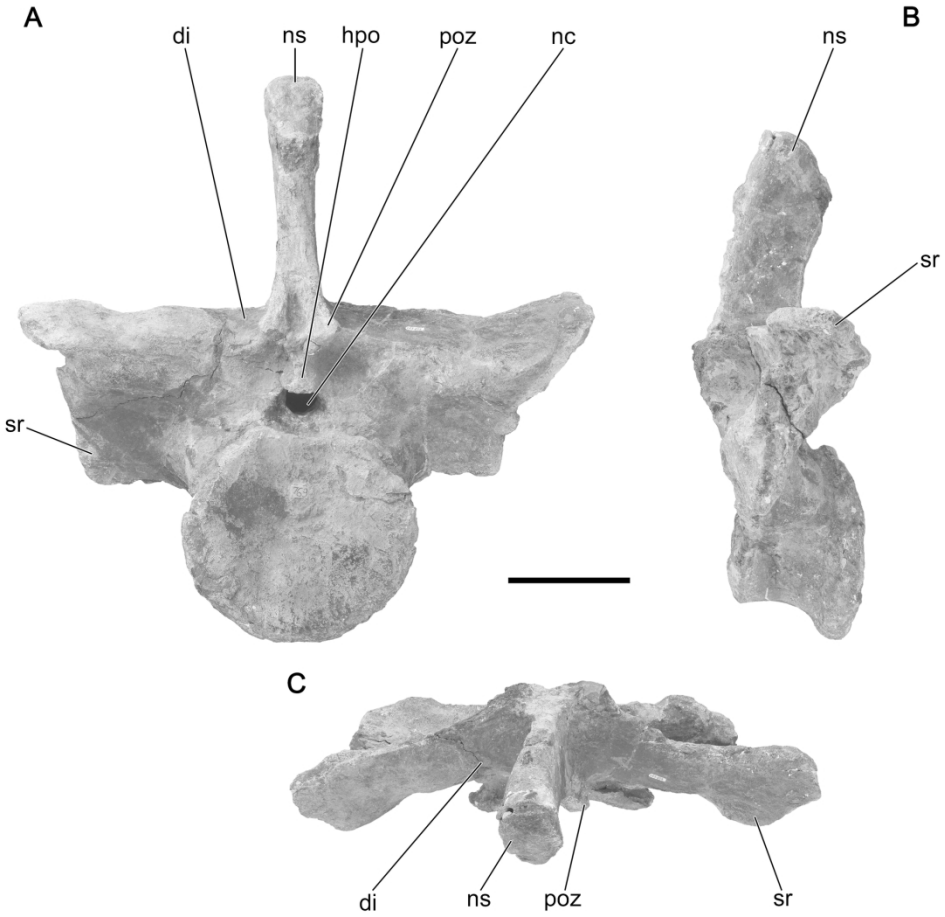

181x168mm (300 x 300 DPI)

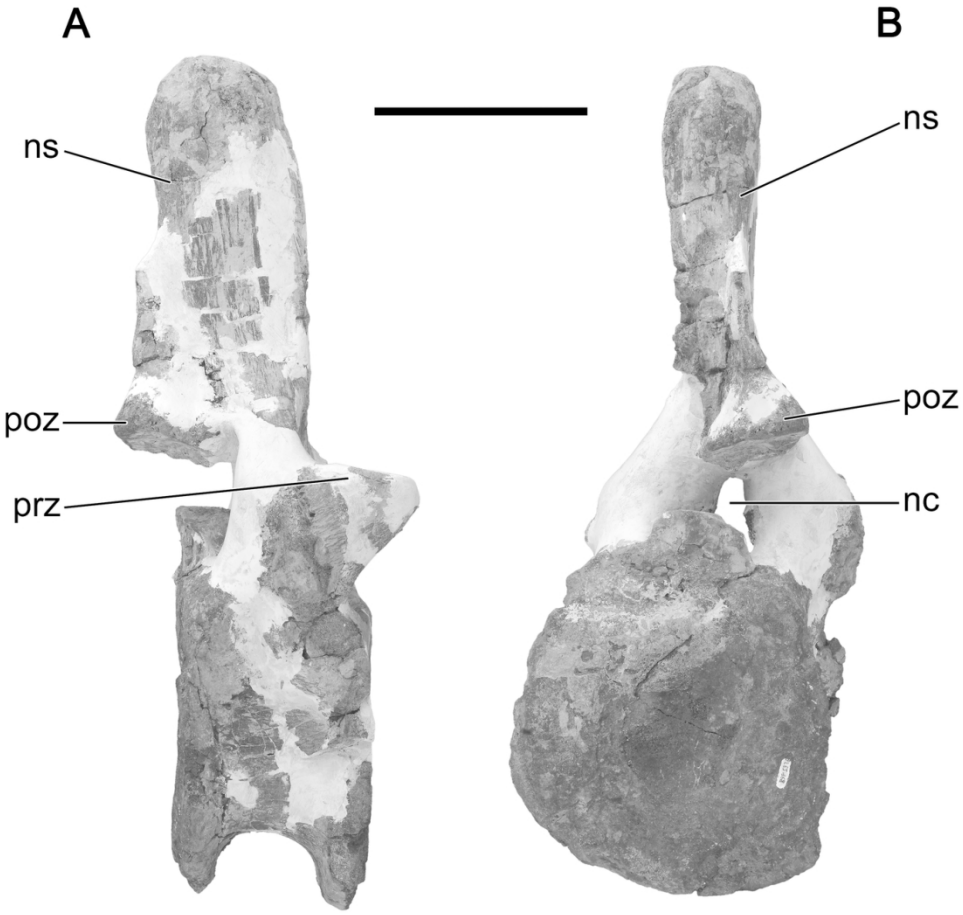

122x113mm (300 x 300 DPI)

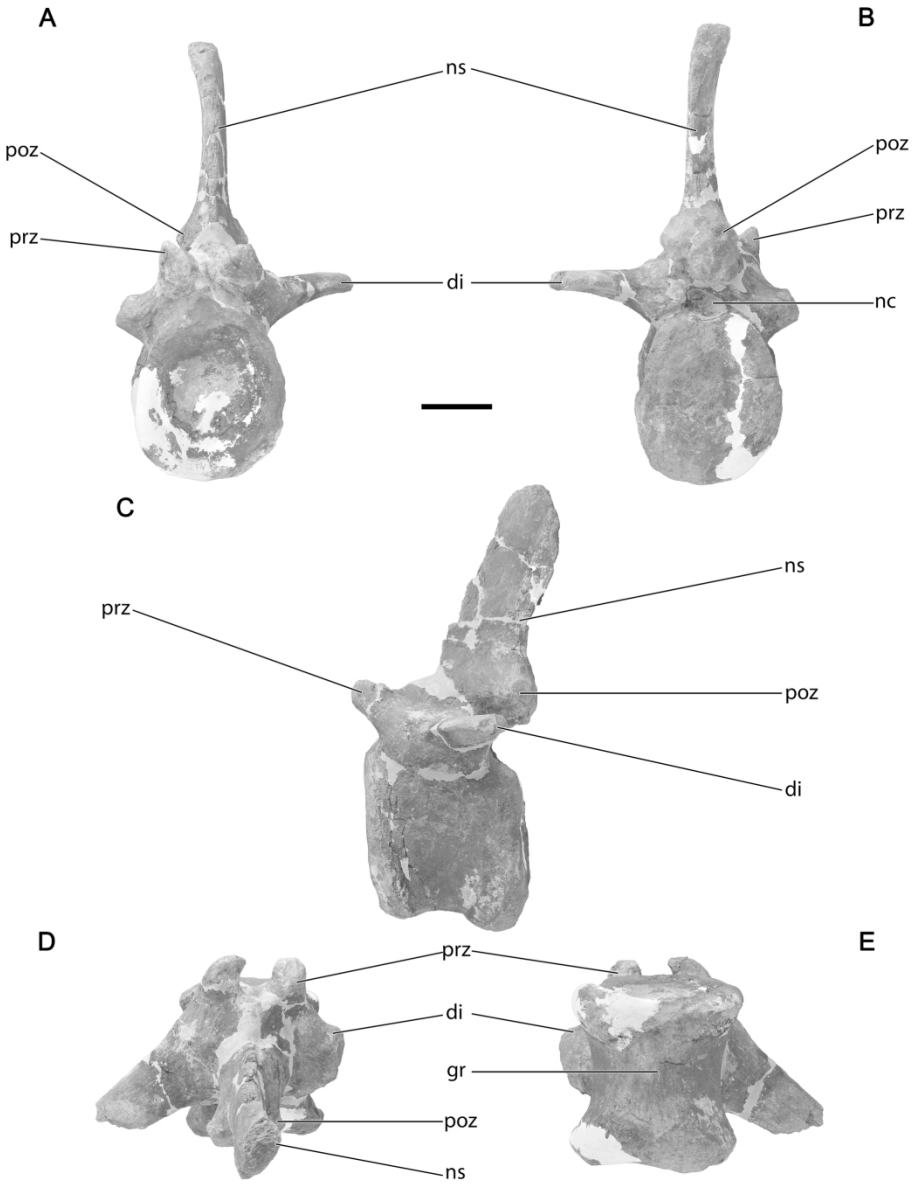

181x232mm (300 x 300 DPI)

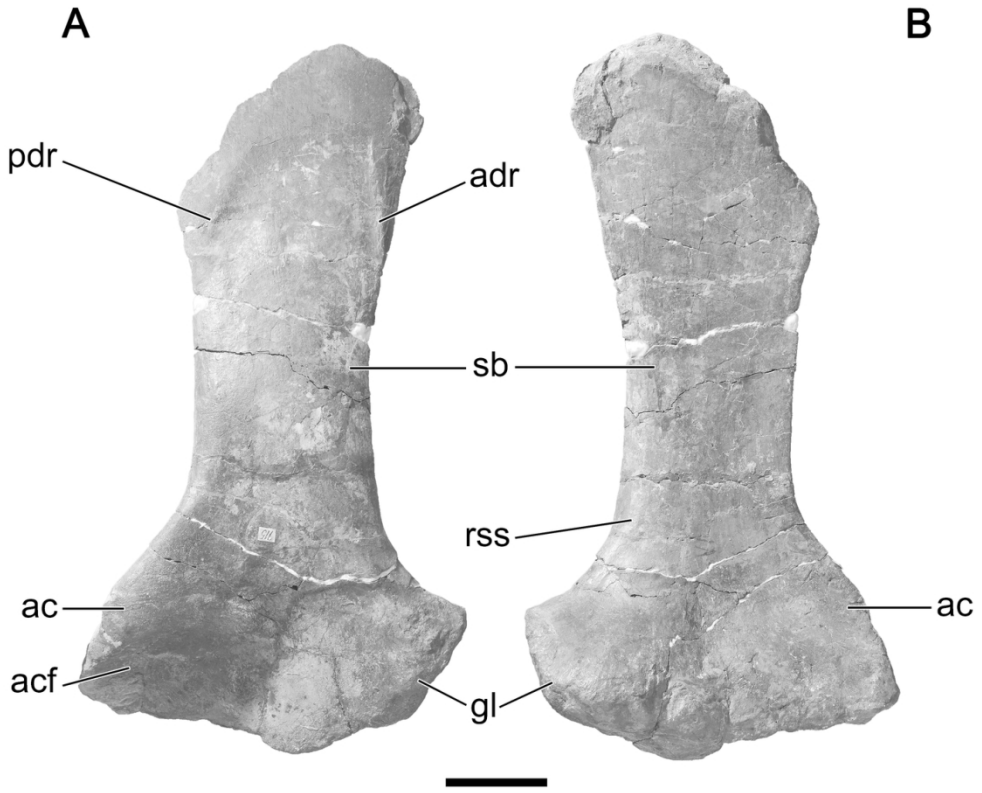

122x98mm (300 x 300 DPI)

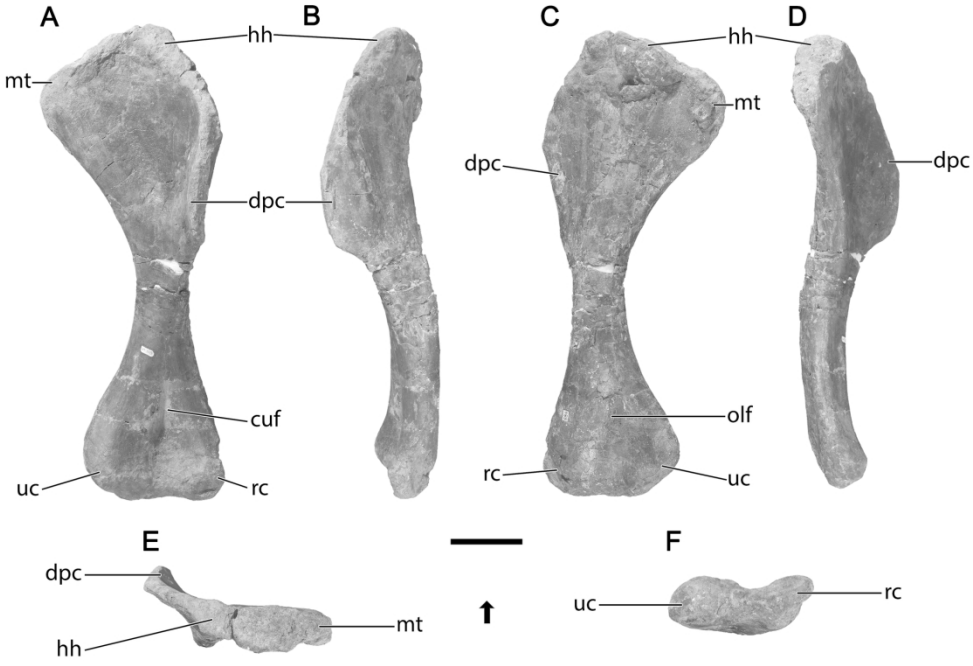

181x121mm (300 x 300 DPI)

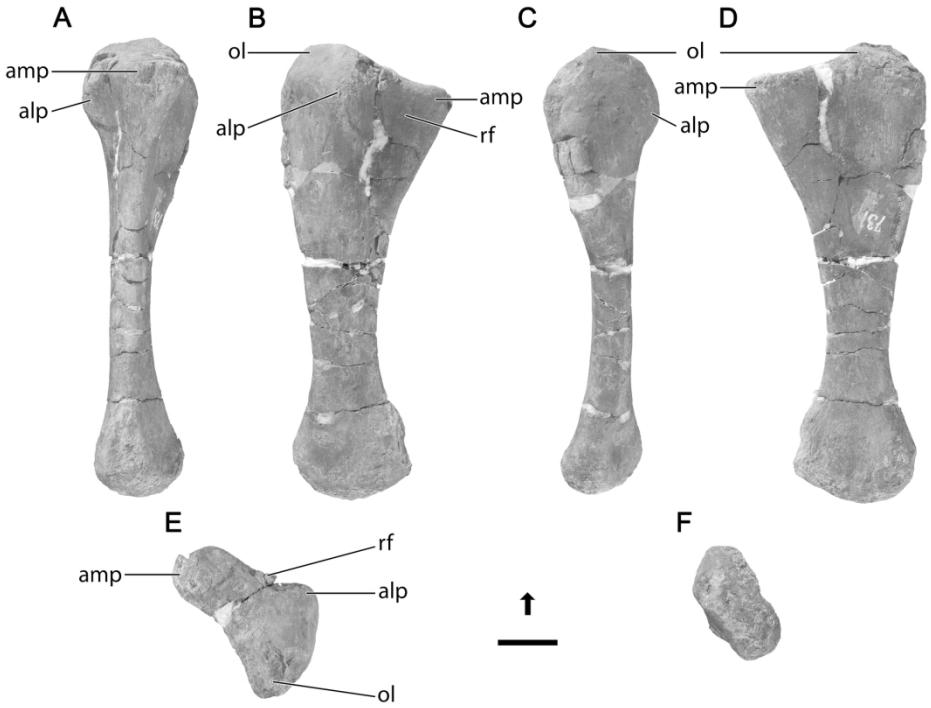

181x131mm (300 x 300 DPI)

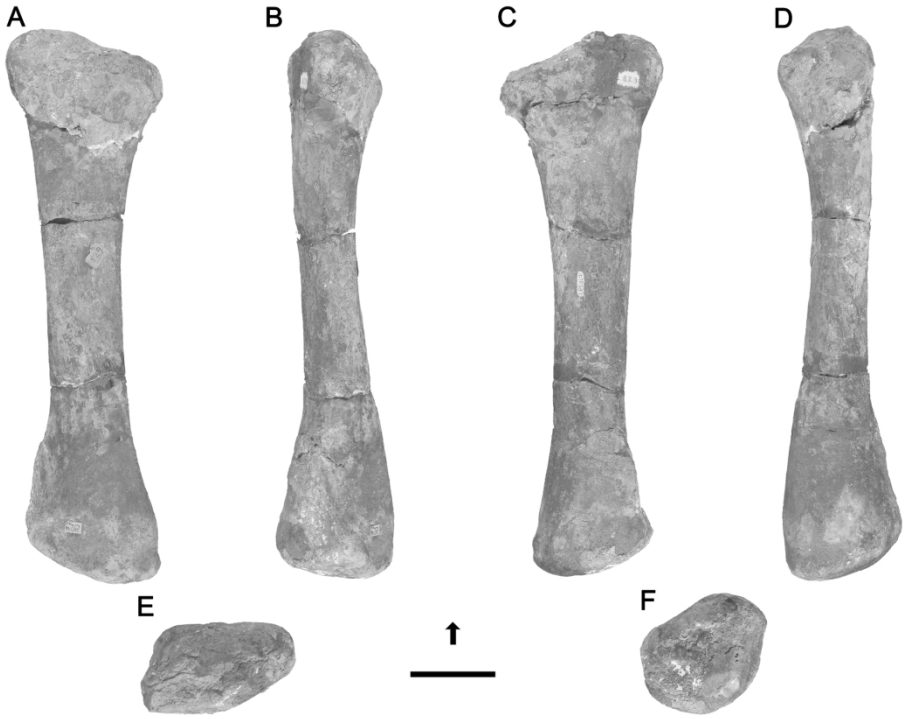

181x131mm (300 x 300 DPI)

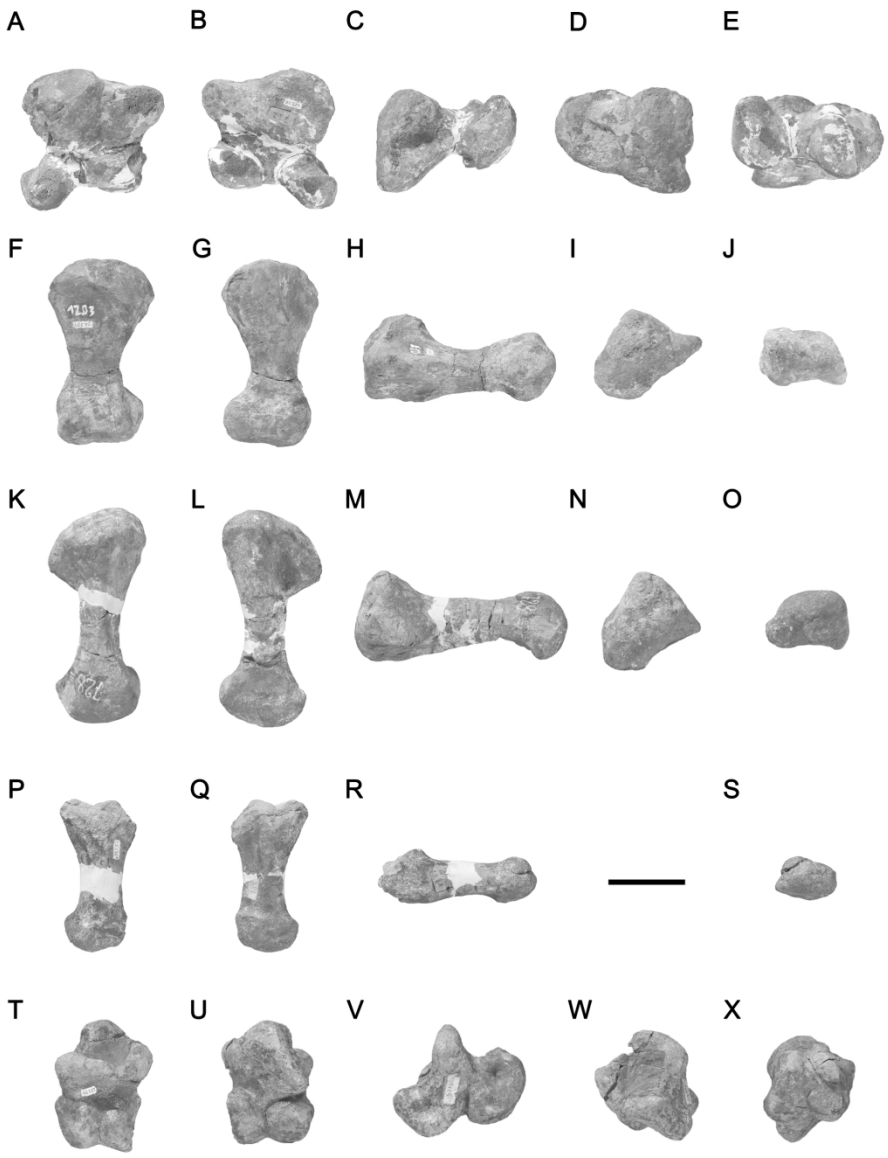

181x232mm (300 x 300 DPI)

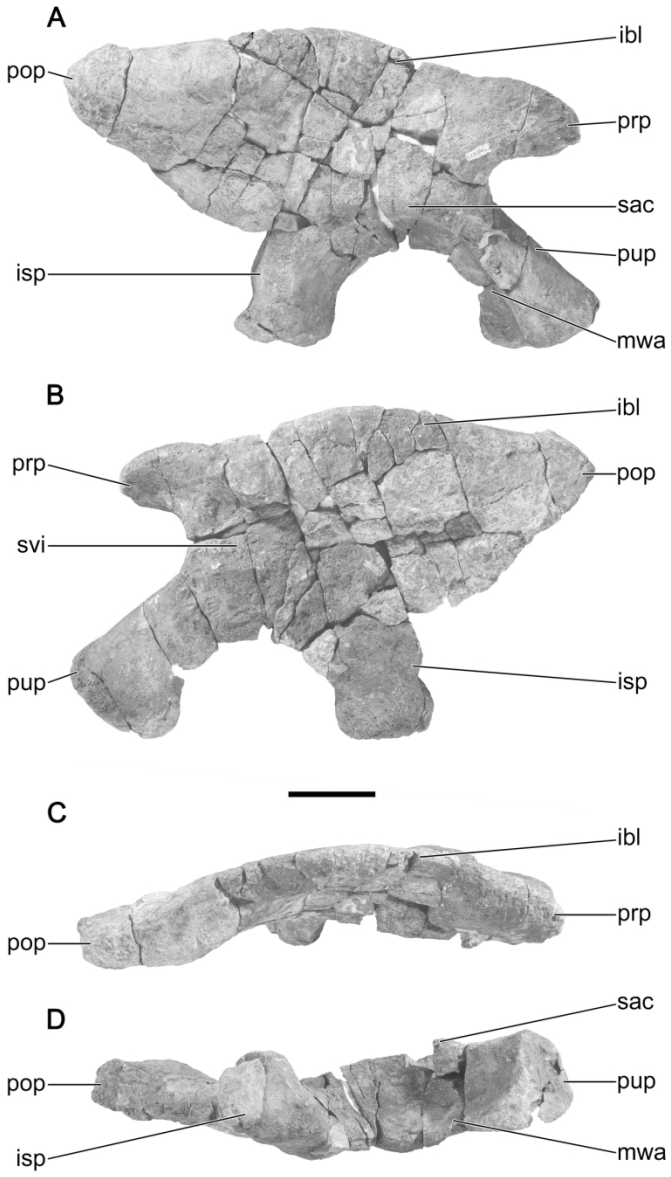

122x214mm (300 x 300 DPI)

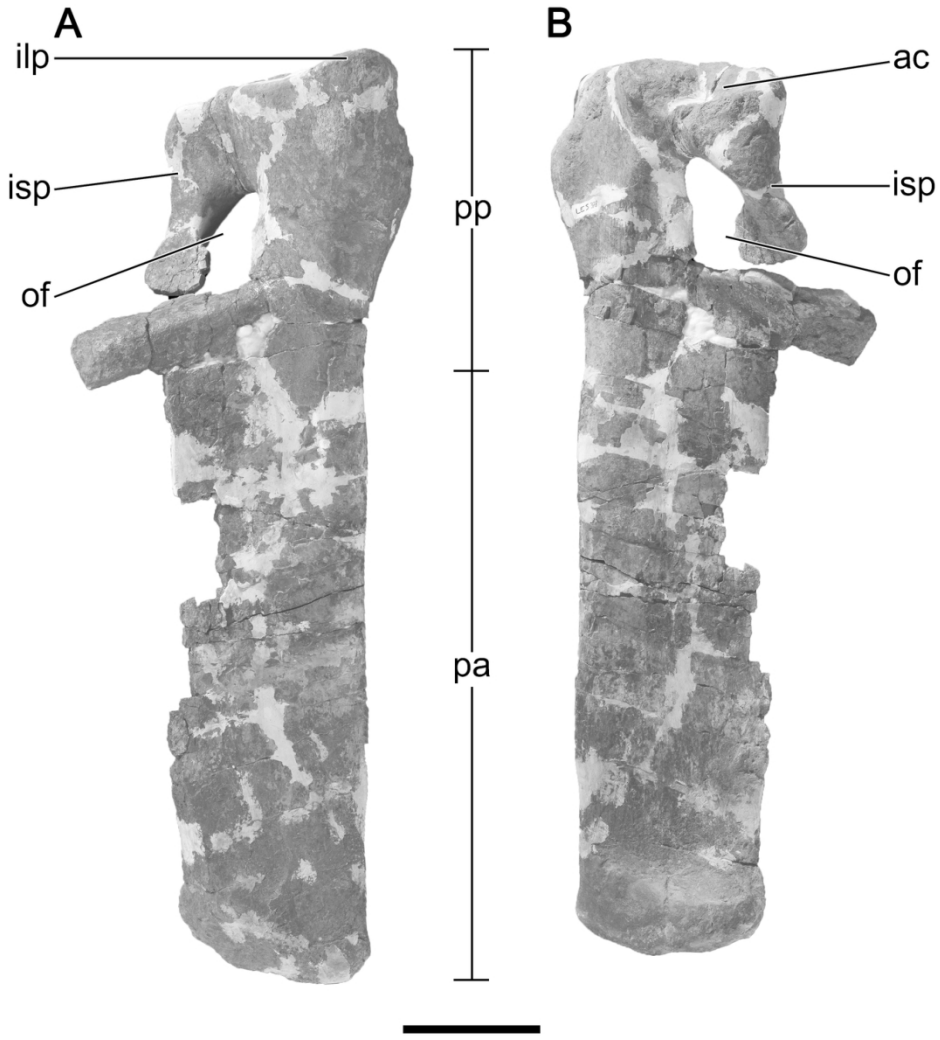

122x130mm (300 x 300 DPI)

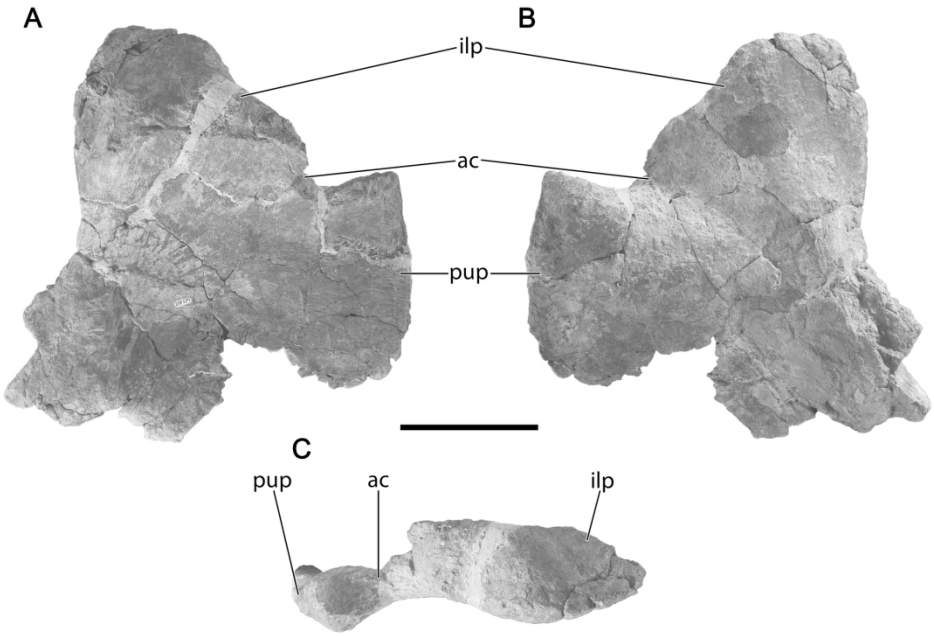

181x120mm (300 x 300 DPI)

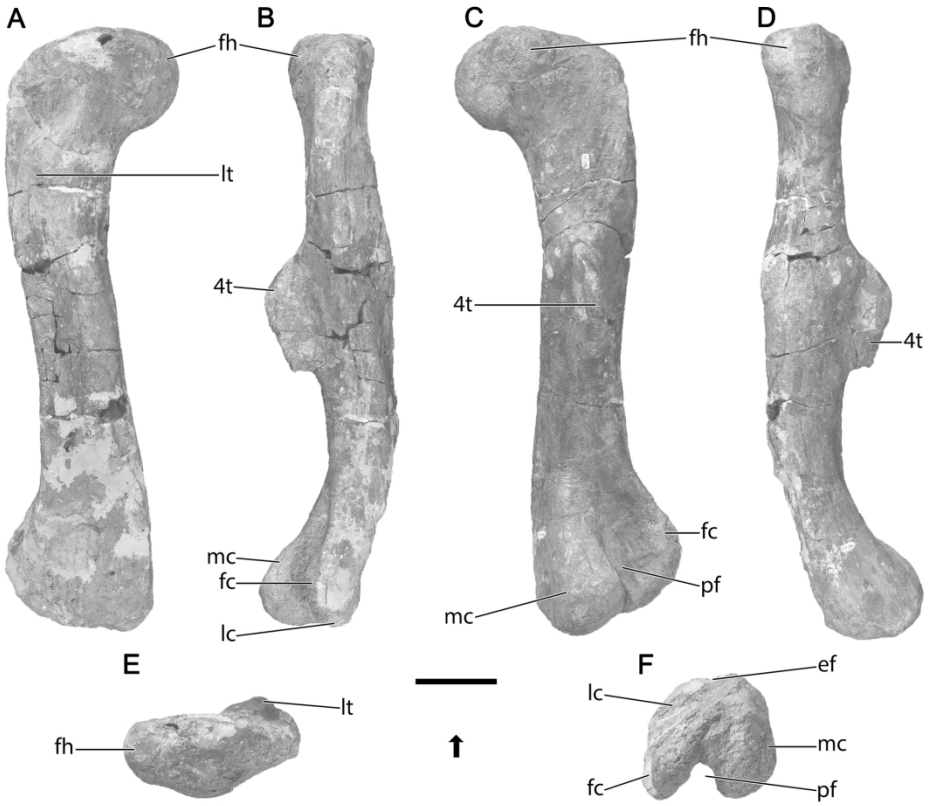

181x149mm (300 x 300 DPI)

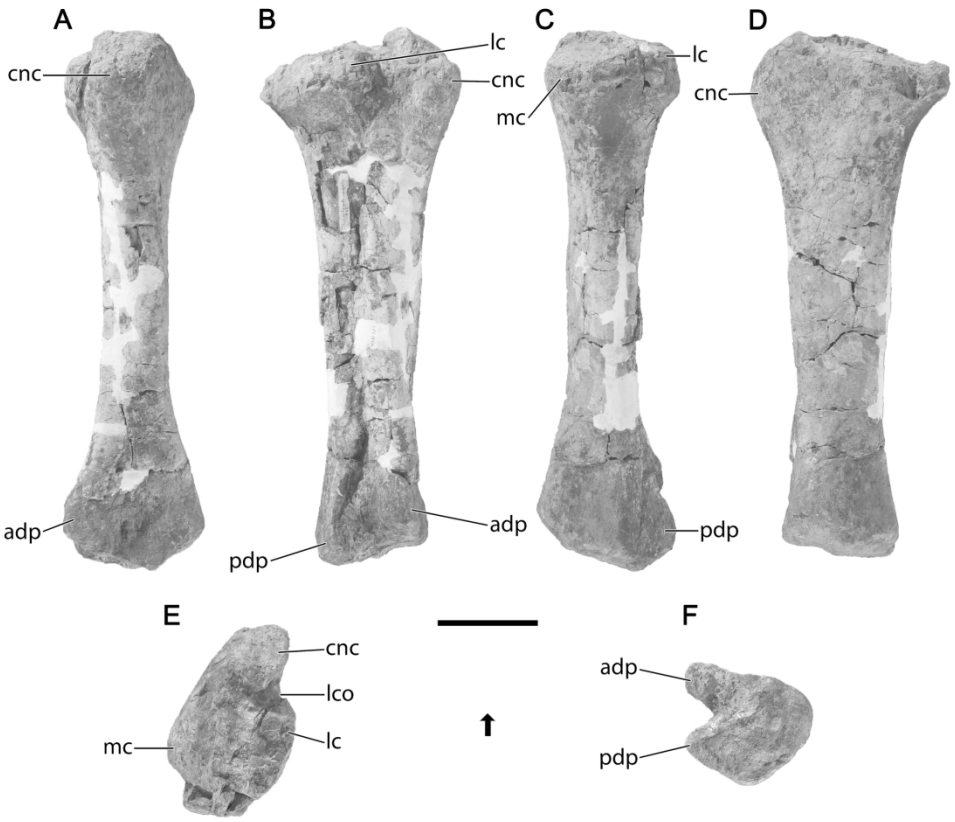

181x149mm (300 x 300 DPI)

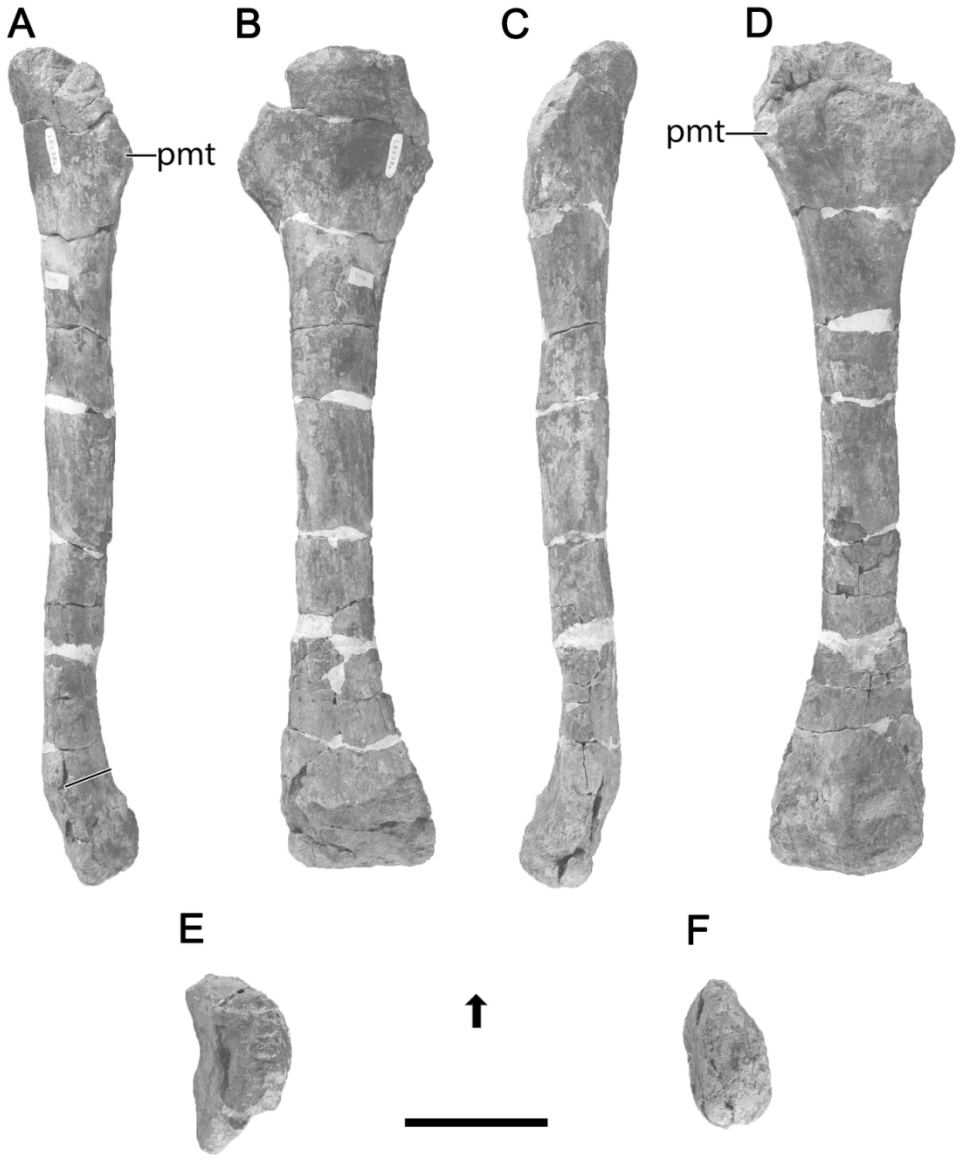

122x142mm (300 x 300 DPI)

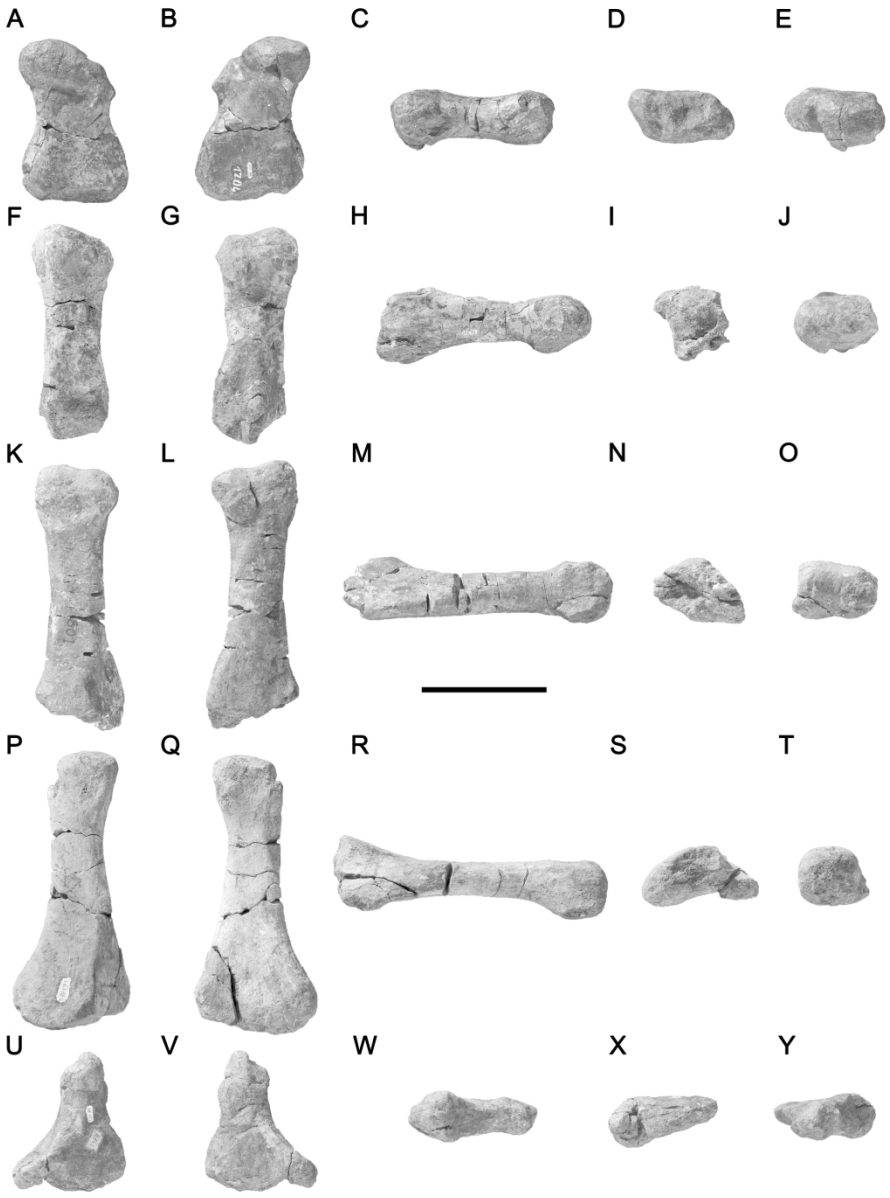

181x232mm (300 x 300 DPI)

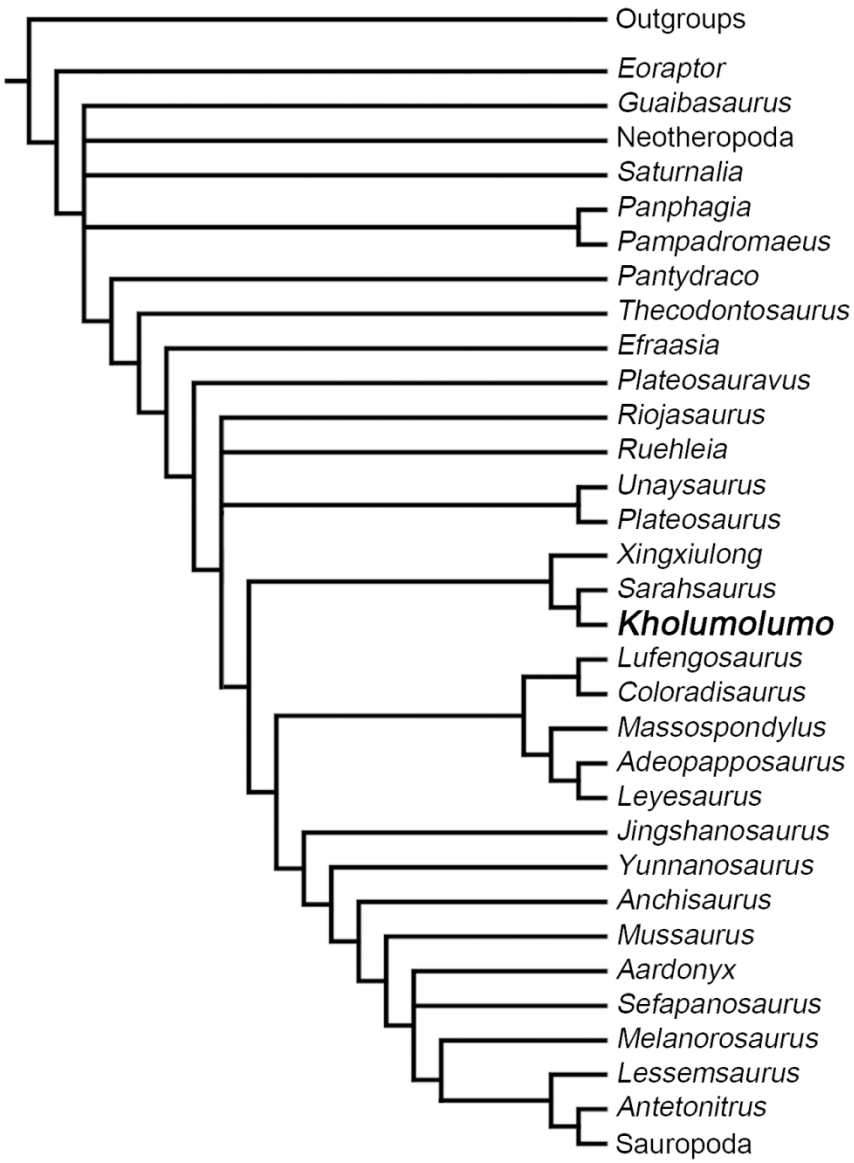
Outgroups
Eoraptor
Guaibasaurus
Neotheropoda
Saturnalia
Panphagia
Pampadromaeus
Pantydraco
Thecodontosaurus
Efraasia
Plateosauravus
Riojasaurus
Ruehleia
Unaysaurus
Plateosaurus
Xingxiulong
Sarahsaurus
Kholumolumo
Lufengosaurus
Coloradisaurus
Massospondylus
Adeopapposaurus
Leyesaurus
Jingshanosaurus
Yunnanosaurus
Anchisaurus
Mussaurus
Aardonyx
Sefapanosaurus
Melanorosaurus
Lessemsaurus
Antetonitrus
Sauropoda